Synthesis and modification of porous boron nitride materials for application in carbon dioxide capture

Fereshteh Hojatisaeidi

A thesis submitted in partial fulfilment of the requirements for the award of Doctor of Philosophy in Chemical, Process and Energy Engineering

School of Engineering

London South Bank University

October 2020

Declaration

I declare that the thesis has been composed by myself with support of my supervisors. The thesis is submitted for examination in consideration of the award of a degree of Doctor of Philosophy in Chemical, Process and Energy Engineering. I would like to emphasise that the work has not be submitted for any other degree or professional qualification. Furthermore, I took reasonable care to ensure that the work is original and to the best of my knowledge, does not breach copyright law and has not been taken from other sources except where such work has been cited and acknowledged within the text.

Dedication

I would like to wholeheartedly dedicate this dissertation to my previous supervisor Professor. Yuda Yürüm who was a true inspiration for me. May his soul rest in peace. I would like to wholeheartedly thank my dearest mom and dedicate this dissertation to her for all her emotional support, although remotely. Last but not least, I dedicate this dissertation to my husband who encouraged me along the way to pursue my dreams toward a PhD. Above all, I truly appreciate all that my father instilled in me without which I could not succeed in my PhD. He sadly passed away shortly before my viva; however, he will always be remembered for his jovial lifestyle.

Acknowledgements

First and foremost, I would like to thank God for anything I have and do not have in my life.

I would like to thank my supervisor, Professor Basu Saha, for his help, support and encouragement throughout this study. I appreciate his trust in me and for offering a position in his research group.

Also, I extend my huge appreciation to my second supervisor, Professor, Geraldine Durand, from TWI, for her guidance, support, the research outlook and boosting my self-confidence.

Special heartfelt thanks to the Sotacarbo team in Italy, Dr. Mauro Mureddu, Dr. Alberto Pettinau and Dr. Federica Dessì. It was a great pleasure working with them in this project.

I would like to say a big thank you to all of the technical support staff at London South Bank University, especially Mr. William Cheung who was always on hand when I needed any help or advice. I am greatly thankful to Mr. Ken Unadat and Mr. Charles Coster for their technical support and guidance in the laboratories.

I have received great support from the School of Engineering, especially from Dr Sandra Dudley and Dr Suela Kellici. I would like to thank them for all their support and facilitating the research journey for me. In addition, special thanks to London Doctoral Academy (LDA) team represented by Prof. Graeme Maidment, Mr John Harper, Prof. Peter Doyle and Mrs Louise Thompson (Campbell).

I believe that I have been extremely lucky in working with supportive and collegiate people in Professor Saha's lab. A warm thank you to them: Dr Victor Onyenkeadi, Dr Zahra Echresh Zadeh, Dr Omar Aboelazayem, Dr Bisi Olaniyan, Mahiuddin Alamgir, Shahenda Mahran and Yusuf Umar.

Abstract

Global warming, which is often confused with “climate change”, can cause long-lasting, irreversible, catastrophic and far-reaching effects on the earth and the lives of the future generations. There is a unanimous agreement that global warming is mainly due to human activities and above all, burning fossil fuels for industrial applications and emission of CO_2 as one of the major contributors of global warming.

To mitigate the amount of CO_2 emission and to offset its effect, the governments around the world have united to take necessary actions in an effective and efficient way by a variety of policy changes and adoption of technologies such as carbon capture and storage. For instance, the UK government has set out measures to tackle climate change with a plan for the UK to be a pioneering economy in the world towards a zero-emission economy by 2050.

Among the technologies used for carbon capture, those derived from solid sorbents for CO_2 capture attract growing interest in industrial applications. The popularity of using these technologies is attributed to their lower energy penalty, high selectivity, recyclability and ease of manufacturing. Developments of new materials with low cost is fundamental, even though numerous solid sorbents have been examined for CO_2 capture to date.

Porous boron nitride (BN) has been recognised as a promising alternative to be used in carbon adsorption process due to its unique advantages including its bond polarity, tuneability and high thermal and chemical stabilities. So far, a systematic understanding of how its distinctive properties (pore structure and chemistry) contributes to capture carbon dioxide is still lacking. To develop a favourable porous BN, further work is required to establish the viability of these materials as cost-effective adsorbents.

This research presents synthesis and modification strategies of porous BN and a characterisation of the material for carbon capture application. Various synthesis conditions have been developed to obtain high surface area (>700 m^2/g) pristine BN material *via* template free method. The study pursued two distinct strategies to modify pristine porous BN, aiming to enhance its CO_2 adsorption performance. Firstly, a focus on controlling the pure BN porosity has been implemented by tuning with a polymeric

surfactant as non-metal modification approach. The capacity of pure CO_2 on non-metal modified porous BN has been enhanced by about 34.5% compared to pristine BN in ambient conditions. The study highlights the significant role of porosity/pore size of BN for CO_2 adsorption.

Secondly, a novel approach has been implemented for modifying pore structure and surface chemistry of pristine BN by introduction of Ni (II) into BN framework. The pure CO_2 capture experiment has been assessed, considering three different temperatures and the results confirmed that the basic sites on porous BN contribute to its ability to adsorb more CO_2 relative to pure BN. The method has been validated as a feasible route to improve porous BN performance in CO_2 adsorption process even at realistic flue gas temperatures (above 298 K). Finally, the stability and reusability of pristine BN samples with various porosity and chemistry have been examined over the eight adsorption-desorption cycles.

Overall, this dissertation demonstrated that porous BN materials possess a combination of desirable properties with flexibility for functionalisation and lower regeneration energy. Thus, it can be considered as an effective adsorbent for future large-scale carbon capture technologies.

Table of contents

List of figures

List of tables

List of abbreviations and acronyms

Abbreviation/Acronym	Definition
BECCS	Bioenergy with CCS
BET	Brunauer−Emmett−Teller
BE	Backscattered Electrons
BF	Bright Field
BJH	Barret, Joyner and Halenda
BN	Boron Nitride
BCN	Boron Carbon Nitride
BNNSs	Boron Nitride Nanosheets
h-BN	Hexagonal Boron Nitride
c-BN	Cubic Boron Nitride
a-BN	Amorphous Boron Nitride
t-BN	Turbostratic Boron Nitride
CCC	Committee on Climate Change
CCS	Carbon Capture & Storage
CDR	Carbon Dioxide Removal
COVID	Coronavirus Disease
CNTs	Carbon Nanotubes
CTAB	Cetyl-Trimethylammonium Bromide
CTAC	Cetyl-Trimetylammonium Chloride
DF	Dark Field
DFT	Density Functional Theory
DSC	Differential Scanning Calorimetry
DTAC	Dodecyl Trimethyl Ammonium Chloride
EDX	Energy Dispersive X-ray Spectroscopy
EELS	Electron Energy Loos Spectroscopy
FTIR	Fourier Transform Infra-red Spectroscopy
GHG	Greenhouse Gas
HK	Horvath-Kawazoe
IEA	International Energy Agency
IPCC	Inter-governmental Panel on Climate Change
IUPAC	International Union of Pure and Applied Chemistry
LDF	Linear Driving Force
LIBS	Laser-induced Breakdown Spectroscopy
ILs	Ionic Liquids
MOF	Metal-organic Frameworks
NLDFT	Non-Local Density Functional Theory
PVC	Polyvinyl Chloride

P123	Poly (ethylene glycol)-block-poly (propylene glycol)-block-poly (ethylene glycol)
PB	Polyborazylene
PSA	Pressure Swing Adsorption
SE	Secondary Electron
SEM	Scanning Electron Microscopy
SRA	Structure Redirecting Agent
SSA	Specific Surface Area
TEM	Transmission Electron Microscopy
TGA	Thermo Gravimetric Analysis
TSA	Temperature Swing Adsorption
UV	Ultraviolet
XRD	X-Ray Diffraction

Journal Publications

Hojatisaeidi, F., Mureddu, M., Dessì, F., Durand, G. and Saha, B., 2020. "Metal-Free Modified Boron Nitride for Enhanced CO_2 Capture". *Energies*, *13*(3), p.549. doi:10.3390/en13030549.

Hojatisaeidi, F., Mureddu, M., Cannas, C., Pettinau, A., Durand, G. and Saha, B., "Synergistic effect of the calcination and the Ni loading on boron nitride for carbon dioxide capture", under review in Applied Energy 2020.

Hojatisaeidi, F., Mureddu, M., Pettinau, A., Durand, G. and Saha, B., "Precursor-mediated synthesis of porous boron nitride for gas adsorption properties", working paper to be submitted to Energy.

Other publications

Hojatisaeidi, F., Mureddu, M., Dessì, F., Pettinau A., Durand, G. and Saha, B., 2020. "Porous boron nitride: an effective adsorbent for carbon capture". Royal Society of Chemistry's (RSC) Environmental Chemistry Group (ECG), Bulletin, United Kingdom, July 2020, 16-17.

Conference presentations

Hojatisaeidi, F., Mureddu, M., Dessì, F., A., Pettinau, Durand, G. and Saha, B., 2018. "Synthesis and characterisation of porous boron nitride as a new class of sorbent material" Royal Society of Chemistry 2018, Environmental Chemistry of Water, Sediment, Soil and Air. London, United Kingdom, 21th November.

Hojatisaeidi, F., Mureddu, M., Dessì, F., A., Pettinau, Durand, G. and Saha, B., 2019. "Metal-free activated boron nitride for carbon capture and storage technology" UKPorMat 2019, 4th Annual UK Porous Materials Conference. Cardiff, United Kingdom, 1st - 2nd July.

Hojatisaeidi, F., Mureddu, A., Pettinau, F., Durand, G. and Saha, B., 2019. "Investigating the impact of Ni modification of boron nitride for CO_2 adsorption behaviour" UKCCSRC Programme Conference 2019, Edinburgh, United Kingdom, 4th – 5th September.

CHAPTER 1

INTRODUCTION

Outline of the chapter

This chapter provides a background to the research study, its aims and objectives, contribution to knowledge and provides an outline of the dissertation. The chapter is organised as follows:

1.1. Background

1.2. Motivation

1.3. Aims and objectives

1.4. Contributions to knowledge

1.5. Structure of the dissertation

1. Introduction

1.1. Background

The industrial revolution in the eighteenth century made mass-production of items feasible owing to the automation of work in large factories. This rapid increase in the production of products, combined with the increased population in the world have led to an exponential rise in greenhouse gas (GHG) emissions around the globe. There is almost no doubt on the influence of the human activities on climate change and analyses show that the recent emissions of GHG is the highest in history (IPCC, 2014). The increase in GHG emissions has far reaching and major implications ranging from ecological and environmental to health impacts. These include but are not limited to rising sea levels, respiratory diseases, disruption in food supply chains and extreme weather conditions. Figure 1.1 shows the average temperature anomaly since 1850 in the world in which a non-linear increasing trend is clearly visible.

The term greenhouse gas (GHG), refers to a set of gases including carbon dioxide (CO_2), nitrous oxide (N_2O), methane (CH_4) and fluorinated gases with CO_2 having the lion's share of these emissions. From the graph in Figure 1.2., one can observe the cumulative CO_2 emissions by region in the last 70 years, showing that while the amount of emission has been almost constant in this period, China has experienced an exponential growth in emissions due to an increase in electricity demand. The overall trend also represents a fivefold increase in emissions worldwide. The recent unprecedented circumstances associated with the COVID-19 outbreak has temporarily reduced the GHG emissions by almost 17% (Le Quéré *et al.*, 2020) in the world, which is unlikely to be a sustainable trend in the foreseeable future.

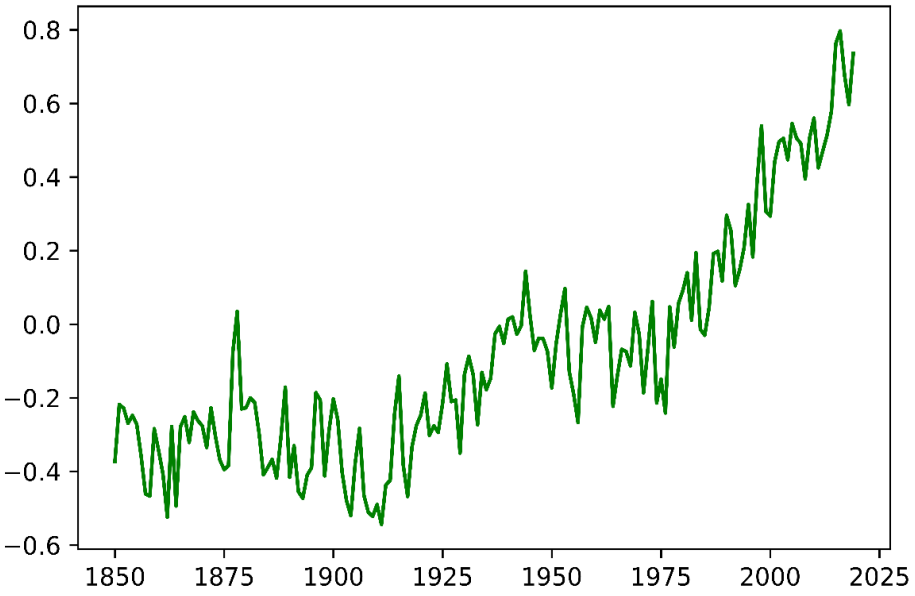

Figure 1.1 Global average temperature anomaly (Adapted from Hannah Ritchie and Max Roser (2017))

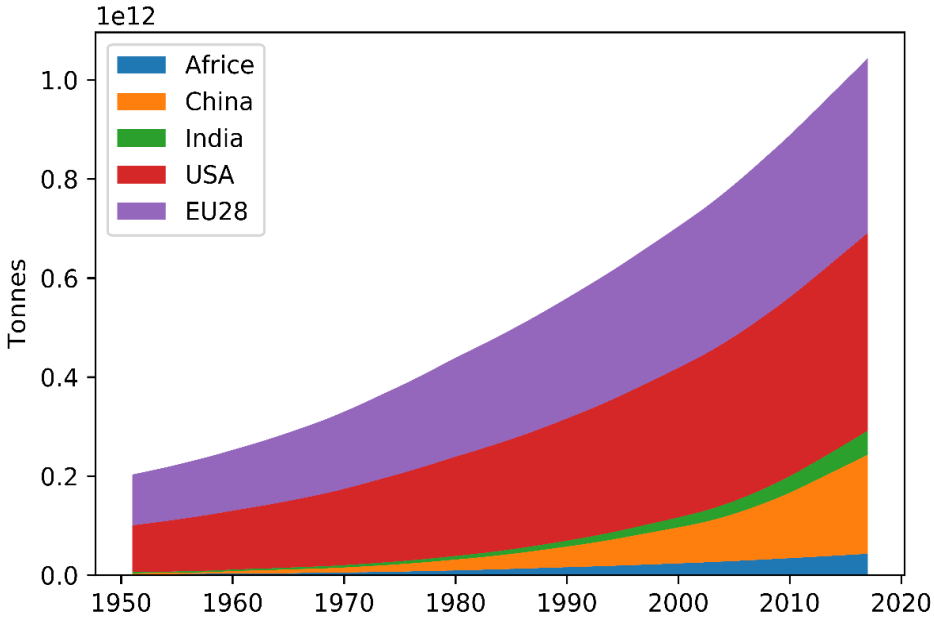

Figure 1.2 Cumulative CO_2 emissions by region in the last 70 years (Adapted from Hannah Ritchie and Max Roser, 2017)

Around the world, there is a unanimous agreement that a neglect on a rapid response to the alarming statistics on GHG emissions is likely to produce an irreversible effect on the planet even if the GHG emissions by human beings stop at some point in the near future. The main challenge with these gases is the fact that they remain in the atmosphere for a very long time causing serious complications for the human being, plants and animals. The anthropogenic share of the GHG emissions is mainly due to burning of fossil fuels for industrial use and because of industrialisation and population growth in the last century. These include emissions generated from the transportation sector, industry and electricity production.

Undoubtedly, one main concern with regards to greenhouse gas emissions is the climate change, which endangers the majority of people on the planet with socio-economically disadvantaged communities at the highest risk. The cost of climate change is estimated to reach almost $8 trillion by the mid-century leading to increased poverty, drought, flood and crop failure (Galey, 2019). These effects will hit some of the poor and less resilient economies in the world the most which are home to a large number of the bottom-of-the-pyramid population. However, some strong economies such as Canada, India, Germany and Japan are also sensitive to the climate change. The unpromising future of the world in absence of efficient and effective actions to curb the detrimental effects of climate change motivated countries in the world to unite and commit to take systematic actions as set out in Goal 13 among the 17 sustainable development goals. Sustainable development goals (SDG) are a set of 17 inter-connected goals identified by the United Nations and adopted by all the member states to tackle global challenges on peace, justice, inequality, poverty and environment. The Goal 13 (climate action) deals with taking urgent actions to combat climate change and its negative impacts on environment and human lives. In line with the Paris agreement, one fundamental target in SDG 13 is to keep the temperature rise well below 2 degrees and closer to 1.5 degrees. Reaching the global target of keeping the temperature increase to below 1.5 °C requires rapid, efficient and collective efforts from all the nations in the world and all sectors of industry.

The UK government has launched a set of initiatives to remove 40,000 tonnes of CO_2 from the earth's atmosphere every year (Department for Business, Energy, 2019). The same trend is found in other parts of the world such as the Boundary Dam project (Canada), Kemper County (USA), Gorgon Injection Project (Australia), Abu Dhabi

CCS project (United Arab Emirates) and Sleipner (Norway) to name a few. The combined capacity of carbon capture in the world is estimated to be close to 100 million tonnes of CO_2 per year (The Global CCS Institute, 2019).

Carbon capture and storage (CCS), as one of the mainstream technologies to reduce emissions, has a huge potential to capture CO_2 generated from electricity generation and other industrial applications. CCS involves three main stages, namely capturing carbon dioxide using an efficient and cost-effective method, transporting carbon dioxide and storing it safely for reuse in power and industrial sectors. Currently, there are several operational projects at various stages of development for demonstrating carbon capture process. Although the recent pandemic has slowed down the progress of these projects, the world is set to reach the pre-defined goals. In the UK, the Government's guidance on UK carbon capture, usage and storage sets out plans for the UK to be a global leader in CCUS technology by 2030 (BEISC, 2019). The government's plan, named as 'net zero' policy, is to cut GHG emissions to almost zero by 2050 (Roger Harrabin, 2019), which is projected to cost £1 trillion by 2050. This can be translated to an annual removal of between 75 and 175 million tonnes of carbon dioxide equivalent in 2050 (Office for National Statistics, 2019).

1.2. Motivation

Numerous carbon capture technologies have been developed and deployed in the last decade such as variants of adsorption, chemical absorption, membrane technology and cryogenic separation as well as biological CO_2 capture technologies including forestation oceanic fertilisation and microalgae-based carbon capture and utilisation (Singh and Dhar, 2019). However, the energy requirements of the currently available technologies for carbon capture and sequestration remain high, which is regarded as one of the most significant CCS barriers in the short term (Budinis *et al.*, 2018). To address this issue, capturing materials as a type of CCS separation technologies offers enormous potentials in terms of CO_2 uptake, CO_2 selectivity, and stability, which can minimise the regeneration energy consumption compared to other conventional capturing technologies (Abd *et al.*, 2020). Additionally, continued research is also needed to develop techno-economic devices from laboratory scale to commercial scale.

Accordingly, targets for physical solid adsorbents have been led to a renewed interest in designing a cost-effective and highly performing adsorbent in this area. Thus, the research aims at developing a new class of adsorbents for CO_2 capture with a green route with shorter reaction time, less complex procedure and yield enhancement.

This study is focused on porous boron nitride adsorbents, which are quite similar to the carbonaceous materials lattice structure. However, the presence of a polarity-bond in BN provides higher affinity to interact with CO_2 molecules in contrast to carbonaceous materials. Despite several published works on developing porous boron nitride for gas adsorption property, there is a sheer need to study the formation of porous boron nitride and the parameters controlling its porosity and chemistry. In this study, our main motivation is evaluation of an optimum synthetic condition along with strategies to modify and improve porous BN adsorbents properties.

1.3. Research aim and objectives

The aim of this research is to accelerate the development of a new low-cost porous boron nitride nanomaterial for CO_2 capture to achieve a high capacity at ambient temperatures as well as at realistic flue gas temperatures (above 298K or higher).

To achieve the ultimate goal of the project, the following objectives are suggested:

Objective 1: To produce pristine porous BN materials with high purity

This objective is to evaluate the effects of different synthetic conditions including precursors, their molar ratio and solvents during production of pristine BN. These parameters are key factors to optimise the chemical and physical features of pure BN and to improve its adsorption properties. This objective provides a better understanding of the relationship between precursors chemistry and the final production of BN materials properties.

Objective 2: To investigate the effect of non-metal modification strategy of pristine BN on CO_2 adsorption

This objective is to tune BN textural properties by using a surfactant template method. With this method, the key impact of surface area, pore size and volume on the adsorptive properties of BN can be examined.

Objective 3: To investigate the effect of metal-modification strategy of pristine BN on CO_2 adsorption

The surface modification of BN is crucial, due to acid-base interaction between BN and CO_2 acidic molecules. This can be applied by creating basic groups to overcome the weak interaction of CO_2 molecules with BN. This approach will potentially lead to modification of the surface chemistry of porous boron nitride by loading Ni transition metal on the BN surface and subsequently enhancing the adsorption property of carbon dioxide.

1.4. Contributions to knowledge

This work has several worthwhile contributions to the knowledge in terms of material synthetic conditions, modification strategies in order to improve sample's porosity and surface active-sites, characterisation and analysis of results.

Firstly, this work has studied the production of pristine porous boron nitride *via* the template-free method, where the optimal yield has been obtained with a well-defined structure and purity on each BN sample. The effect of nitrogen, boron and solvent precursors have been investigated on BN final production. Very little is currently known about the importance of BN precursors effect in the field of carbon capture. Therefore, our findings make a significant contribution to build porous BN adsorbents in wet chemistry laboratories.

Secondly, this research has performed a non-metal modification strategy by adding extra precursor (structure directing-agent surfactant) to identify the impact of BN pore size on CO_2 adsorption/desorption kinetics. Understanding the direct correlation between porosity and gas diffusion helps design a novel procedure to affect BN pore geometry. To date, only a few studies have investigated the key role of textural properties on enhancing the physical adsorption of CO_2 in other systematic ways. As far as we are concerned, no published research exists similar to our method to examine the adsorption capacity of BN.

Thirdly, a novel strategy for preparation of BN dopped with various nickel (Ni) amounts has been adopted to explore other crucial factors (e.g. polarizability/active sites) explaining the attractive CO_2 sorption properties of BN. Up to now, very little attention

has been paid to the role of basic groups on BN surface, which could result in an enhanced interaction between BN and acidic CO_2 molecules. Our study is the first to address the weak interaction of carbon dioxide and pristine BN by loading Ni *via* simple impregnation and calcination. Furthermore, our study sets out to consider the usefulness of BN-Ni samples at temperatures above 298 K for industrial applications.

In addition, further controlled studies which compared differences in using polar solvents during the fabrication process of BN-Ni samples have been investigated.

Finally, the reusability of pristine BN has been carried out in a laboratory scale through eight cyclic tests above the room temperature. We would like to highlight the fact that our study is the first attempt to conduct cyclic tests on the selected pristine BN samples.

1.5. Structure of the dissertation

A brief description of the chapters in the dissertation is given as follows.

Chapter 2: Literature review

The literature review chapter begins with establishing the context, background and an overview of the importance of carbon capture and storage (CCS) for meeting the climate change targets. This chapter looks at how CCS pathways can be directed into a more cost-effective and applicable deployment. It will then cover different CO_2 separation and capture method(s), explaining the value of studying dry adsorption in forthcoming technologies. After giving a brief review of the relevant academic literature, the applicability and value of using porous boron nitride as an adsorbent for carbon capture has been explained. Given the aim of the research, a synopsis of the current experimental methodologies, research design and modification of porous boron nitride have been reviewed. Furthermore, in this section, some of the fundamental challenges of CCS by solid adsorbents are discussed, the key research questions are provided, and existing knowledge gaps are identified.

Chapter 3: Methods and characterisation

In this chapter, detailed experimental studies have been performed on porous BN using the bottom-up synthetic approach. Various characterisation and process techniques have been carried out to investigate the materials' properties and CO_2 adsorption performance.

Chapter 4: Precursor-mediated synthesis of porous boron nitride

Pristine porous BN samples have been synthesised through the template-free method. The main objective of this chapter is to obtain the optimal yield of porous BN by evaluating different precursors during the hydro or solvo thermal evaporation steps. Various analytical techniques have been applied to characterise the structure, morphology, and chemistry yields of BN samples. The effect of precursor variables and their interactions into BN frameworks have been discussed. Optimum synthetic conditions have been confirmed experimentally, which result in porous BN samples with high purity and porosity levels.

Chapter 5: Metal-free modification of porous boron nitride

An initial objective of the modification strategy has been reached in this chapter on the question of whether metal-free modification of BN enhances CO_2 capturing capacity. A facial synthesis modification procedure has been applied to tune pristine BN pore size/geometry using structural directing-agent surfactant (Pluronic P123 triblock copolymers). The influence of using surfactant has been analysed and compared with pristine BN sample by characterising their chemistry, structure, thermal stability and textural properties.

Chapter 6: Metal modification of porous boron nitride

The second objective of the modification plan of this study has been achieved in this chapter by considering the impact of Ni loading in both porosity and surface chemistry of BN. A simple impregnation-calcination step has been applied with different levels of

Ni compound into the boron and nitrogen precursors. The surface metal modification results have been discussed using materials characterisation techniques.

Chapter 7. Evaluation of porous boron nitride for carbon dioxide capture

The main aim of this research has been achieved in this chapter, where the applicability and efficiency of using porous BN (either pure or modified samples) to capture pure CO_2 have been investigated. Experimental dynamic adsorption process has been assessed at low CO_2 partial pressures across a range of favourable adsorption temperatures. The role of surface functionality outcome on porous BN affinity to interact with CO_2 molecules has been argued and compared to pure BN samples' value results. Finally, the reusability of pristine BN samples has been examined based on cyclic temperature swing adsorption/desorption process.

Chapter 8: Conclusions and recommendations for future work

The overall conclusions for this research with sections on the significant finding and recommendations for future work have been provided in this chapter.

CHAPTER 2

LITERATURE REVIEW

Outline of the chapter

This chapter presents a detailed review on carbon capture methods and applications based on solid sorbent materials. It focuses on experimental synthesis and modification of porous boron nitride adsorbent where different synthetic and modification methods have been addressed. The chapter is organised as follows:

2.1. Introduction

2.2. Global greenhouse gas (GHG) emission

2.3. The value of carbon capture and storage (CCS)

2.4. CCS development and applications

2.5. CO_2 combustion and capture processes

2.6. Sorbents regeneration processes

2.7. Adsorbents for CO_2 capture

2.8. Boron nitride nanomaterials

2.9. Experimental investigation of porous boron nitride

2.10. Chemical modification of boron nitride

2.11. Application of porous BN in CO_2 capture

2.12. Conclusions and knowledge gaps from the literature

2. Literature review

2.1. Introduction

The specific objective of this dissertation is to improve the performance of porous boron nitride materials to capture carbon dioxide and to use these adsorbents for tackling climate change. This literature review firstly provides an introduction into the significance of carbon capture and storage (CCS) to tackle climate change (section 2.2 and 2.3). It then offers an overview of various technologies to capture CO_2 and how these technologies could be enhanced in terms of cost, efficiency and regenerability (section 2.4–2.6). Subsequently, the literature review presents adsorption processes, focusing on the research on dry-sorbent materials in section 2.7, and then sheds light on the literature of using BN as a solid sorbent. Section 2.8 highlights the structure and chemistry on BN while section 2.9 addresses various methods for BN synthesis with a focus on those, which bring about porous structure by template and non-template methods. The review then covers those studies on surface modification of BN for different purposes in section 2.10. It comprises of two key themes, namely: (a) non-metal modification and (b) metal modification. Section 2.11 deals with the studies published in the last decade on using BN for carbon capture. It is hoped that this review summarises the most relevant studies to ours as well as find the current gaps in the literature of which this dissertation is an attempt to fill some.

2.2. Global greenhouse gas (GHG) emission

Greenhouse gas (GHG) emission has brought about significant challenges to governments around the world. These challenges include but not limited to the rise of sea levels and devastating social effects. GHGs include various gasses among which carbon dioxide (CO_2) is the most commonly emitted gas by human activities. As Figure 2.1 depicts, CO_2 has been the most important component of GHGs in the last three decades. This, in turn, has led to detrimental environmental effects including global warming and endangered species and strong policies are needed to reduce these detrimental effects on the environment. According to Global Carbon Capture & Storage Institute (2018), the world economies remain heavily dependent on fossil fuels, which are the source of 85% of the world's energy. It is worth noting that nearly

a quarter of all CO_2 emmisions come from industries such as coal, cement, steel and chemical production (IEA/UNIDO, 2011). As shown in Figure 2.2, the demand trend for fossil fuels has been doubled between 2000 and 2016. This significant increase calls for an amplified effort in decarbonisation industries and power sector. While fuel switching such as using natural gas rather than fossil fuels and adopting renewable energies can reduce CO_2 accumulation, accelerating in decarbonisation is extremely challenging without use of carbon capture and storage (CCS) technologies.

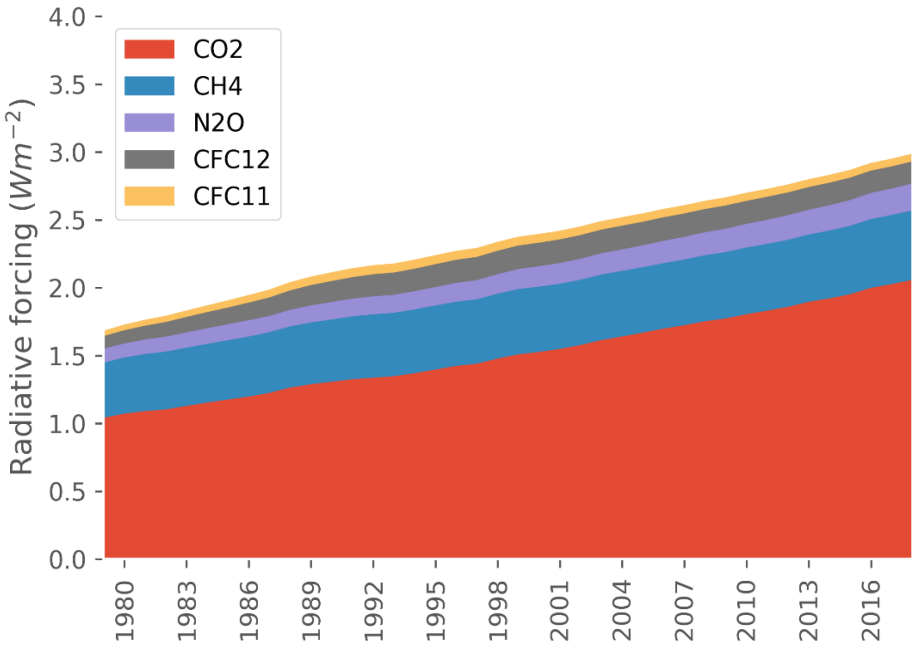

Figure 2.1 The inter-annual variation in radiative forcing by greenhouse gases (Adapted from Butler and Montzka, 2013)

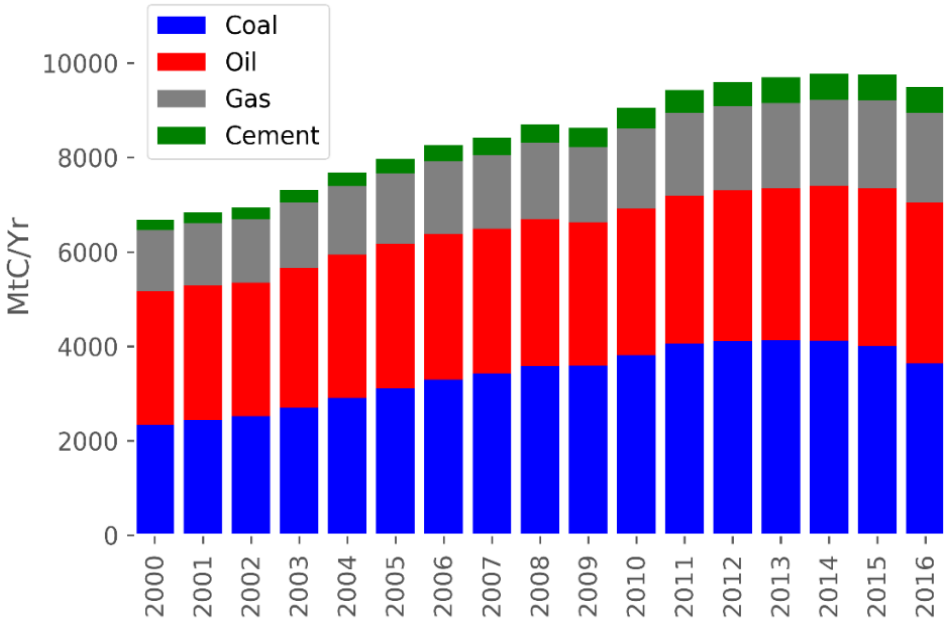

Figure 2.2 Annual global fossil fuel carbon emissions (Adapted from Global Carbon Project, 2017)

2.3. The value of carbon capture and storage (CCS)

Numerous studies such as the Inter-governmental Panel on Climate Change (IPCC), the International Energy Agency (IEA) among others have emphasised the essential role of carbon capture and storage (CCS) technologies to achieve net zero emissions target (Rogelj *et al.*, 2018; Transform. Ind. through CCUS, 2019). For instance, the benefits of CCS in achieving the UK's net-zero target is provided by Committee on Climate Change's (CCC) in May 2019 (Committee on Climate Change, 2019). According to this report, CCS is considered in all the mitigation options advised by CCC to the UK government. Moreover, it also supports delivering the negative emission technologies as well as cut emissions in heavy industries by producing low-carbon hydrogen.

Additionally, CCS is one of the most crucial and cost-effective pathways to accomplish deep decarbonisation in industry and power sectors (GCCSI, 2020). As the demand for industry production and electricity is increased by population growth, the utility of CCS in decarbonising the industry and power sectors has been accelerating globally. Importantly, technologies based on carbon dioxide removal (CDR) and bioenergy with

CCS (BECCS) will be needed to be developed for future negative emissions and is widely recognised as vital in the journey to net zero by 2050. While there are challenges such as process cost and scaling-up the innovative technology, deploying negative emission technologies is of utmost importance to meet long-term climate targets. Hence, transition to low-carbon economy is ongoing with the progress of novel technology to contribute to reduction of primary barriers for development of CCS.

2.4. CCS development and applications

As we discussed in the previous sections, reduction of greenhouse gas emissions is fundamental to meet the net zero target by the mid-century. We will now move on to explain applications of CCS in different sectors ranging from the chemical industry to power generation. CCS is an indispensable part of a variety of technologies and processes and its replacement not only leads to doubling the cost, but also reduces the risks associated with meeting climate targets (GCCSI, 2020). As noted by the United States Environmental Protection Agency, CO_2 emissions from sectors such as electricity and heat production have the largest source of emissions in total (Figure 2.3). Process emissions from chemical industry production such as cement, steel, aluminium and ammonia contribute to almost one-quarter of industrial emissions; however, it cannot be avoided by using alternative fuels (*Transform. Ind. through CCUS*, 2019). Thus, decarbonisation of these sectors will be taken into account to address the climate change challenges. Among portfolio technologies, CCS is considered as the most effective contributor to the industry subsectors regardless of the fact that challenges will remain for the industrial sector. Another major contribution of CCS application has been found in low-carbon hydrogen production for almost two decades. The technologies used so far for low-carbon hydrogen production with CCS comprise gas reforming, coal gasification and electrolysis (Joffe *et al.*, 2018).

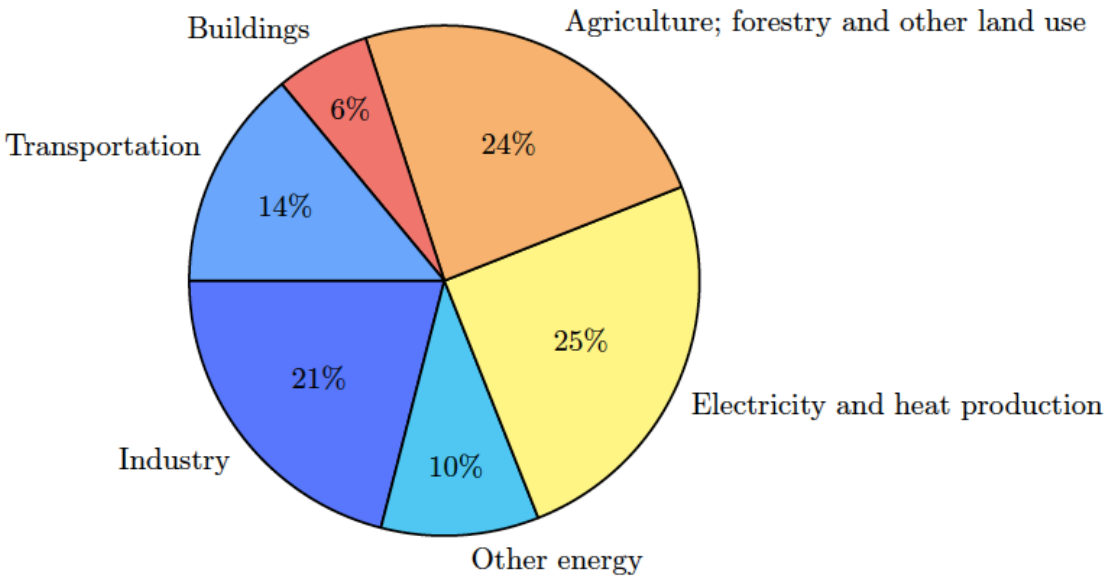

Figure 2.3 CO_2 emissions by sectors (Adapted from United States Environmental Protection Agency, accessed: 7 October 2020)

Overall, the process of using CCS in industry has been materialised in commercial scale; however, for some industries like iron, steel and cement production, there is still a need for successful deployment. In the power sector, the extra cost of the capturing process is the main setback for large-scale implementation. Globally, the demand for CCS with low cost services has increased and so, there is a sheer demand for new technologies for this purpose.

2.5. CO_2 combustion and capture processes

As previously stated, a large amount of CO_2 is emitted during the combustion of natural gas, thereby various strategies to capture CO_2 through mix gases have been applied in industry. After CO_2 sequestration from the mix gases, carbon dioxide is compressed into liquid in order to be transported through pipelines for geological storage (Coutris *et al.*, 2015). To date, the capture technologies that have been demonstrated at pilot plant scale or higher scales are classified as (i) pre-combustion, (ii) post-combustion and (iii) oxy-fuel combustion (Lee and Park, 2015). Figure 2.4. depicts the combustion processes in power generation.

The pre-combustion approach is integrated with gasification step to produce syngas. As Figure 2.4 shows, the first step is the reaction between fuel and oxygen gas, which

occurs at a high temperature, and pressure. The syngas produced at this stage is conducted through a water-gas shift reaction to produce H_2 and then shifted to the combustion process to produce power and heat in power plants (Broom and Thomas, 2013). The separation approach for pre-combustion mainly involves H_2/CO_2 separation based on physical absorption of CO_2 followed by releasing the CO_2 after pressure drops (Romano *et al.*, 2010). However, physical adsorption using amine modification system is also feasible (Su *et al.*, 2009). One limitation of the pre-combustion technology is that the energy is not preserved efficiently during CO_2 capturing process and there is a need for an in-depth supporting system.

In the post-combustion carbon capture approach, first the fossil fuels or biomass is fed into a combustion process, then the flue gas which contains CO_2 and N_2 is conducted to the separation process (In *et al.*, 2005). Therefore, the capture process involves the separation of CO_2 from N_2 flue gas in a presence of water vapour. This technology is applicable in a majority of existing coal-fired power plants as well as natural gas fired boilers. In spite of this benefit of post-combustion capture, some barriers such as low CO_2 partial pressure and advanced process requirement to achieve high capture volume exist that hinder the implementation of the separation process.

The oxyfuel combustion is another recently developed CCS technology. Therein, pure oxygen is used in the combustion process, which requires an air separation unit to generate pure oxygen for combustion. Therefore, oxyfuel combustion has exorbitant costs as opposed to other approaches. It is imperative to take into account that oxy combustion is valuable due to high concentration of CO_2 in flue gas, which can be reasonably purified. Currently, the oxyfuel combustion is carried out on coal-fired power plants and is planned for large-scale demonstration projects (Rubin *et al.*, 2012).

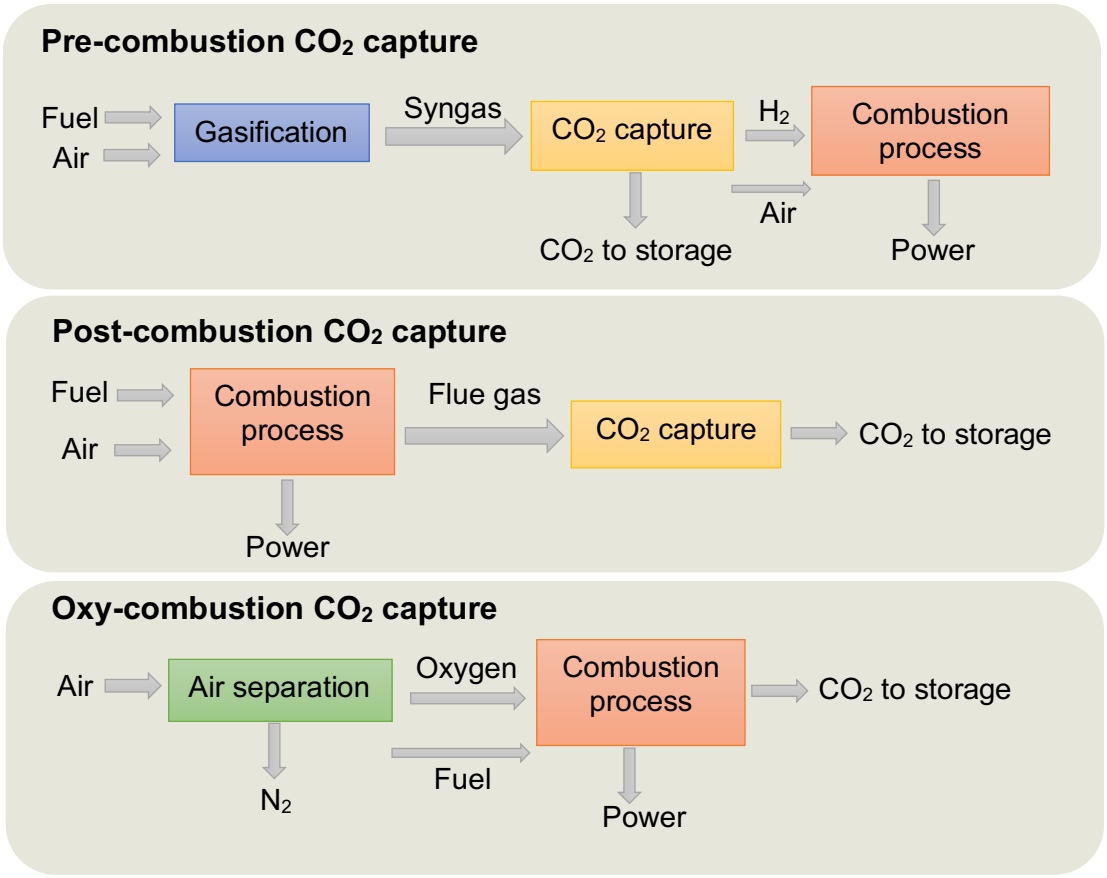

Figure 2.4 Diagrams demonstrating post-combustion, pre-combustion and oxy-combustion system (Adapted from Figueroa *et al.*, 2008)

The trend of innovative advances of CO_2 capture and separation methods among post, pre and oxy combustion processes is shown in Figure 2.5. What stands out in this figure is the growth of cost reduction benefits of advanced technologies once they approach commercialization. This means that by the next generation, there will be significant improvements in efficiency and cost over highly novel technologies.

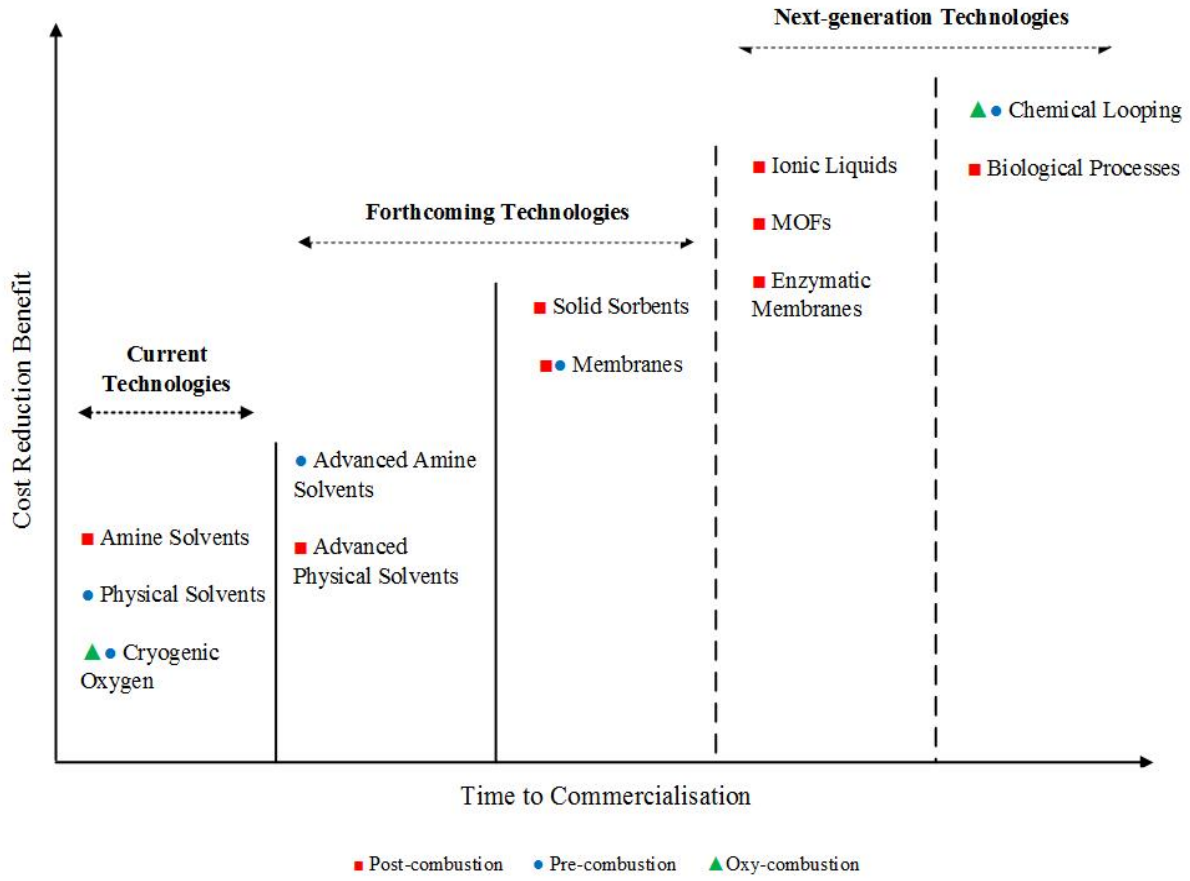

Figure 2.5 Disruptive CO_2 capture technologies. (Adapted from Figueroa *et al.*, 2008)

Among the current available technologies, CO_2 capture from post-combustion emission gases is the most commonly used technology in power plants and other industries. Post-combustion carbon capture is a prime candidate to be retrofitted in the power sector in order to reduce GHG emissions. The classification of technologies for post-combustion capture of CO_2 is shown in Figure 2.6.

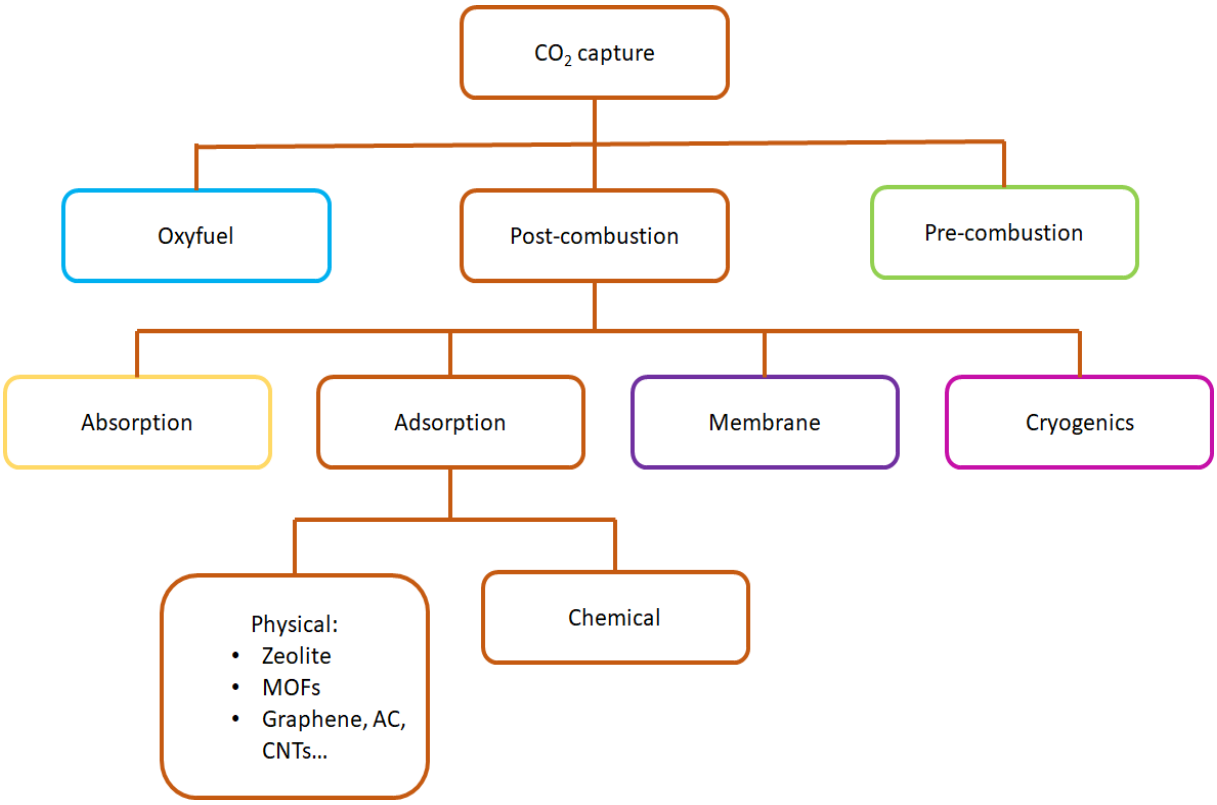

Figure 2.6 Methods of CO_2 separation and capture (Adapted from Younas *et al.*, 2016)

Generally, the choice of methods is mainly dependent on the condition in which the flue gas is conducted including level of impurities, the temperature, the CO_2 pressure and concentration (Rubin *et al.*, 2012).The physical absorption process involves a reaction between amine-based solvent and CO_2 with a low partial pressure. Thus, amine-based solvents can capture CO_2 from flue gas and the solvent is recovered to absorber. Traditionally, absorption technology is considered as the most mature option for CO_2 separation while it suffers from negative environmental footprint and its complex regeneration process, which is also costly. Membranes are another adsorptive porous metallic, polymeric and ceramic material that can be used to capture and separate CO_2 from a gas steam. In this process, membrane acts as a filter from which the flue gas passes through the material and is absorbed. Given that the selectivity of CO_2 is a noteworthy issue, membrane pore walls could enhance selective diffusion of CO_2 over other gases such as N_2, O_2 and SO_2. Although in the currently used technologies, membrane is used for gas purification in the production of hydrogen, it is more applicable for high pressure processes in pre-combustion plant (Lock *et al.*, 2015).

Cryogenic gas separation is one of the commonly used technologies in natural gas value chain with high concentration of carbon dioxide yield and selectivity (Idem *et al.*, 2006). In this separation, CO_2 is recovered with high purity under particularly low temperature and high pressure. The obtained liquid phase of CO_2, which is obtained through refrigeration and separation process, can be transported easily. A major drawback of this approach is the high consumption of refrigeration energy (Leung *et al.*, 2014).

Unlike absorption processes which use a liquid solvent to separate CO_2 from flue gas, solid sorbent could also capture and separate CO_2 on its surface as shown in Figure 2.7. The process based on adsorption is reversible and sorbents that are commercially used are porous solids and can be recycled. The regeneration cost of adsorption is relatively lower than conventional solvent-based adsorption given that there is no need for large quantities of water to regenerate solvent solution (Webley and Danaci, 2020).

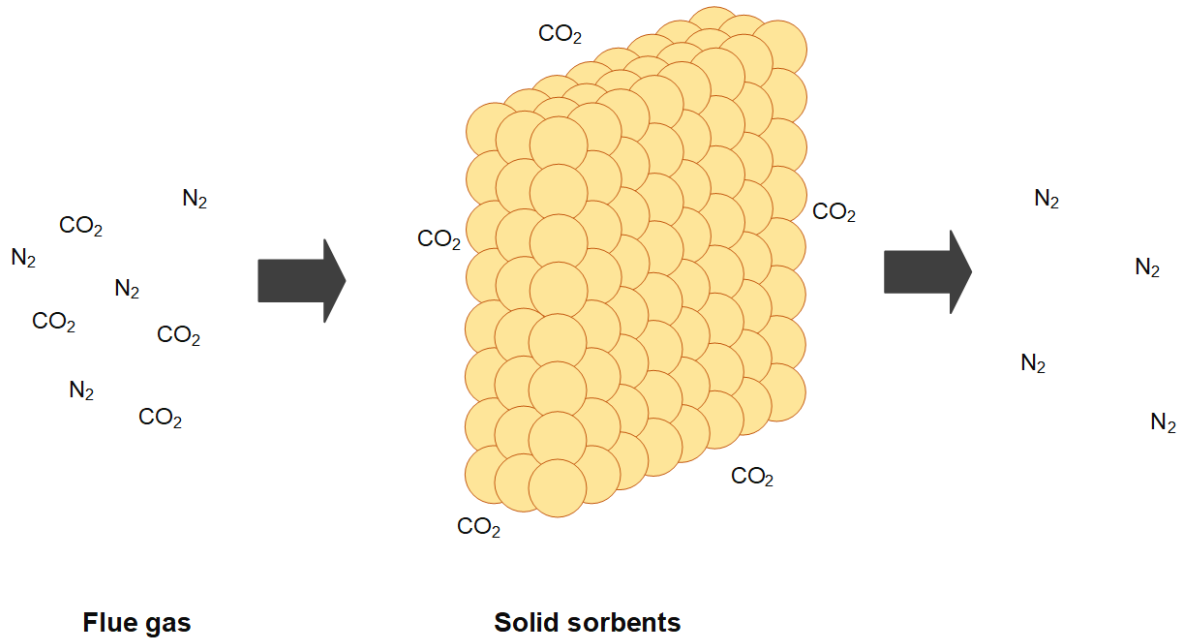

Figure 2.7 Illustration of CO_2 adsorption and separation on the surfaces of a solid sorbent (Adapted from Rubin *et al.*, 2012)

As indicated previously, the traditional technology is based on absorption in aqueous organic amines; however, the intensive energy consumption, equipment corrosion and toxicity, make exploration of new materials for CO_2 capture highly demanding (Li et

al., 2013; Lee and Park, 2015). Hence, the challenge of selecting the porous solid is to design durable sorbents for CO_2 capture with the aim of achieving high purity, recovery, productivity and low energy consumption.

2.6. Sorbents regeneration processes

Adsorption regeneration step by nanoporous materials is divided into classical techniques such as temperature swing adsorption (TSA) and pressure swing (PSA) or vacuum swing adsorption (VSA). The decision of how to select cyclic adsorption processes depends on specific separation. In the TSA process, due to the fact that the reaction is exothermic, the adsorbent is regenerated by increasing its temperature, while in the PSA process, the regeneration occurs by reducing the pressure. (Broom and Thomas, 2013).

For instance, Belmabkhout *et al.*, (2009) measured the CO_2 adsorption on MCM-41-100 at high pressures up to 25 bar, using high PSA operating dry adsorption. The author concludes that their optimal material shows a high volumetric uptake and selectivity over N_2, H_2 and CH_4 at high pressure and dry conditions. Another example of PSA cyclic separation of CO_2 is reported by Delgado *et al.* (2007) which measured the separation of carbon dioxide/methane on basic resin. The result of their study indicates gradual increase of adsorption capacity with the number of cycles which plateaus at a constant value after 16 cycles. Moreover, they evaluated a Linear Driving Force (LDF) model to explain the breakthrough PSA curves.

In order to apply the CO_2 regeneration technology for large-scale applications with high purity and recovery, thermal swing sorption is a favourable process. In contrast to PSA, working capacities and selectivity are large in the adsorption process by TSA (Webley and Danaci, 2020). The TSA performance is based on heating and cooling during the constituent adsorption/desorption cycle time. Therefore, temperature and sorbents sensibility to heat are the critical parameters which need to be optimised for the regeneration heat process (Dijkstra *et al.*, 2018). In addition, a modelling work needs to be validated for the small-scale pilot separation processes. To this end, the relevant infrastructures needed for this development which are associated into the physical characterisation, amount of gas adsorption isotherms and sorption kinetics of solid adsorbents should be taken into account.

2.7. Adsorbents for CO_2 capture

Solid adsorption is an alternative process to solvent-based chemisorption which was first considered in the early 1990's for carbon capture (Kikkinides et al., 1993; Ishibashi et al., 1996). Novel CO_2 capture adsorbents (zeolites, carbonaceous materials, metal organic frameworks, functionalised adsorbent) followed solid adsorption in the following years. Solid sorbents can be applied for a wide range of temperature and pressure conditions for both post-combustion and pre-combustion applications. Another strength of adsorption is being economically favourable due to the low cost and easy regeneration of absorbents. Moreover, using waste material as an adsorbent causes minimal environmental footprint as opposed to using solvent compounds (Bui *et al.*, 2018). One of the challenges in this area relates to the manufacturing of new adsorbents that enables the researcher to enhance good diffusion kinetics and providing improved performance. Regarding dry sorbent materials, there have been several properties such as selectivity, CO_2 working capacity, cycling stability, energy consumption and tolerance against water, which need to be determined for CO_2 capture. Moreover, a systematic understanding of how these materials contribute to CCS processing in actual conditions should be investigated.

In the remainder of this section, the most common CO_2 adsorbents and their main attributes, strengths and weaknesses in the context of CO_2 capture have been summarised. The research advantages of using porous boron nitride as a new adsorbent for carbon capture has also been discussed.

2.7.1. Carbonaceous material

Inorganic porous carbons such as graphene, activated carbon and carbon nanotubes (CNTs) are common options for CO_2 adsorption. They are low cost materials with high chemical stability, surface area, and easy structure modification. These materials are extensively considered in CO_2 physisorption studies (Younas *et al.*, 2016).

It is now well-established from a variety of studies that these materials have potential for green and sustainable synthesis due to being derived from biomass and renewable sources (Sevilla and Fuertes, 2011b; Primo *et al.*, 2012; Wei *et al.*, 2012). Despite all advantages of using these materials for CO_2 adsorption, the CO_2-uptake value is favoured at high partial pressures of adsorbate. Hence, CO_2 capacity in carbon-based

materials shows poor sorption and selectivity over mix gases. Previous research showed that a variety of modifications can be made to increase adsorption capacity on carbonaceous materials. For instance, KOH treatment, which is one of the best activating reagents can enhance CO_2 adsorption of carbonaceous materials and increase the number of pores and surface area (Sevilla and Fuertes, 2011; Wei et al., 2012; Ello et al., 2013). Furthermore, pure carbon materials are less polar and thereby, exhibit a weak affinity to CO_2. To overcome this barrier, various studies confirmed that the N-doped porous carbons may provide the polar sites as well as negatively charge the carbon frameworks (Zhang *et al.*, 2015b; Singh *et al.*, 2017).

2.7.2. Metal-organic frameworks (MOFs)

MOFs are crystalline materials consisting of metal ions linked by organic ligands. The uniform micropores size and extra framework cations of these materials are key factors for using MOFs in CO_2 capture (Zhang, 2013). The incorporation of MOFs by functional group as well as doping metals in the framework modifies the adsorption properties by changing the surface chemistry (Wu et al., 2012; Yazaydın et al., 2009). Kinik *et al.* (2016) and Sezginel et al. (2016) tried to enhance separation performance of MOF through direct interaction between ionic liquid (ILs) and MOF. Their results suggest that IL-MOF interactions strongly affect the gas affinity of materials at low pressures while available pore volume plays a key role for gas adsorption at high pressures (Cota and Martinez, 2017). In addition, the usage of MOFs is often limited because of their poor chemical stability as they can react with flue gas components like water, NO_X and SO_X (Duan *et al.*, 2017).

2.7.3. Zeolite-base adsorbent

Zeolites can be described as microporous crystalline aluminosilicate minerals with identical pores structure, which have been used as commercial adsorbents and catalysts. The presence of narrow pore size and polarity makes zeolite an efficient shape-selective material for separation applications (Yang et al., 2008). Previous research concluded that efficiency of CO_2 adsorption by zeolite depends on the structure, size, purity, cationic form and molecular polarity (Samanta *et al.*, 2011; Zukal *et al.*, 2017). Importantly, the CO_2 adsorption capacity on zeolite is increased with gas

phase pressure and is decreased with the rise in adsorption temperature. Furthermore, due to the strong adsorption behaviour of zeolite for moisture, the CO_2 uptake is decreased in the presence of the moisture contents (Younas *et al.*, 2016). It is possible, therefore, that zeolites show a weak CO_2 capture performance in the gas mixtures containing water. Another intrinsic limitation is that regeneration of zeolite and desorption of CO_2 is costly and requires considerable amounts of energy.

2.7.4. Advantages of using porous boron nitride (BN)

Recently, boron nitride (BN) materials are considered as a new class of sorbents for carbon capture applications. The primary reason to turn our attention to BN materials is its unique advantages compared to other materials. The key factors encouraging the CO_2 capture performance of BN can be attributed to its stability in a wide range of temperatures, high surface area/porosity and the ionic character of BN bond (Jiang *et al.*, 2015). Another interesting feature of these promising materials is their flexibility to structural/pore geometry change. This approach opens a new route to modify the surface chemistry of BN to achieve a better sorbent material for CO_2 diffusion in dynamic conditions.

In this case, there have been numerous crystalline forms obtained so far such as hexagonal nanosheet, nanotubes or porous turbostratic to name a few. More details of structural and chemistry properties of BN nanomaterials is provided in the following section. With regards to expanding BN-based CO_2 capture capability, other advanced research on surface modification and doping also considered the best ways to improve its CO_2 uptakes and selectivity.

Generally, the following sections describe the procedure and methods used in designing and modification of this material, highlighting its application in CO_2 capture.

2.8. Boron nitride nanomaterials

Boron nitride nanomaterials (BN) have been established as one of the most promising inorganic ceramic materials with different structures and properties. The chemical compound of BN, involving boron (B) and nitrogen (N) covalent bonds exists in various crystalline forms. The most common crystalline structure of BN is the hexagonal form

(h-BN), which is also called as a white graphene with a layer structure. The cubic form (c-BN) of BN, known as the second toughest material, is of less attraction among scholars compared to hexagonal form. There are also two scarce rhombohedral and wurtzite forms (Pakdel *et al.*, 2014a). Much of current literature on BN structure pays particular attention to the hexagonal forms. This lattice form can also be tailored into non-crystalline or disorder structure of turbostratic BN (t-BN) and amorphous BN (a-BN) materials. Mostly, BN materials with pores structure are referred to turbostartic and amorphous structures due to their low crystalline order and high impurities and defects. A recent systematic literature by Weng *et al.* (2016) concluded that porous BN structure has a better performance relative to other structural models in terms of adsorptive applications of BN. In addition, 2D dimensional layer of h-BN interact by weak van der Waals forces with interlayer spacing of 0.333 nm (Lin and Connell, 2012). As can be seen in Figure 2.8. the sheet of 2D BN can be rolled and shaped into 1D tube structure. After preliminary work of BN nanosheets in the form of nanomeshes (Corso *et al.*, 2004), other forms of nanosheets were extended to the nanoplate (Kostoglou *et al.*, 2016), flake like (Marchesini *et al.*, 2017b) and microsponges (Weng *et al.*, 2014) to name a few. The literature on one-dimensional (1D) BN nanomaterials is also highlighted in several morphologies such as nanowires (Chen *et al.*, 2006), nanofibers (Lin *et al.*, 2016), nanoribbons (Li *et al.*, 2013c) and nanorod (Zhang *et al.*, 2006). Collectively, some morphologies at different nanoscales which have been produced so far, are illustrated in Figure 2.9.

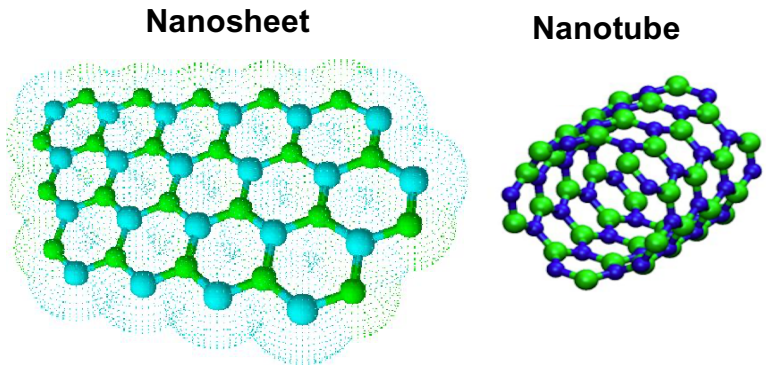

Figure 2.8 Structure of 2D BN nanosheet which wrapping to make 1D BN nanotube (Adapted from Golberg *et al.*, 2010)

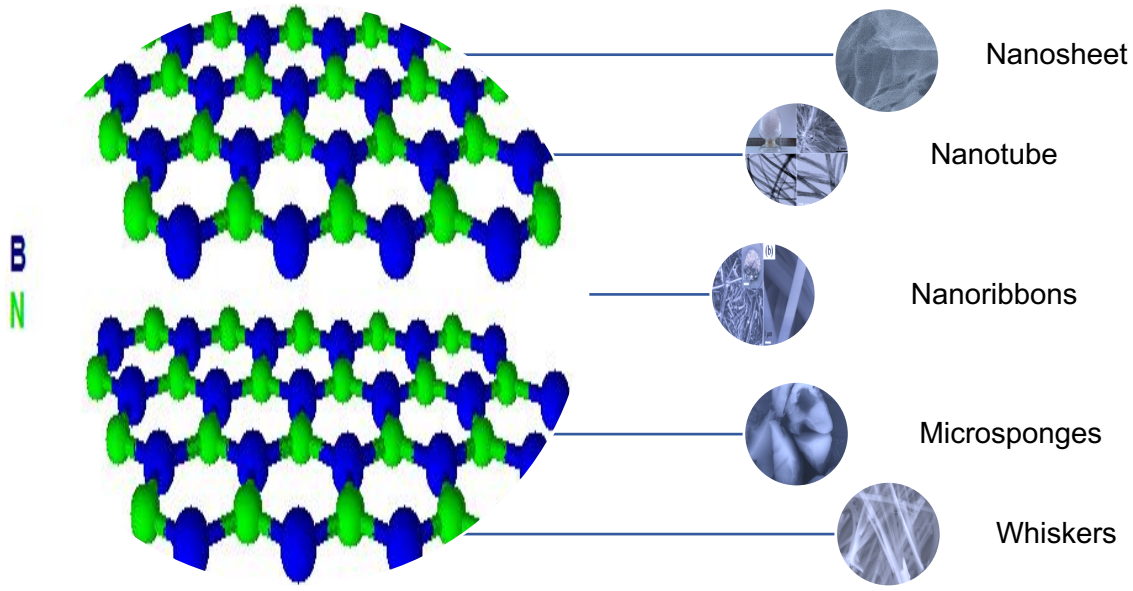

Figure 2.9 Microscopic structure images of diverse BN nanostructures reported so far (Adapted form Hojatisaeidi *et al.*, 2020; Lin *et al.*, 2016; Li *et al.*, 2013c; Weng *et al.*, 2014; from top to bottom).

As mentioned above, BN materials are quite similar to carbon-carbon network structures. While the C-C bond in graphite is covalent bond with no ionic characteristic, the covalent bond in B-N exhibits partially ionic character with 1.45 Å in length (Marom *et al.*, 2010). Thus, the distribution of electrons in B-N shift to the electronegative N atoms creating the electron-deficient B atoms and causes polar structure. There is a large volume of published studies describing the role of polarizability and ionic character of BN in the field of adsorption such as water treatment (Song et al., 2017), hydrogen storage (Li *et al.*, 2013b) and carbon capture (Janik et al., 1994). Furthermore, experimental studies on boron nitride nanostructure have shown superior mechanical properties and thermal conductivity of these materials (Boldrin et al., 2011, Andrew et al., 2012, Chen et al., 2004). Therefore, BN nanostructure are very useful in nanofiller composite materials, anti-oxidation lubricants and protective coatings in industry (Weng et al., 2016, Pakdel et al., 2012). Another feature of BN materials is their strong luminescence properties in the UV range which promotes its application in photoluminescence property (Gao *et al.*, 2009). In this write-up, among all these properties of BN material, we will mainly focus on the ionic character of B-N bond, high surface area and superior total pore volume and high thermal stability.

These are the fundamental properties, which are required and make the BN a promising candidate for carbon capture applications.

2.9. Experimental investigation of porous boron nitride

Following on from the discussions in the previous section, BN nanomaterials appear in a variety of structures and crystallography features. This variation provides a large set of applications in various sectors of industry. In the literature on adsorptive applications of BN, the relative importance of porous structure has been the subject of considerable discussion. Data from Scopus source has identified a considerable amount of literature published on porous boron nitride as depicted in Figure 2.10.

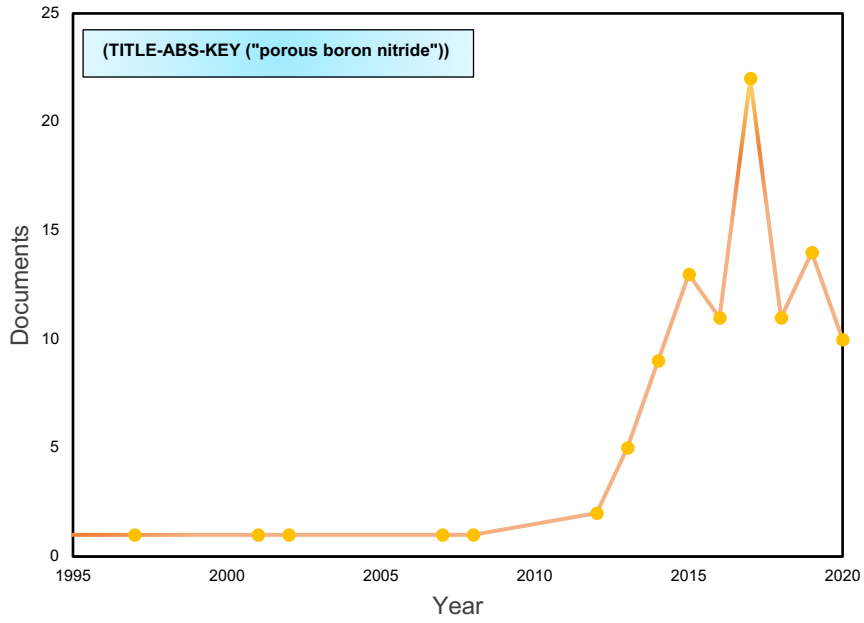

Figure 2.10 Scopus analyse search results with keyword: “porous boron nitride" [Accessed date: 20 June 2020]

What is striking about this graph is that the demand for synthesising porous BN has remarkably increased between 2010 and 2020. Consequently, much more information has become available on the chemical methods of porous BN in both theoretical and experimental domains. However, debate continues about the best strategy for management of the chemistry features of porous BN using in particular sorption properties. As in this work the pore size/shape of adsorbents properties is considered,

the following sections describe the most common synthetic approaches for preparation of porous BN that have been used by scholars. The studies presented thus far provide evidence that porous BN materials could be obtained from different morphologies (e.g. ribbon, whiskers, flake, etc.) to different structures (1D, 2D, 3D) towards their applications. The most similar chemical characteristic of synthesised porous BNs is their low crystallinity, which take a formation of turbostratic and amorphous structure. However, there are fundamental differences among these materials in terms of their micro-meso porosity networks. A great deal of previous research into synthesis methods have focused on producing materials with high surface area and a large number of pores. In this regard, researchers attempted to evaluate the impact of different process parameters on the growth of porous BN. Therefore, it is a major challenge to choose the best synthesis condition, which depends on the application area. For instance, in this research, we aim to design a highly performing porous BN for CO_2 capture and separation process. Thus, from a chemistry point of view, the best approach for this application is the one which offers a high pore volume with a dominant level of ultra-micropores. The themes identified in porous BN characteristics are presented in Figure 2.11.

Herein, the experimental work is presented which reviews the synthetic approaches leading to porous BN. Methods can be widely classified into those using template and those without during the synthesis. These methods have been recently challenged by multiple studies demonstrating the influence of process parameters on BN structural and chemistry growth. Raw materials and their molar ratio, temperature, carrier gas and post-treatment have emerged as the most obvious factors in the literature to date. Overall, a summary of the main findings, together with an overview of different fabrication processes is provided in this section.

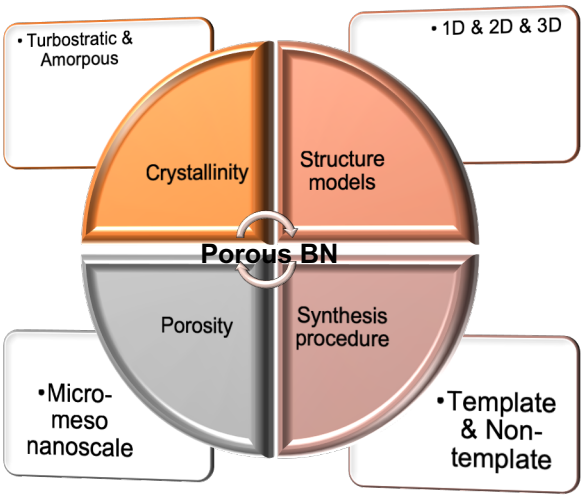

Figure 2.11 Themes identified in porous BN

2.9.1. Template synthesis porous BN

In a wet chemistry laboratory, the porous boron nitride can be obtained through chemical reaction of boron precursors and nitrogen precursors *via* heat-treatment step. In template direct synthesis, the porosity of BN tailors by using the presence of template (hard, soft and dynamic) during BN synthesis, which is then needed to be eliminated by the post treatment method. This section attempts to provide a brief summary of the literature relating to porous BN synthesis using hard and soft templates. It should be noted that in this section, only the most popular and well-known templates are discussed.

Hard templates:

As explained earlier, in order to yield porous BN, the controlled chemical reaction can be employed during the mixture of boron and nitrogen precursors, followed by heat-treatment. Commonly, most of the strategies for obtaining the porous structure of BN with specific morphology and high surface area involve utilizing hard templates. These hard templates typically include mesoporous silica, activated carbon, zeolites and graphene aerogels. The specific surface area (SSA) for these porous BNs are reported to be from 100 to 900 m^2g^{-1}. The initial growth of porous BN using the hard template method is highlighted by Han *et al.* (2004). In their work, the measurement of specific surface area was 167.8 m^2g^{-1} using activated carbon as a hard template. Afterward, in many studies, mesoporous carbon/silica were adopted as the hard template such

as SBA-15 silica and mesoporous carbon (CMK-3) (Dibandjo et al., 2005; Vinu et al., 2005). A key study comparing mesoporous silica and carbon is that of Dibandjo *et al.*, (2005) in which they investigated the impacts of SBA-15 and CMK-3 on mesoporous boron nitride. In an analysis of surface area, they found that mesoporous BN using mesoporous carbon molecular sieves shows a high surface area of 500 m^2g^{-1} and it has a uniform structure compared to the silica template. Moreover, ammonia and HF treament were used to remove carbon and silica templates respectively. In a follow-up study, Rushton and Mokaya, (2008) synthesied mesoporous BN using mesoporous silica through nitridation at 1150 °C under ammonia flow. The product exhibited a specific surface area of 327 m^2g^{-1} and a pore volume of 0.5 cm^3g^{-1}. A recent study by Maleki *et al.*, (2016) involved new polymeric templates for the synthesis three-dimentionally (3D) BN foam. They prepared BN composite using polymeric hard template, pyrolyzed at 1150°C under ammonia atmosphere to eliminate the template. The obtained porous BN revealed high oil uptake due to its high hydrophobicity. Aditionally, introducing carbon template (e.g. glucose spheres) into boron and nitrogen affects on morphology/shape of boron nitride nanoparticles (Han *et al.*, 2017). Han *et al.* (2017) demonstrated that spherical structure of BN is formed by glucose under combination of hydrothermal and heat treatment process. The textural properties of BN are improved by preparing micro-meso amorphous BN from zeolite (Schlienger *et al*., 2012). According to Schlienger *et a*l., (2012), high specific surface areas up to 570 m^2/g are achieved by impregnation of carbonaceous templates with polyborazylene (PB) *via* ceramisation temperature at 1200°C. Similarly, a broader perspective has been adopted by Salameh *et al.*, (2018) which controlled the crystallinity and textural properties by adjusting the temperature in a range of 1000 to 1450°C under nirtogen flow. Their study found that reducing temperature to 1000°C increased SSA BET surface area to 728 m^2g^{-1} with a 3D mesopores structure. Their finding presented robust monolit 3D boron nitride as a potetial for hydrogen storge.

Considering all the evidence above, it seems that the major drawback of using hard templates is the porosity achieved through this method, which is very low due to inefficient filling of precursors within template pores. Furthermore, it is difficult to eliminate templates and often leads to a failure of a part of the pore structure, affecting the performance of the product (Xie *et al.*, 2016).

Soft templates:

The soft template does not have a rigid structure. Common soft template method involves use of various structure redirecting agents (SRA) such as cetyl-trimethyl ammonium bromide (CTAB), polyvinyl chloride (PVC), cetyl-trimetyl ammonium chloride (CTAC), triblock copolymer poly (ethylene glycol)-*block*-poly(propylene glycol)-*block*-poly(ethylene glycol) (p123), etc. (Li *et al.*, 2013c; Xiong et al., 2017; H. Li et al., 2017). Some authors attempted to use dodecyl trimethyl ammonium chloride (DTAC) as a soft template for production of spherical hexagonal boron nitride at different nanoscales (Ning *et al.*, 2016; Zhang *et al.*, 2014). While Ning *et al.*, (2016) focuses on the microsructure and adsorption performance of h-BN by using different molar ratios of boron source, Zhang *et al.*, (2014) is more concerened with the effect of template content and nitriting temperature on the micro morphology of h-BN. The former author prepared h-BN with the use of borax and boric acid in different molar ratios and heated certain amount of urea and DTAC under amonia atmosphere. Zhang *et al.*, (2014), on the other hand, studied the same procedure with different amounts of soft template (DTAC). These experimental methods confirmed that the precursors content and temperature treatment may have some influence on the shape and size of BN production. Another soft template approach was reported by Xiong *et al.* (2015) with the use of 1-butyl-3 methylimidazolium tetrafluoroborate ([Bmim]BF4) *via* calcination under N_2 atmosphere. In their synthetic procedure ([Bmim]BF4) applied as a soft template and carbon source to prepare boron carbon nitride (BCN). In another major study, highly porous activated boron nitride prepared with the presence of oxygen and carbon impurities (Li *et al.*, 2013c). Their finding demonstrated porous BN with 2078 m^2g^{-1} specific surface area by introducing the triblock copolymer (P123) as a structure-directing agent into boric acid and melamine precursors under two steps of heating process. As far as we are concerned, this outcome reveals the highest surface area of porous BN, which has been reported so far. Collectively, these soft templates have been used for enhancing the porosity of the resulting BN materials as a result of their advantages such as good repeatability, ease of processing and not requiring HF for removal of silica ones (Mishra and Saravanan, 2018).

Dynamic templates:

Several recent systematic studies examined the dynamic template method to control the synthesis of porous BN. For instance, Xiao *et al.* (2016) separated BN layers with Magnesium-based intermediates during synthesis. The results of their research support the idea that Magnesium diboride (MgB_2) is formed like a sandwich with BNNS and Mg-based by-products are decomposed during the reaction. Furthermore, the combination steps of freeze-drying and thermal decomposition were conducted by Lin *et al.* (2016) to produce one-dimension (1D) BN nanofiber. Their heating process was performed in a range of 1000–1300°C under nitrogen flow. Prior to the pyrolysis treatment, the aqueous solution of boric acid and melamine was placed in vacuum freeze dryer for several days. As noted by the author, a freeze-drying process contributed to the formation of 1D nanostructure. In a follow-up study, Zhao *et al.* (2017) obtained ultrathin uniform ribbon-like boron nitride with the same procedure. Their strategy is described as a self-sacrificed template using boric acid and melamine as raw materials, followed by vacuum freeze drying and calcined up to 1050°C. A similar procedure was followed by Xiong *et al.* (2020) to obtain 3D boron nitride monolith. As opined by Xiong *et al.*, (2020), the 3D monolith structure exhibited a higher adsorptive performance compared to powder, and therefore it can be easily recovered and separated.

In another comprehensive study of dynamic route, Han and Yu, (2018) reported a high round spherial boron nitride using ammonia borane (BH_3NH_3) as a precursor toward the pressure-induced vapour synthesis. The formation of well-dispersed spherical structures was achieved after further heat treatment (up to 1300°C) of ammonia borane in the sealed vessel. In all the studies reviewed in this section, formation of boron nitride is recognised as a specific morphology. Thus, applying dynamic efforts improve the nano-architectural properties of BN rather than its textural aspects.

2.9.2. Template-free synthesis porous BN

The previous section showed the template development of porous boron nitride in a wide range of morphologies, sizes and chemical structures. However, all the previously mentioned methods suffer from some serious drawbacks. Perhaps, the most serious disadvantage of template method is that it requires additional steps (e.g.

HF and ammonia treatment) to remove the template. Another key problem with this approach is that the majority of BNs produced with template may contain impurities and lower surface area. Therefore, the template-free theory has been vigorously challenged in recent years by a number of researchers. This method of BN production has been associated with precursors decomposition, which does not call for removing the template. Furthermore, the cost of template and additional steps in the synthesised BN *via* template method has led to development of alternative template-free methods.

We turn now to the experimental evidence on non-template routes, which has been the subject of many studies in last decade. In the section that follows, the procedures and methods used in this investigation will be described in detail. Generally, non-template method involves heating the mixture of boron and nitrogen precursors under various conditions. Recent developments in this methodology have highlighted the need for highly porous BN associated with shorter reaction time and higher yield. Consequently, trends in template free production of BN have led to a proliferation of studies on how considering the dynamic and chemical conditions can result in a well-defined porous structure. Figure 2.12. presents the different parameters that affect the porosity and structure yields of BN using non-template method. Numerous reports advocate that different conditions including the molar ratio of precursors, decomposition temperature, solvent mediate and carrier gas play major roles in the formation of BN with diverse structures and properties.

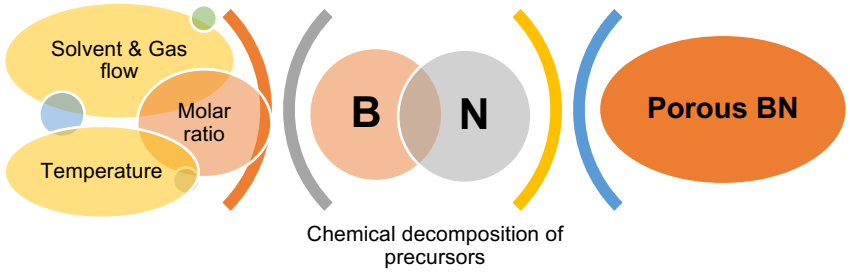

Figure 2.12 Schematic of parameters in template free synthesis of porous BN (Adapted from Mishra and Saravanan, 2018)

Before proceeding to examine the role of the process conditions in BN synthesis, it is important to establish the targets and specifications. For instance, with respect to designing a high-performing adsorbent, it has been commonly assumed that changing

material properties such as surface area, pore size, chemistry and defects could influence adsorption performance. Therefore, benchmarks to design highly performing adsorbents can be treated as follows: 1) optimising synthetic conditions in order to achieve fascinating BN properties 2) controlling those parameters which have correlated to adsorption properties.

A considerable amount of literature has been challenged on controlling various parameters and is summarised in Table 2.1. Classification of publications on Table 2.1 indicates that many researchers have been working on the production and gaining fundamental insights into boron nitride formation in the last decade. In fact, preliminary studies indicate that synthesis conditions probably have a significant impact on the morphology and porosity of BN nanomaterials. In a randomised controlled study of raw materials, boric acid and urea/melamine are typically used as boron and nitrogen precursors respectively. In a small scale study, boron trioxide, dicyandiamide and biuret were also employed (Chang *et al.*, 2018; Weng *et al.*, 2014; Marchesini *et al.*, 2017a).

The literature on chemical decomposition of precursors is commonly carried out in high temperature treatment (between 800–1400ºC) and depending on gas carrier (e.g. nitrogen or ammonia), various structure and morphology can be produced. Prior studies have noted the importance of temperature in determining the BN crystallinity. The results offer that in low synthesis temperature (< 900ºC), the formation of BN leads to a a-BN or t-BN with poor crystalline order (Hagio, Tsuyoshi and Nonaka, Kazuhiro and Sato, 1997). In contrast, hexagonal BN with high crystalline order is obtained when the synthesis temperature is increased (> 1000ºC) (Ansaloni and de Sousa, 2013). However, it has been commonly assumed that the material's surface area decreases due to high crystal order structure. In reviewing the literature, it can be seen that by far the greatest demand is for achieving the high surface area with tuneable porosity of BN nanomaterials. This surge in popularity of BN with high SSA and porosity could be justified by its superior performance in adsorption and catalytic applications. Among the few studies on the topic, the work of Marchesini et al. (2017) is the most relevant to this study and is a function of thermal decomposition characteristics of the N-based precursors in the form of NH_3, H_2O, CO, N_2, etc. The chemical reaction between various nitrogen-based gases derived from a precursor and boric acid (H_3BO_3) results in the formation of BN. The highest surface area of

1924 m^2/g with 1.2 cm^3/g total pore volume was obtained using melamine and urea in a molar ratio of 1:5. While the use of multiple nitrogen precursors may contribute to tune the porosity of BN material, no significant differences of SSA were found in multiple boron synthetic routes, as reported by Zhang *et al.*, (2015).

In another investigation into template-free synthesis of BN, Marchesini *et al.*, (2017b) found that intermediate preparation is a principal factor of high surface area. Therein, comparing the intermediate drying time with the formation of porous BN shows that further dried in an oven, the surface area could be more than doubled (form ~400 to 1000 m^2/g) with improved microporosity. It is also interesting to note that Wu et al. (2016) provided an insight on the impact of using different solvents prior to heat treatment. The authors demonstrated that different boiling points of the solvents influence the intermediate decomposition during thermal treatment and hence on the structure of the resulting porous BN. Clearly, it was revealed that when the mixture of methanol and distilled water were used as a solvent, the highest surface area obtained, however, urea with high molar ratio to boric acid was also required in the reaction mixture. The first set of analyses examining the impact of urea concentration on the number of BN layers was reported by Nag *et al.*, (2010). In their study, fewer layers as well as a high surface area are obtained with increasing urea concentration in the mixture. In their analysis of precursors, boric acid/urea ratios of 1:48 exhibited the highest surface area after annealing at 900ºC in nitrogen atmosphere. Prior to the work of Nag *et al.*, (2010), the role of urea proportion was largely unknown.

Additionally, other studies have found that utilising various precursors as well as carrier gas could also obtain different structures and formations of BN. For example, a mixture of boric acid/dicyandiamide under ammonium gas yielded BN microsponges with BET surface area of 1900 m^2/g *via* one-step thermal treatment (Weng *et al.*, 2014). Surprisingly, prior to the above experiment; Weng et al., (2013) reported porous microbelt BN with lower SSA of 1488 m^2/g that is thought to be related to the use of melamine instead of dicyandiamide as a nitrogen raw material.

Moreover, a number of studies have discovered that the mix carrier gas such as nitrogen/hydrogen or nitrogen/ammonia have a pivotal role in the formation of BN with relatively high surface area (>900 m^2/g) *via* annealing process (Li *et al.*, 2016; Maiti *et al.*, 2017; Florent and Bandosz, 2018). According to Florent and Bandosz, (2018), the

use of nitrogen containing 0.5% ammonia appears to be more effective compared to chemical decomposition of melamine diborate (M.2B) under nitrogen/hydrogen flow.

It is also well known that similar to urea, the concentration of melamine with boric acid can give rise to high porosity. For instance, microscopic analysis data from Tu *et al.*, (2018) and Song *et al.*, (2017) indicate that higher proportion of boric acid to melamine could result in significant drop of surface area. Using the melamine concentration approach, researchers have been able to tune the porosity of BN. However, one needs to consider that further use of melamine leads to carbon impurities. Overall, the literature review on nitrogen precursors has highlighted that an excessive use of nitrogen sources (e.g. urea, melamine, dicyandiamide and biuret) shows high pore structure in the final BN material.

Furthermore, high temperature post treatment is another way of template-free approach which is investigated by Li *et al.*, (2013b). In their major study, Li *et al.* (2013b) identify a great feature of BN whiskers including high surface area, pore volume and abundant defects for hydrogen storage and water treatment applications. Similarly, further works have been established in the literature through two steps pyrolysis or calcination to produce porous BN (Kostoglou *et al.*, 2016; Ji *et al.*, 2016; Li *et al.*, 2018). Recently, Li *et al.*, (2018) prepared porous BN nanosheets by dissolving boron trioxide with ethylene diamine to get a homogeneous mixture. The mixture was then treated at 280ºC in three-neck flask for one hour. The prepared precursor was carried out in ammonia flow at 500ºC first then the temperature increased to 1300 ºC. The final product exhibited a high thermostability with 3D structure and had 474 m^2/g surface area.

All these possible synthetic routes could also affect the morphology and structure of BN. Apart from all factors, precursor is recognised as an important factor to determine the morphology. For instance, the use of melamine can result in rod-like, fibre, ribbon and whiskers feature whereas utilising urea leads to layered-like or flake like morphologies. It is apparent from table 2.1 that there are a few spherical and flower-like features of BN. Other parameters such as temperature and carrier gas are generally seen as factors strongly related to various structures of BN. A recent study by Matveev *et al.* (2020) reported a new synthetic procedure to obtain a highly crystalline hexagonal BN. In this case, ammonia was employed as a nitrogen source

as well as carrier gas in chemical decomposition step. Hexagonal BN was formed after heating at 1000 for an hour. There are also a few studies, which used argon as a carrier gas, where no significant effect of argon on BN samples has been reported.

Taken together, all these results suggest that there is an association between each parameter during fabrication process and the materials properties. Therefore, a significant analysis and discussion on synthesis parameters is needed to optimise the synthetic condition. Noticeably, the selection of particular synthetic route can impact the efficiency and effectiveness of BN material in individual applications. The experimental methods, which have been reviewed above, are meant to be used on BN nanomaterials in different applications. For instance, much of the adsorption research has focused on identifying and evaluating the highly porous structure of BN which is more conducive for adsorption processes. In view of all that has been mentioned so far, one may suppose that template-free approaches are important contributory factors to the development of porous BN with high surface area and tuneable pore size. Despite these promising results, challenges in adsorbents development remain. As far as we are concerned, there is still a limited understating on the formation mechanisms of BN and the status of research needs to improve for given applications, particularly adsorption. Hence, further studies which take these variables into account will need to be undertaken.

Table 2-1 Influence of various conditions in the template-free fabrication of porous BN

Precursors	Solvent/Carrier gas	Temp ºC	Morphology& Structure	BET (m^2/g)	Fabrication Process	Ref
Boric acid/Urea	Deionized water/Ar	1200	BN nanoflower	-	High-temperature post-treatment	(Kumar *et al.*, 2020)
Boric acid/ammonia	NH_3	1000	Crystalline hexagonal BN	-	one-step heat treatment	(Matveev *et al.*, 2020)
Boric acid/Melamine	Deionized water/NH_3	1050	BN bundle	871	Boric acid nitridation with ammonia	(Song *et al.*, 2019)
Boric acid/Melamine	Deionized water/N_2	1000	BN microrod	103 - 616	Dried in vacuum oven & spray dryer followed by two steps pyrolysis	(Han *et al.*, 2019)
Boric acid/Melamine	Deionized water/N_2	1000	BN microrod	36 - 653	one-step heat treatment	(Wang *et al.*, 2019b)
Boron trioxide/ ethylene diamine	NH_3	1300	3D porous nanosheets	474	Two steps pyrolysis	(Li *et al.*, 2018a)
Boric acid/Urea	Water: Methanol/N_2	900	Layered graphene-like BN	1033	one-step heat treatment	(Wang *et al.*, 2018a)
Boron trioxide/Urea	Ultrapure water/ N_2	1000	Layered structure	798	Two steps pyrolysis	(Ji *et al.*, 2016)
Boron trioxide/h-BN	Acetone/Ar	1000	3D porous BN	0.92 – 2.5	Solid state sintering process	(Gautam *et al.*, 2016)

Precursors	Solvent/Carrier gas	Temp ºC	Morphology& Structure	BET (m^2/g)	Fabrication Process	Ref
Boric acid/Borax/Urea	Deionized water/NH_3	675	Spherical h-BN	230	Multiple B-precursors route	(Zhang *et al.*, 2015a)
Boron oxide/guanidine hydrochloride	Methanol/N_2	1050	3D flower-like nanosheets	1114	One step cylinder compressing	(Chen *et al.*, 2018d)
Boron trioxide/Urea	Water: Propanol/N_2	900	BN nanosheets	556	One-step heat treatment	(Chang *et al.*, 2018)
Boric acid/Melamine	Distilled water/N_2	900	Ultrathin nanosheets structures	189	One-step heat treatment	(Tu *et al.*, 2018)
Boric acid/Melamine	Distilled water/N_2@NH_3	1000	Nanorod porous BN	1571	one-step heat treatment	(Florent and Bandosz, 2018)
Boric acid/Urea	Distilled water/N_2	1050	Flake-like morphology	1016	Intermediate preparation	(Marchesini *et al.*, 2017b)
Boric acid/Urea/Melamine/Biuret	Distilled water/N_2	1050	From fibres to flakes 3D porous	1924	Multiple N-precursors route	(Marchesini *et al.*, 2017a)
Boric acid/Melamine	Distilled water/N_2	1100	Rod-like structure	1062	One-step heat treatment	(Song *et al.*, 2017)
Boric acid/Melamine	Distilled water/N_2@H_2	1100	Flower-like porous BN	1140	Two steps heat treatment	(Maiti *et al.*, 2017)

Precursors	Solvent/Carrier gas	Temp ºC	Morphology& Structure	BET (m^2/g)	Fabrication Process	Ref
Boric acid/Urea	Water: Methanol/N_2	1900	2D wrinkles structure	1900	Solvent mediate/ One-step heat treatment	(Wu *et al.*, 2016b)
Boric acid/Melamine	Distilled water/N_2@H_2	900	Porous whiskers	964	One-step heat treatment	(Li *et al.*, 2016)
Boric acid/Urea	Ethanol/N_2	850	Porous nanoplate	212.73	Two steps Pyrolysis & calcination	(Kostoglou *et al.*, 2016)
Boric acid/Dicyandiamide	Distilled water/NH_3	800	Porous microsponges	1900	One-step heat treatment	(Weng *et al.*, 2014)
Boric acid/Melamine	Distilled water/NH_3	1000	Porous microbelt	1488	One-step heat treatment	(Weng *et al.*, 2013)
Boric acid/Melamine	Distilled water/N_2	1460	Whiskers - Ribbon like	1687	High-temperature post-treatment	(Li *et al.*, 2013b)
Boric acid/Urea	Distilled water/N_2	900	Single/few-layered flake structure	927	One-step heat treatment	(Nag *et al.*, 2010)

2.10. Chemical modification of BN

As previously stated, porous BN nanomaterials with wide-band gap semiconductors are referred to as insulators (Pakdel *et al.*, 2012). This intrinsic characteristic and the ionic bond of BN play significant roles in determining the electronic and magnetic properties of BN. Moreover, as described in the previous section, the unique textural properties of BN (high surface area and porosity) is a key feature, which has been recognised so far. The most obvious finding of studies to date is that these properties can be tuned in terms of both electronic structure and surface pore network to optimise the BN performance. With respect to applicability of porous BN in variety of areas, the challenges and strategies to facilitate and promote its performance need to be investigated. One interesting finding is that chemical modification and functionalisation of BN can lead to generating novel characteristic of BN materials (Weng *et al.*, 2016). A considerable amount of literature has been published on chemical modification of BN in order to control its morphology, porosity and electronic properties. One should note that in the process of controlling the material properties of BN, it is of utmost importance to identify the purpose of changing the structure/porosity and chemistry of BN. One major debate in early research concerns with the wide optical band gap of BN materials that is believed to disrupt the BN electronic and optical applications. Therefore, several methodologies such as doping and surface modification have been suggested to narrow the band gap of BN materials (Lim *et al.*, 2013; Yin *et al.*, 2020; Wang *et al.*, 2020). Another considerable aspiration of optimising new BN is to improve its storage and adsorptive capacity (Lale *et al.*, 2018; Xiong *et al.*, 2018). This can be achieved by controlling the defect, pore structure and surface functionalisation (Shtansky *et al.*, 2018; Xiong *et al.*, 2020a).

The experimental and theoretical aspects of BN modification is another key factor, which needs to be explained in this section. The main issues reviewed hereby are: i) identification of the link between BN material properties and its ability to tune; ii) review of a number of studies, which have focused on surface modification procedures to improve the BN applicability. Generally, chemical modification of BN can be classified depending on different objectives into non-metal and metal modification. Thus, this section analyses the previous BN modification findings and presents the justifications for use of each method accordingly.

2.10.1. Non-metal modification

The non-metal modification method is one of the most practical ways of developing new features of BN, with the aim of enhancing the process ability of materials. In this case, different methods have been proposed to classify metal-free modification of BN.

Generally, the surface of BN nanomaterials could be chemically modified by covalent or non-covalent chemical bonding. In the section that follows, the reaction of each of these methods into BN skeleton is discussed in detail and from both experimental and theoretical perspectives.

Covalent Functionalization

Covalent functionalization with functional groups is an important way to enhance the interaction of boron nitride with various materials and redefining its self-properties to suit various applications. In this section, an overview of the progress in functionalized boron nitride nanomaterials is presented. It includes physical and chemical routes, which describe novel h-BN with enhanced water solubility, biocompatibility, surface affinities and reduced band gap. The dipole formation of BN, which consists of polarized B-N bonds, makes the electron-deficient cloud in B atoms interact with nucleophilic groups. Thus, covalent functionalization of h-BN is feasible *via* a reaction between the vacant p orbitals in B and the reactive radicals (Weng *et al.*, 2016). To date, numerous functional groups, such as hydroxyl (-OH), amino (-NH_2) and ether (-OR) have been introduced into BN surface through chemical functionalisation. It has been previously observed that BN with different dimension models (e.g., 1D and 2D) can be chemically bonded *via* various procedures. An important observation to point out here is that since BNNTs or BNNSs are commonly used as the precursors, the covalent functionalisation methods differ from those discussed hitherto. Mostly, these methods are based on chemical exfoliation, plasma treatment and hydrothermal reaction with ball milling.

Regarding the electrophilic nature of B atoms in BN surface, hydroxyl group (–OH), Amino (–NH_2) and amine (–NHR) groups can covalently attach to and modify the materials. The hydroxyl group is the most important chemical modification for BN materials. A number of procedures have been developed to link the –OH group on the

surface of BN nanomaterials. For instance, Zhi *et al.*, (2009) oxidized the surface of boron nitride nanotube with hydrogen peroxide (H_2O_2) in an autoclave at 120 ºC. Therein, –OH groups reacted with BNNTs and chemically bonded to the B sites due to dissociated of H_2O_2 in a sealed reactor. Through the FTIR analyser, they found that the hydroxyl functional group is connected to the surface of BNNT rather than being embedded into its structure. This has been also confirmed by XPS spectroscopy and the final product comprised ~6% wt% oxygen content. Direct sonication is another key method which was reported by Lin *et al.* (2011) in which the hexagonal boron nitride nanosheets were hydroxylated in aqueous solution using bath sonication. The exfoliation of h-BN was also confirmed with sonication-assisted hydrolysis, obtaining a monolayered nanosheet. Later, Sainsbury *et al.*, (2012) introduced hydroxyl group in the h-BN lattice with a chemical exfoliation method. Their study involved two-steps using an organic peroxide reagent (di-*t*-butyl peroxide) and the mixture of H_2SO_4/H_2O_2 to yield hydroxyl-functionalize BNNSs (OH–BNNSs). As indicated previously, BN nanomaterials can be grafted to hydroxyl groups under plasma air conditions (Pakdel *et al.*, 2014b). In a study conducted by Pakdel *et al.*, (2014b), it was shown that $^{\bullet}OH$ radicals were generated in the air plasma and can be feasibly functionalised both in plane and edge sites of BNNS surfaces. Another possible edge hydroxylation of BN nanomaterials has been developed by Lee *et al.*, (2015) through a ball milling techniques in the presence of sodium hydroxide. With the same consideration, Xiao *et al.*, (2015) confirmed the presence of –OH at the edge position of BN with electron energy loss spectroscopy (EELS), using hot steam treatment. Most recently, one-step simple dispersion of h-BN in isopropanol has been proposed for a large-scale production modification of h-BN nanosheets (Zheng, 2020). In their analysis of ultrasonic-assisted polar organic solvents, use of isopropanol with hydrogen bonds can modify and exfoliate h-BN nanosheets with a better peeling effect.

Similar to hydroxyl group, alkoxy (–OR) groups can be also introduced onto BN surfaces with the sonication assistance boron nitride nanotube (Kim *et al.*, 2015). The procedure involved using multi-walled BNNTs that were sonicated in various alcohol types for three hours. FTIR spectra detected the B–O, B–O–C stretching, and O–B–O bending vibration mode, suggesting the well dispersed –OR groups in alcohol solvents.

In addition, the positive charge of B atoms enables BN to interact with $–NH_2$ through Lewis base interaction. The first amine functionalised BNNTs was reported by Xie *et al.*, (2005). They demonstrated the homogeneous dispersion of BNNTs with PEG chains, yielding the functionalised BNNTs in aqueous solutions. It is noted that later this method has been improved, applying temperature treatment (Lin *et al.*, 2010). The plasma technique is another way to achieve amine-functionalised BNNTs which was proposed in Ikuno *et al.* (2007). They used NH_3 plasma irradiation to covalently bond $–NH_2$ groups to the BNNTs surface. Further investigation of $–NH_2$ functionalization of BN nanomaterial was carried out under sonication (Liao *et al.*, 2014) and ball milling approaches. Lei et al. (2015) functionalized the few-layer BN using ball milling techniques based on urea-assisted solid exfoliation of commercial h-BN. They obtained a light NH_2-BNNS aerogel with a low density and good solubility in water. A great deal of current research into amino-functionalized boron nitride has focused on polymerization of BNNSs in order to produce nanocomposite membrane. These new polymer nanocomposites were obtained for a certain target like hydrogen separation and thermal/mechanical enhancement properties (Wang *et al.*, 2018b; Zhang *et al.*, 2019; Ou *et al.*, 2020).

It is now well established from a variety of studies that other functional groups (e.g. –OCOR, –NHCOR, –COR, etc.) can be introduced to either pure BN or hydroxylated and aminated BN. The electrophilic functionalisation of BNNTs with acyl and amino group was first studied by Zhi *et al.* (2005). Moreover, oxidized surface of pure BN (OH-BN) is chemically active for esterified (–OCOR) functionalisation (Zhi *et al.*, 2009). In follow-up studies, Ciofani *et al.*, (2012) and Huang *et al.*, (2013) used oxosilane groups to bond –OH groups on BNNTs to design a polymer composite for dielectric and biomedical applications. Acylation (–COR) of boron nitride can be obtained with the presence of –NH2 groups. For example, in a recent work by Hao *et al.*, (2020) functionalized boron nitride nanoplate with 3-mercaptopropyl trimethoxysilane (MPTMS) and poly(ethylene glycol) diacrylate (PEG). In addition to the functional groups explained above, hydrogen and florine modification of BN materials were also reported with effect on material's band gap and magnetic structure (Li *et al.*, 2013d; Tang *et al.*, 2005).

Element doping

Elemental doping strategy is considered as a fundamental way to tune the micro pore and electronic structure of BN nanomaterials. Over the past decade, most research in non-metallic doping elements has emphasised on making important changes of pristine BN for some unique properties, including photocatalyst, dry sorbents and hydrogen storage to name a few. In general, carbon and oxygen are the most popular dopants which chemically doped BN to meet the practical applications. Oxygen doping into BN nanomaterials has been investigated both theoretically and experimentally (Silva *et al.*, 2006). According to theory calculations in Silva *et al.* (2006), the tube structure of oxygen replacing with nitrogen atom found to be more stable configuration instead of boron substitution. In analysis of ON substitution, the formation of narrow band gap BN structure is more favourable which can be attributed to the fact that an electron is injected from O to the π bond. This new magnetic property of BN opens a new route for optical and catalytic applications (Wu and Zhang, 2009; Gou *et al.*, 2009). Similarly, the influence of oxygen on the electronic properties of BN was reported by Singh (2015). Their comparative study indicated the different behaviour of electronic properties of carbon and boron nitride nanotubes due to oxygen doping. While the energy bands are gradually modified in BNNTs and exhibited the metallic characteristic, the metallicity of oxygen doped zigzag carbon nanotubes is reduced.

Moreover, some authors are interested in using oxygen modified BN for hydrogen storage and adsorption properties (Lei *et al.*, 2014;Tokarev *et al.*, 2016; Zahedi *et al.*, 2016). In one well-known recent experiment performed by Lei *et al.* (2014), the highest storage capacity was recorded from oxygen-doping of the BN nanosheets *via* the sol-gel method. The present study raises the possibility that the oxygen impurities are obtained by means of using boron trioxide precursor. Lu *et al. (2018)* performed a combination of theoritical and experimental calculations for preparing BN nanomaterials with oxygen doping and ferromagnesium behaviour. In addition, a recent article (Zhang *et al.*, 2019a) focused on tribological properties of O-doped BNNSs in which the interlayer fiction of BNNSs is changed, regarding the effect of oxygen atoms on the geometry and electron distribution of BN sheets.

Carbon substitution to BN structure is a class of metal-free modification of BN which is thermodynamically and energetically favourable (Bhowmick *et al.*, 2011). Much of

the current literature on metal-free modification of BN pays particular attention to production of boron carbon nitride (BCN) due to its large surface area and abundance of active sites. Only in the past ten years, studies of BCN materials directly addressed how its unique properties contribute to a good performance for semiconductors photocatalyst activity (Chen *et al.*, 2019), electrochemical reaction (Chen *et al.*, 2020), oxidation reaction (Wei *et al.*, 2020), hydrogen reduction (Zhou *et al.*, 2020) and adsorbents (Peng *et al.*, 2018). Several attempts have been made by researchers to synthesise BCN material *via* various procedures such as CVD method (Yin *et al.*, 2005), using metallic substrates (Yin and Chen, 2011; Lu *et al.*, 2013), arc discharge (Ben Belgacem *et al.*, 2016), biomass derivatise (Tu *et al.*, 2018). This section describes the design and implementation of BCN toward metal-free precursors-mediate ways, which results in porous BCN. Similar to the pristine porous BN, fabrication of BNC involves utilising a variety of precursors followed by thermal and calcination conditions. Carbon-based materials such as graphite, activated carbon, are the most common carbon raw materials for determining BCN with various forms of carbon. For example, some scholars (Huang *et al.*, 2015; Karbhal *et al.*, 2016), proposed a green synthesis route using glucose to generate C-doped into boric acid and urea mixture. Recently, a series of experiments, with the addition of coconut shells, activated charcoal and starch as a carbon derivate, were performed to investigate BCN with super characteristic and applications (Kumar *et al.*, 2011; Kumar *et al.*, 2013; Li *et al.*, 2018b; Chen *et al.*, 2020; Zhou *et al.*, 2020). Commonly, the obtained borocarbonitride composition prepared by urea solid state and gas phase routes can be classified into microsphere, nanotubes, nanoribbons and nanosheets structure, depending on the carbon source. As previously stated, solid state reaction of melamine with boron source comprises carbon impurities in BN structural networks. Therefore, several lines of evidence suggest efficacy of using melamine for the formation of BCN without adding an extra carbon sources (Gautam *et al.*, 2015; Peng *et al.*, 2018; Florent and Bandosz, 2018; Chen *et al.*, 2018a). The main differences of these methods are using a wide range of sintering temperatures and a variety of precursors concentrations. Furthermore, other organic precursors such as polymeric monomers and [C16mim]Cl ionic liquid reactants may cause incorporation of carbon atoms into B-N frameworks under solid-gas phase reaction (Chen *et al.*, 2018a; Zhang *et al.*, 2018; Chen *et al.*, 2018a). Most recently, Wei *et al.* (2020) proposed a new methodology for hierarchical porous sheets BCN, using choline chloride as a solvent

into urea and boric acid mixture. The homogeneous mixture was calcined at 900°C under an ammonia flow. It is worth noting that data from several sources have identified the combination of C and O impurities in BN materials using energy dispersive X-Ray spectroscopy (EDS) (Örnek *et al.*, 2018, 2019; Bhattacharyya *et al.*, 2019).

Surfactant-organic compound modification

As it was pointed out in the previous sections, surfactant compounds like liquid ionic, cetyltrimethylammonium chloride (CTAC), and tri-block copolymer (P123 or F127) act as template in production of porous BN. This section demonstrates how organic surfactants contribute to modify the porosity in BN porous materials during the decomposition process. The main challenge faced by researchers is creating pores into BN frameworks, and subsequently evaluating the impact of porosity distribution on the BN adsorption properties. To the best of our knowledge, the highest porosity of BN is reported in Li *et al.* (2013a) yielding a surface area of 2078 m^2/g with large pore volume of 1.66 cm^3/g. This method relied on structure-direct agent approach using tri-block copolymer (P123) as a surfactant into melamine-boric acid mix solution followed by a two-step pyrolytic process. P123 surfactant provides the means for surface modification of precursors by causing hydrogen-bonding with melamine. The P123 compound was removed during the post-treatment, and thereby more gasses were released. Surfactant modification-based method is one of the most practical ways of obtaining a highly activated BN, which exhibits a great adsorption performance for environmental remediation. In a follow-up study, Xiong *et al.* (2016) synthesised the porous modified BN using the same method. In their research, the calcination process was carried out at 1000°C for three hours, whilst Li *et al.*, (2013a) performed two stages of pyrolysis in higher temperatures and duration time. The obtained nanowire activated BN displayed a surface area of 295 m^2/g with abundance of mesopores, which is favourable for desulfurization.

Later in Xiong *et al.* (2017), the researchers optimised the usage of vary surfactant (such as PVP, F127, P123) in order to obtain a promising adsorbent for desulfurisation application. Their study suggested that the activated BN with Pluronic P123 exhibits the highest adsorption capacity on DBT among other surfactants. Moreover, the use

of P123 into porous boron carbon nitride was confirmed to be efficient in adsorbing the dyes in waste water as a result of tuning the nanoscale structure (Wang *et al.*, 2017). Therefore, tri-block copolymer surfactants, in particular the Pluronic P123, could be a major factor, if not the only one, improving the porous structure of pure BN.

2.10.2. Metal modification

Metal nanoparticles and metal oxides have been also explored to modify boron nitride in terms of i) electronic and magnetic properties ii) pore size/shape iii) thermal conductivity iv) hydrophobicity. It is now well-established from a variety of theoretical studies that metal nanoparticles (alkali/alkaline earth metals and transition metals) have a potential to change the BN electrical, magnetic and optical properties (Grad *et al.*, 2003; Gómez Díaz *et al.*, 2013; Iqbal and Ayub, 2016; Zhou *et al.*, 2018; Liu *et al.*, 2019; Asif *et al.*, 2020). In a recent review of experimental research, various studies have assessed the efficacy of transition metal atoms (Ag, Cu, Au, Co, Ni, Pt, *etc.*) into BN materials for a case application. Traditionally, the fabrication methods which have been proposed to develop these transition metals or metal oxide into BN can be categorised into a) consuming the bulk or commercial-based BN b) using the BN precursors. The former procedure is based on sonication and exfoliation mediate; whereas the latter relies on impregnation-pyrolysis approach. In the remainder of this section, we address both classification methodologies and the mechanism beyond each in detail and based on recent publications in the field.

Gao *et al. (2014)* reported a new and convenient synthetic procedure to obtain a composite of h-BN embedded with silver NPs. The procedure consists of the sonication of BN with certain volumes of $AgNO_3$ followed by microwave assistance to accelerate growth of metallic nanoparticles. Conversely, Pang *et al.* (2018) doped silver NPs by means of impregnating boron and nitrogen precursors with $AgNO_3$ and then calcining at 900°C in N_2 atmosphere. Noticeably, it was shown that this approach is more profitable in adsorptive activities of BN owing to its high surface area.

Both metallic Cu NPs and CuO have been combined with BN materials to obtain high performance of catalytic activities in studies such as Wu *et al.*, (2016b) and Oh *et al.* (2020). While Cu NPs can boost the catalytic performance by advancing the electron mobility of BN, CuO supported on h-BN provides high stability of heterogeneous

catalysts. In both of the above-mentioned studies, impregnation-calcination method was assessed, although Oh *et al.* (2020) conducted the calcination step in air atmosphere at 400°C with the aim of converting Cu^{2+} to CuO.

Furthermore, an efficient catalyst could be obtained by synthesising a BNNS–Au NPs composite. Fu *et al.* (2016) prepared BNNS–Au NPs composite by in-situ growth of Au on BNNS dispersion. As noted by authors, the outstanding catalytic activities of processed composite was also extended for Pt, Ag and Pd NPs with BNNS. In the same vein, He *et al.* (2020) deposited AuNPs on the surface of BN through wet impregnation of $AuClO_4 \cdot 3H_2O$ into ultrasonicated h-BN.

Studies such as those conducted by Du *et al.* (2017) showed that Co-loaded BN nanoparticles act as a heterogeneous catalyst with high chemical stability. The core-shell of BN/Co nanoparticles is formed with the amount of boron oxide, urea and cobalt nitrate were physically mixed and sintered in high temperature at 1250 ºC. Obviously, the cobalt precursor concentration would affect on its catalytic activity as determined in their kinetic study. In another major study, Hao *et al.*, (2018) found a novel Co-doped BCN with spherical framework by annealing boron oxide, ammonia chloride and glucose. Therein, during the thermal decomposition, glucose formed spherical shape into BN structure and ammonia chloride released gases that formed interconnected porous structure. Unlike Du *et al.*, (2017), Hao *et al.*, (2018) obtained the high surface area of 443 m^2/g and studied its electrochemical properties.

Recently, a number of studies have been published for loading Ni into BN nanomaterials. In this case, Cao *et al.*, (2018) found that pristine h-BN acted as a support for the Ni particles dispersion, given to its surface defect engineering. The preparation of Ni/h-BNNS has been considered as electron donor/acceptor reactions which can improve the catalytic conversion and adsorption of CH_4 and CO_2. The study of the structural morphology of nickel oxide was carried out by Kokulnathan and Wang, (2019), in which they established a 3D flower like NiO embedded with BCN materials. A combination of hydrothermal method and ultrasonication were used for the 3D flower-like NiO/BCN composite. The results of their study found that NiO could further increase the accessible active surface area as well as electron charge transfer of BCN for electrochemical applications. Their approach was also applied for modifying porous BN with NiO to obtain a proper adsorbent for wastewater treatment (Song *et al.*, 2020;

Li *et al.*, 2020). Another novel strategy was presented by Jiang *et al.*, (2020), producing NiNPs/BNNS catalyst *via* exfoliation of bulk BN followed by gamma-ray irradiation. To this end, gamma-ray irradiation was induced to reduction of Ni^{2+} ions in order to *in-situ* growth of NiNPs in the interlayers of h-BN.

Furthermore, the interaction mechanism of charge transfer between BN and metal ions was confirmed further by investigating other transition metals (Ce and Pt) which can serve as active sites to improve the BN performance (Luo *et al.*, 2019; Wu *et al.* 2020). By drawing on the concept of the interaction between BN and Pt catalyst, (Li *et al.*, (2020b) developed Pt/BN catalyst through impregnation reduction method, exposing porous BN to an ethylene glycol solution consisting K_2PtCl_4. In their DFT analysis, they have been able to clarify that a electron back-donation process took placed to contribute to the strong interaction between Pt metal and BN support.

The studies presented thus far provide evidence that transition metals can be introduced into BN either as a metal nanoparticle, or metal oxide. Given that there have been numurous synthesis stategies for metal modification of BN, the selection of a specefic procudue is application-dependant. The highest impact of metal modification of BN from the studies disscussed so far include: a) boosting electron mobility b) controling the charge and magnetic state and c) increasing the active sites and surface area. However, there is still room for further progress to determine new themes of BN/metal hybrids for a particular application.

2.11. Application of porous BN in CO_2 capture

Following on the discussion above, boron nitride nanomaterials have been the subject of many classic studies in a wide range of fields. Apart from all valuable applications, the utilisation of BN materials for CO_2 adsorption is a major area of interest within the literature. Recently, there has been renewed interest in porous feature of BN for the gas sorption properties, in particular CO_2 sorption. Therefore, the issue of selecting a unique synthesis and modification method has received considerable attention. The CO_2 capture performance of the BN porous materials in different conditions has been investigated in recent years as shown in Table 2.2.

An initial attempt to synthesise porous BN for gas sorption was made by Janik *et al.* (1994), preparing t-BN with surface areas up to 712 m^2/g for the adsorption of carbon dioxide. It was investigated that the gas adsorption behaviour mostly relies on the microporous nature of BN.

Table 2.2 demonstrates that the template-free strategy has been widely used to produce pristine porous boron nitride. However, Xiao et al. (2016) investigated pure porous BNNS by using magnesium diboride (MgB_2) as a dynamic template and tested adsorption of CO_2 over N_2. More importantly, the CO_2 uptake of their work was relatively low, while it demonstrated good selectivity of CO_2 over N_2.

One practical way to achieve a high CO_2 adsorption capacity over pristine BN was reported by Nag *et al.* (2010). They made a few-layer BN by controlled chemical composition of urea, indicating that the sample with the lowest layer thickness shows a high CO_2 uptake. In addition, Marchesini et al. (2017a) pointed to some of the ways to obtain tuneable structure by preparing an intermediate prior to heat treatment. Although intermediate preparation has a significant impact on porosity, it required a long drying time. Hence, they have also investigated that tuneable and highly porous boron nitride could be tailored using multiple N-containing precursor, which showed enhanced CO_2 capture capacity (Marchesini et al., 2017b).

The literature on CO_2 capture of porous BN has highlighted that surface modification of boron nitride is critical to increase the CO_2 adsorption capacity (see Table 2.2). Recently, a number of publications considered the important role of micropore size in the rate of adsorption kinetics diffusion (see Chen *et al.*, 2018a; Florent and Bandosz, 2018; López-Salas *et al.*, 2018 for further information). In this case, Chen *et al.*, (2018a) and Florent and Bandosz, (2018) attempted to hold the view that the incorporation of C atoms into BN matrix modifies the porosity/ultra-microporosity of BN which results in a larger CO_2 uptake.

Functionalised BN with nitrogen groups is another effective way to promote BN capability towards CO_2 capture. In this case, some studies suggest that the nitrogen group is a principle factor of edge sites adsorption by hydrogen bonding (Owuor *et al.*, 2017; Chen *et al.*, 2018c). However, Huang *et al.* (2017) proposed that the electron-donating with amine groups into electron-deficiency of BN causes increase in the adsorption of CO_2. Despite these promising results of the amino fuctionalization

approach, questions remain. One of the issues that emerges from the above findings is that amino groups with porous materials are disabled by weak intermolecular forces which in turn decreases physical CO_2 adsoption (Qi *et al.*, 2019).

In another BN functionalised approach, Yang *et al.* (2019) found that the introduction of basic sites into BN materials could be promoted to bond with acidic CO_2. The authors highlighted three main mechanisms for CO_2 sorption occurring on the factionalised BN/ZnO, in which vacancies/defects, alkaline-edge groups and polarity of Zn–O bonds provide adsorption sites.

From a theoretical point of view, BN characteristic bonding and properties provide a useful account of how to modify its surface to enhance the adsorption/desorption of CO_2 on porous BN materials. In this regard, theoretical studies proved that it is critical to modify electronic and defect engineering of BN to increase its affinity toward CO_2 molecules (Sun et al., 2013; Paura *et al.*, 2014; Guo et al., 2015). This may be explained by the fact that the electron-deficiency of these materials leads to a weak affinity to CO_2 Lewis acidic molecules. Therefore, inducing extra electrons into BN is favourable to interact with CO_2.

Together, the key factors of surface area, pore size/shape, defects and surface chemistry of BN can influence on and link to the CO_2 adsoprtion process. Basically, all of the reviewed studies in this section support the idea that by changing the structure/porosity and surface chemistry of BN, one could obtain an enhanced CO_2 adsorption uptake and selectivity.

All in all, it seems that controlling the parameters of boron nitride properties and developing novel structures with high capacitive performance for carbon capture remains a major challenge to overcome.

Table 2-2 Summary of experimental studies on CO_2 adsorption using porous BN with brief synthesis conditions

Description method	Surface area [m^2/g]	Adsorption conditions		CO_2 Capacity (mmol/g)	Comments	Reference(s)
		T (k)	P (bar)			
Porous BN - Template-free synthesis form polymeric precursors followed by pyrolysis in vacuum under NH_3 (800 – 1000 ºC)	437-712	273	1	0.4-5.5	CH_4/CO_2 selectivity was correlated to the micropores size of samples.	(Janik *et al.*, 1994)
Few layered porous BN – Template-free synthesis form thermal evaporation of boric acid and urea in different molar ratio (1:6, 1:12, 1:24, 1:48, 1:72) followed by pyrolysis at 900 ºC in N_2.	927 (for sample 1:48)	195	p/p_0= 0.85	7.27	The urea concentration could be controlled the number of layered BN and consequently increased its surface area.	(Nag et al., 2010)
Hierarchically porous BN nanosheets – Dynamic template method with magnesium diboride (MgB_2) template and ammonium chloride, heated under NH_3 at varied temperature (450−1050 °C).	236 (for BN was treated at 750°C)	298	1	0.45	Mg atoms acted as a sandwich structure to promote the BN crystallisation. The obtained sample exhibited good CO_2/N_2 adsorption selectivity.	(Xiao *et al.*, 2016)
Porous flake BN – Template-free synthesis using boric acid and urea dried in oven at varied duration time (0− 200h), followed by heat-treatment at 1050 °C in N_2.	1016 (for BN with longer dried time)	298	1	0.6	The porosity of BN could be tuned by drying the intermediate for longer time at lower temperature.	(Marchesini, et al., 2017a)
Porous BN with variety morphologies – template-free synthesis using different molar ratio of Urea/ melamine/ biuret and boric acid precursors mixed and heated at 1050 °C in N_2.	1924 (for melamine/urea 1:5)	298	1	1.6	Using multiple N-precursor could result in high surface area and CO_2 capacity.	(Marchesini, et al., 2017b)
		298	20	8		
		283	20	10		

Description method	Surface area [m^2/g]	Adsorption conditions		CO_2 Capacity (mmol/g)	Comments	Reference(s)
		T (k)	P (bar)			
3D BN Foam – Synthesised in two steps: 1) exfoliation of h-BN with Intermolecular of bonding of PVA 2) freeze-dried mixture for 24 h	124	-	56	7.26	Nitrogen functional groups in 3D foam BN increased BN surface area and CO_2 uptake capacity.	(Owuor *et al.*, 2017)
Amino functionalised BN nanosheet – Synthesised through impregnation using polyethylene amine (PEI) with different loading (wt%)	3 (for 54.9% PEI loading)	348	1	3.12	PEI were inserted into BN nanosheet *via* acid-base interaction. The strength of interaction between CO_2 molecules and PEI functionalised BN attributed to the both physically and chemically adsorbed CO_2.	(Huang *et al.*, 2017)
3D porous BCN nanorod – template-free synthesised using boric acid and melamine in different molar ratio (1:2, 2:1, 1:4), followed by heat treatment at 1000 °C under N_2 containing 0.5% NH_3	1571 (for BM4)	293	1	2.49	Samples are exhibited a highly porous structure of by introduction of C atoms into BN samples.	(Florent and Bandosz, 2018)
Porous microbelt BCN – template-free synthesised using boric acid and melamine in different molar ratio (1:4, 2:1) followed by heat treatment at 800 °C in Ar	877 (for BCN 1:4)	298 273	1 1	3.74 5.5	Pore size plays an effective role in C-doped BN compared to surface area and pore volume. Relatively high CO_2 adsorption capacity observed for BCN samples due to its ultra-micropores and defects structure.	(Chen et al., 2018)

Description method	Surface area [m^2/g]	Adsorption conditions		CO_2 Capacity (mmol/g)	Comments	Reference(s)
		T (k)	P (bar)			
3D flower-like BN – dynamic-template synthesised using Guanidine hydrochloride and boron trioxide (5:1 molar ratio) in methanol, followed by cylinder compression (3 tons), Heated at 1050 °C in N_2.	1114	273	1	1.7	OH, and NH_3 functional groups are attributed to promote CO_2 capacity. The major contribution of CO_2 adsorption occurred via in-plane van der Waals interaction, while a minor contribution was from H- bond on the edges.	(Chen *et al.*, 2018d)
		298	1	0.8		
3D BCNO formed by using melamine, boric acid and glucose *via* freeze-drying and pyrolysis at 1000 °C in N_2.	347	298	1	1.8	3D architectures and narrow micro porosity are attributed to capture CO_2.	(López-Salas *et al.*, 2018)
Porous BN aerogel – Synthesised by using the homogeneous dispersion of CNT/GO through 3 steps: 1) hydrothermal 2) freeze-drying 3) pyrolysis at 1600 °C under boron oxide and N_2.	716.56	273	1	4.46	BN aerogel exhibited a polar structure with high pore volume, which is favourable for CO_2 molecules diffusion and selective adsorption of CO_2/N_2.	(Kutty *et al.*, 2018)
		298	1	3.8		
Porous BN fibres – Synthesised by using boric acid and melamine and hexamethylenetetramine precursors and heated at 1050 °C in N_2.	1042	273	1	2.85	Extra micropores distributions obtained by introduction of hexamethylenetetramine during procedure.	(Wang *et al.*, 2019a)
Porous BN fibres – Synthesised on two steps thermal treatment: 1) annealed at 1050 °C in N_2 2) post-annealed at 1400/1500/1600 °C under N_2/NH_3.	844 (for 1400-NH_3)	273	1	1.61	Post temperature treatment effected on pore structure of BN fibres. NH_3-treatment at high temperature could be improved adsorption capacity due to chemisorption of N-H groups.	(Liang *et al.*, 2019)

Description method	Surface area [m^2/g]	Adsorption conditions		CO_2 Capacity (mmol/g)	Comments	Reference(s)
		T (k)	P (bar)			
3D spherical functionalised BNNS with ZnO and NH_2^- through ball milling and solvothermal evaporation steps.	71.2	273	1	2.81	CO_2 adsorption occurred on 3D s-BNNS/ZnO *via* 1) in-plane van der Waals interaction 2) on the edge sites *via* H bonds 3) chemical adsorption with basic sites of ZnO which is dominated the adsorption capacity	(Yang *et al.*, 2019)
		298	1	1.78		

2.12. Conclusions and knowledge gaps from the literature

The past decade has seen a rapid development of boron nitride nanomaterials in several fields of interest. In all the studies reviewed in this section, porous BN is recognised as a tuneable pore structure with flexible morphology, structure and chemical modification through synthetic methods. Two important themes emerge from the papers reviewed so far including production of porous BN with high surface area and porosity *via* using template or non-template strategy as well as discovery of new features of BN by introducing organic functional groups or metallic species.

Concerning the first theme, template-free approach is often favoured for its superiority in terms of obtaining high porosity and surface area with less number of synthesis steps and chemicals. However, such studies remain narrow in understanding the effect of various parameters during the synthetic method. The question raised by this review is finding the factor with the highest impact on CO_2 adsorption application. To the best of our knowledge, precursor is one of the key factors to optimise the chemical and physical properties of BN for CO_2 adsorption. Given that few studies exist on this issue, considerable work should be done to determine the role of precursors in the structure of pristine BN.

In the second theme, a considerable potential of BN for CO_2 adsorption was reported in those works, which employed surface modification strategies. This is because surface modification of BN can strengthen interaction to CO_2 molecules by providing either high porosity or adsorptive sites. On one hand, controlling the microscopic properties of BN with different techniques (e.g. surfactant-assistance, heteroatoms-doped) is widely applied to increase CO_2 sorption capacity due to BN with optimal pore size exhibits high kinetic selectivity (this fact is fundamental in order to tune the BN pore size with a potential for capturing more CO_2 compared to pure BN). On the other hand, negatively charged BN surface or its enhanced polarizability provide remarkable increase in its thermodynamic properties for CO_2 adsorption. In fact, physical CO_2 capture commonly occurs at plane sites of BN by weak van der Waals interaction between CO_2 molecules and BN materials. The existence of lattice defects and other functional groups contribute to enhancing CO_2 capacity with acid-base or H-bond interaction.

Hence, from thermodynamic and kinetics perspectives, several methods including the heteroatom functionalisation, polymeric surfactant modification, basicity and polarizability enhancement can further increase the CO_2 uptake performance of porous BN. This finding, while preliminary, suggests that adsorption capacity of BN is correlated with textural parameters and the surface chemistry of BN.

Among various families of modification strategies, studies of polymeric surfactants and their impact on BN pore size distribution for carbon capture are limited in the literature published to date. According to the positive role of structure-directing agent surfactant on BN pore geometry, one can infer that surfactant modification may boost BN affinity to capture more CO_2. Moreover, the majority of studies proved the significant impact of metal modification on electronic, magnetic and surface chemistry of BN. However, not many of these influences were experimentally studied in application of BN for carbon capture. We hypothesise that transition metal oxides could enhance the CO_2 adsorption of BN by creating basic groups given their basic features.

Given the knowledge gaps outlined above, research questions that could be asked include: (i) how to optimise the chemical and physical properties of pristine BN production by considering the influence of precursors chemistry and concentration during the non-template procedure; (ii) how to modify the porosity of BN by introduction of metal-free surfactant; (iii) how nickel oxide as a transition metal oxide could improve the interaction between Lewis acidic CO_2 molecules and BN materials.

Overall, a reliable pathway for tuning the BN surface area and pore volume needs to be established. The effect of loading organic surfactant as well as nickel compound on surface chemistry of BN should also be investigated in more detail, with focus on its electronic, basic and pore size distribution properties. Finally, the CO_2 adsorption test needs to be applied on pristine and modified BN to evaluate the BN's applicability in carbon capture and to find the link(s) between its properties and CO_2 adsorption performance.

CHAPTER 3

METHODS AND CHARACTERISATION

Outline of the chapter

This chapter describes the methodology of synthesis porous BN using bottom-up approach. Experimental procedure and various materials characterisation techniques are considered. The chapter is organised as follows:

3.1. Introduction

3.2. Porous BN synthesis

3.3. Characterisation techniques

3.4. Conclusions

3. Methods and characterisation

3.1. Introduction

Research on production of porous BN *via* wet chemical reaction relies on two particular steps of hydrothermal or solvothermal evaporation and pyrolysis. While the former step in this process is based on intermediate preparation of precursors, the latter involves crystallisation growth of BN through decomposition of precursors. Therefore, factors including the order structure, shape-morphology and size of BN particles are determined in the pyrolysis stage. As indicated previously in the literature review section, temperatures, carrier gases and time are the most important parameters identified in pyrolysis or heat-treatment processes. A more detailed account of the methodology and synthetic conditions during the decomposition process is given in the following section (section 3.2). Following on from the aims of this study, the most suitable porous BN materials will be synthesised for providing the targeted CO_2 adsorption capacity. Moreover, findings in this study would make an important contribution to the area of green synthesis, which is comprised of shorter reaction time, reduction of energy and yield enhancement. Hence, the proposed methodology for the BN modification strategies is relatively similar to the production of pristine BN, without complicating it further.

In addition, characterisation of BN samples is important for an increased understanding of its nanoscale structure and bulk chemistry properties. The remaining part of this chapter (section 3.3) will proceed with a brief description of various techniques used to identify BN properties and its performance for CO_2 capture.

3.2. Porous BN synthesis

Porous BN powders were synthesised with a bottom-up approach in a wet chemistry laboratory. In the first step, the mixture of solid precursors containing nitrogen sources (urea or melamine) and boron sources (boric acid or boric acid-borax) were either dissolved and heated in ultrapure water or a mixture of water-methanol solvents. Then the dried powders were placed in alumina boat crucible and transferred into a tubular furnace for thermal decomposition. The tubular furnace was a PTF series Protherm, equipped with a quartz horizontal tube with 20x500 mm dimensions. An illustration of the pyrolysis setup with tubular furnace is shown in Figure 3.1. For all the samples in

this pyrolysis procedure, the precursors were heated for three hours under nitrogen (oxygen free cylinder, BOC Ltd) at a flow rate of 100 mL/min during the reaction time. The program controller Eurotherm 3208 Series was set up to gradually increase the temperature from the room temperature to 1173 K at rate of 5 ºC/min with three hours dwelling time, and then to naturally cool the furnace to ambient temperature at the same rate. In order to avoid air from entering the tube, both ends of the furnace were tightened with flange cuffs. Moreover, gas bubbler filled with water was used at the outlet gases. Hereby, it should be emphasised that in both modification strategies, the extra precursors, Pluronic P123 triblock copolymers (Mn _ 5800, Sigma-Aldrich) and Ni $(NO_3)_2.6H_2O$ (Aldrich, 99%) were added to the mixture of BN precursors before the heat-treatment process. This led to prevention of pores being filled and the porous order structure from being weakened.

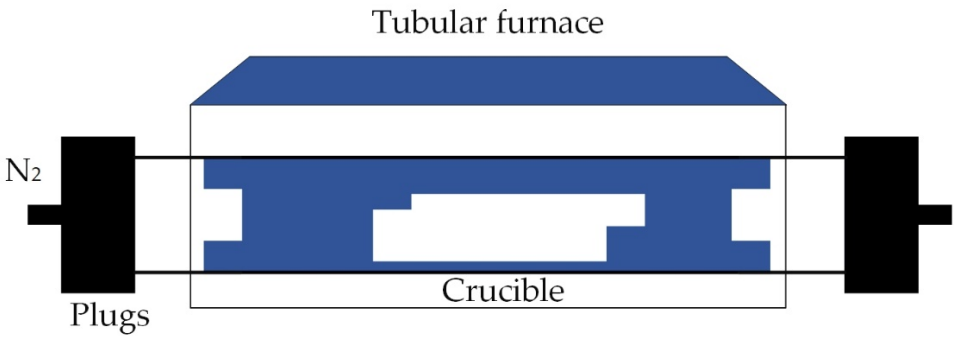

Figure 3.1 Schematic of tubular furnace for pyrolysis process

3.3. Characterisation techniques

3.3.1. Crystalline structure: X-ray diffraction

X-ray diffraction (XRD) is a technique, which is widely used for characterisation of unknown crystalline solid materials (e.g. minerals, inorganic compounds). This technique has the potential to determine the crystal structure and atomic spacing. The regular structures of solid are examined by X-ray diffraction (XRD). Therefore, amorphous materials are not traceable in a diffraction pattern. Powder samples for XRD analysis are homogenised and finely grounded prior to the operation. The X-rays are diffracted at different angles (θ) when their atoms strike on a crystal lattice. These diffractions are associated with planes of atoms and are detected by scanning the sample in a range of 2θ angles (Figure 3.2.). The position and intensity of diffraction

peaks are determined by the distance between the parallel set of planes of atoms (d_{hkl}) and the atoms configuration in the entire crystal, respectively. Moreover, the Miller indices (*hkl*) of diffraction peaks are analysed in XRD data to identify different planes, such that each d_{hkl} attributes to a family of lattice plane. Then, the Bragg's law (1) calculation is used to provide the *d*-spacing of planes from the following equation:

$$n\lambda = 2d\ sin\theta \quad (1)$$

Where:

θ: is the angle of incidence X-ray;

n: is an integer;

λ: is the wavelength;

d: is the spacing between atom planes;

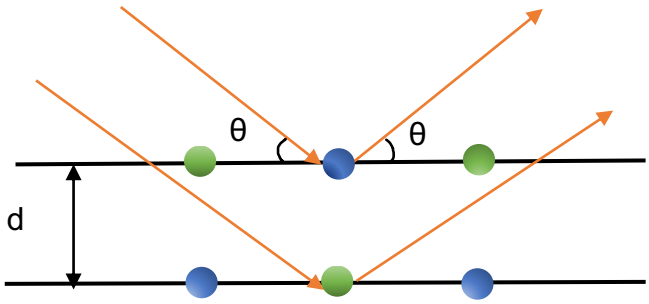

Figure 3.2 X-ray diffraction (XRD) principle

Powder X-ray diffraction (XRD) was performed using an X-ray diffractometer (Bruker D8 Advance) in reflection mode. The operating conditions ran at an anode voltage of 40 kV and an emission current of 40 mA using monochromatic Cu Kα radiation and fixed X-ray wavelength (λ= 1.541 78 Å). The diffraction data can be divided into two main peak positions (2θ) and intensities. The distinct limitation of powder diffraction compared to single crystal diffraction is that individuals' planes are not detectable in the former.

Crystal structures for BN materials are mainly consisted of hexagonal and turbostratic order. The XRD pattern in hexagonal boron nitride (h-BN) shows sharp peaks with high intensity; however, the turbostartic BN (t-BN) structure in XRD exhibited two broad peaks with low intensity. The unit cell lattice of sample phases is determined by measuring peak positions over the range of 2θ. The unique characteristic planes for t-BN are (002) and (100) which are also attributed to the presence of a few-layered boron nitride nanosheets. In addition, the interlayer spacing value (d_{002}) for hexagonal 2-dimensional BN is 3.33 A° which is obtained from XRD analysis (Alkoy *et al.*, 1997). For turbostratic materials, the degree of ordering increases (d_{002} spacing value) with decreasing its crystallization.

3.3.2. Bulk chemistry: Fourier transform infrared spectroscopy (FTIR)

Fourier transform infrared spectroscopy (FTIR) is a chemical characterisation method to identify chemical compounds, and functional groups. FTIR spectroscopy is a type of absorption technique based on molecular vibration mode with infrared light. The absorption occurs when photons have enough energy for excitation to the next vibration energy level while the infrared photons interact with a molecule with dipole change. All FTIR spectrometers rely on the Michelson Interferometer (the core of FTIR spectrometers). In an interferometer, the infrared waves strike a beam splitter, which passes light through the mirrors. After recombination of light with beam splitter, it absorbs a sample and conducts to the detector. The common region for infrared absorption spectroscopy is applied around 4000 cm^{-1} - 400 cm^{-1} since this region is the absorption radiation of most organic and inorganic ion compounds. The interferograms peaks are plotted into infrared adsorption spectrum as a function of absorption intensity (% transmittance) against the wavelength.

The chemical properties and intermolecular bonding of the BN material can be characterised by Fourier-transform infrared (FTIR) spectroscopy. The spectra of BN were recorded from 4000 to 400 cm^{-1} using a Nicolet Avatar 370 spectrometer equipped with an ATR diamond. First, the background spectrum needs to be collected, before collecting the single-beam spectra of the sample. The FTIR background spectrum is the information including the interferometer, detector, and source.

According to the data analysis of pure BN sample, the sample spectrum of absorption frequency is recognised as the normal mode of in-plane B–N and out-of-plane B–N–B vibration bonds.

3.3.3. Nano-scale morphology: Scanning electron microscopy (SEM)

A scanning electron microscope (SEM) is a type of electron microscope that is designed to make high quality images from bulk specimens. In general, the electron microscopes focus a beam of electrons instead of light on to a specimen, which yields the surface and composition information. The electron beam in SEM is accelerated and emitted from a filament (cathode) in electron gun and followed into the metal plate (anode) with a positive voltage in a range of 1 to 30 keV. Then, the sample is irradiated by the beam and the interactions occur inside the sample. These interactions are detected and transformed into an image. In particular, the characteristics to obtain through SEM examination are: (i) topography (the surface features of a sample and its texture) (ii) morphology (the shape and size of the particles making the sample) and (iii) composition (the elements and compound that the sample is composed and the relative amount of them). Most of the SEM instruments consist of following components:

- Electron gun (filament)
- Electromagnetic lenses
- Scanning coils
- Sample stage
- Detectors
- Vacuum system

The electron beam follows a path through the electromagnetic lenses in the column of microscope. Once it hits the sample, other electrons backscattered, and secondary electrons are ejected from the sample. Detectors collect the secondary or backscattered electrons and transfer them to a signal which produce an image. Furthermore, as can be seen in Figure 3.3, different signals occur when the incoming electron beam hits the sample. The secondary electron (SE) is generated from the collision between the primary electrons and the sample's outer electrons. Only

electrons close to the surface can escape due to SE low energy electrons (~10-50 eV) (Vernon-Parry, 2000). Contrary to SE, the backscattered electrons are generated with high energy electrons (elastic scattering)(Vernon-Parry, 2000). Therefore, images in backscattered electron have a lower resolution compared to secondary electrons (SE) and it is suitable for observing compositional difference. Characteristic X-Ray signals are emitted when an electron in the outer shell moves down and releases energy in the form of X-rays (Vernon-Parry, 2000). The amount of released energy in the X-ray is a function of the difference between shells of individual elements. Therefore, the Energy Dispersive X-ray Spectroscopy (EDX) can be utilised in order to collect the released energy and in order to highlight the chemical compositions of the sample.

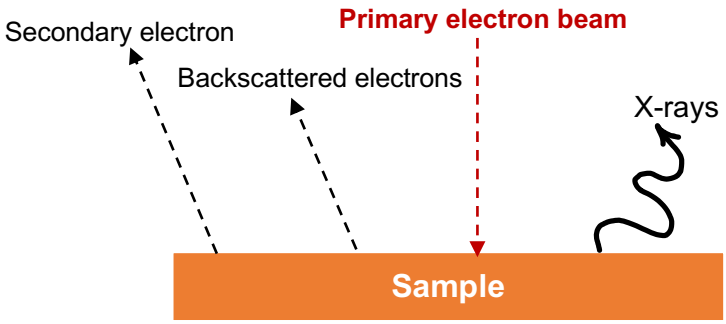

Figure 3.3 Signals from the sample in SEM

The morphology of porous BN samples was evaluated, using a scanning electron microscope (SEM, PEMTRON PS-230) in secondary electron mode (SE detector) at 10 kV. The microscope was equipped with an energy dispersive X-ray (EDX, OXFORD X-act) with energy resolution at 5.9 keV for the local elemental analysis. For imaging in the SEM, the specimen should be electrically grounded and conductive. To do so, the samples were ground, deposited on carbon tape, and coated (BIO-RAD sputter coater) with gold to reduce charging in the microscope.

3.3.4. Nano-scale morphology: Transmission electron microscopy (TEM)

Transmission electron microscopy (TEM) is another electron microscopy technique which is used to study the inner structures such as the growth of layers, crystal defects,

dislocations and grain boundaries. The magnifications in a TEM is much higher than an SEM and users can magnify their samples by more than 50 million times.

Similar to SEM, in a TEM microscope, electrons are produced from electron guns and pass through the samples, using magnetic lenses. Based on the angle of incident, the beam is partially transmitted and diffracted (Williams and Carter, 1996). The resultant beam is conducted through the magnetic objective lens and the aperture in order to eliminate the diffracted beam. Thus, the final image is obtained when the transmitted beam is passed *via* intermediate and projector lenses (Pennycook *et al.*, 2010). The magnified image is recorded on a fluorescent or CCD screen. This high contrast image is called Bright Field Image.

Porous materials may lead to more electron beams to pass as a result of their low-density properties. For porous BN, transmission electron microscopy (TEM) characterisation was carried out using a JEOL 1400 Plus. Generally, TEM sample preparation is quite a complex procedure and samples need to be very thin and flat. Prior to the test, finely ground samples were dispersed in *n*-octane and subjected to an ultrasonic bath and the suspensions are then dropped on carbon-coated copper grids for the TEM observations.

3.3.5. Textural properties: Nitrogen sorption isotherms at 77 K

The solid powder material exhibits different properties within its structure such as cracks, cavities and pores form its bulk form. These unique characteristics of powder were investigated *via* a volumetric Micrometrics surface area-measuring instrument at cryogenic temperature. The nitrogen adsorption/desorption isotherm plot is collected by calculating the amount of nitrogen adsorbed onto the sample with the volume and pressure sets data. Every standard profile of adsorption-desorption isotherm offers the gas uptake of the sample (low or high surface area) and the size of the pores (microporous – mesoporous or nonporous).

The Brunauer−Emmett−Teller (BET) theory continues to be the most widely used procedure for evaluating the surface area of porous materials (Naderi, 2015). The linear equation for the BET theory is:

$$\frac{P}{V_a(P_0 - P)} = \frac{1}{V_m C} + \frac{C-1}{V_m C}\left(\frac{P}{P_0}\right) \quad (1)$$

where V_a denotes the quantity of gas adsorbed at pressure P. The quantity of gas adsorbed due to a value of specific monolayer capacity is shown as V_m and P is the equilibrium pressure of the gas. C is a constant and P_0 is the saturation pressure of the gas.

The C value indicates the shape of isotherm in the BET plot, in which associated to the monolayer adsorption energy (Thommes *et al.*, 2015). According to the linear equation of the BET plot, a series of V_a *vs.* P/P_0 data points may be difficult to collect. In this case, some micrometrics instruments modify a single point linear in equation (1) to the smaller slope to yield the BET single point model as given in equation (2).

$$\frac{P}{V_a(P_0 - P)} = \frac{1}{V_m}\left(\frac{P}{P_0}\right) \quad (2)$$

Further gas adsorption analysis provides information of pore size (up to 300 nm), total pore volume, adsorption/desorption value, t-plot and micropore report. Based on the IUPAC classification, pores in microporous samples are defined as smaller than 2 nm, mesopores samples are between 2 nm and 50 nm and macropores samples are larger than 50 nm (Lowell *et al.*, 2004). Variation of gas sorption calculation methods is divided as follows:

- Micropore filling: Density functional theory (DFT) and Horvath-Kawazoe (HK), (P/P_o range:1×10^{-9} to 0.02).
- Monolayer complete: BET, Langmuir, (P/P_o range: <0.05 to 0.3).
- Multilayer formation: t-plot, (P/P_o range: > 0.1).
- Capillary condensation: Barret, Joyner and Halenda (BJH), (P/P_o range: > 0.35).

Pore volume distribution as function of pore size in a range of meso – and macropores (>2nm) is achieved using the Barret, Joyner and Halenda (BJH) method. The condition for calculating pore size distributions should be considered by reducing isotherms data about 0.05 P/P_o and saturation, where all pores are filled at 0.995 relative pressure. In addition, density functional theory (DFT) offers a modern, microscopic method based

on molecular simulation for both micro- and mesopores size range. While the BJH method underestimates pore widths of less than 10nm by a degree of up to 20% to 30%, a much more predictable pore size distribution analysis over the complete pore size range (micro-mesopores) can be performed by a DFT method (Cychosz *et al.*, 2017a).

The single point adsorption total volume of pores was calculated at P/P_0 = 0.95 - 0.98 close to unit, where all pores of samples are already filled with liquid N_2, using equation (3)

$$V_{tot} = \frac{P_{standard} V_{adsorbed} V_M}{RT} \quad (3)$$

where:

$P_{standard}$: standard pressure (10^5 Pa).

$V_{adsorbed}$: volume of nitrogen adsorbed at $P/P_0 \sim 1$

V_M: liquid molar volume of N_2 at 77 K (34.65 cm^3/mol).

R: gas constant.

T: standard temperature.

For BN samples, the nitrogen adsorption/desorption isotherms were carried out using a porosity analyser (Micromeritics ASAP2060) at 77 K. Prior to the measurement, the samples were degassed for 1 hour at 363 K followed by 18 hours at 423 K both under vacuum. Pore size distribution plots obtained from N_2 at 77 K by applying both non-local density functional theory (NLDFT) and Barret, Joyner and Halenda (BJH) methods.

3.3.6. Thermal stability: thermogravimetric analysis (TGA)

The basic principle of a thermal gravimetric analyser relies on heating a material under gas flow environment (air, N_2, CO_2, He, Ar, etc) at a defined rate. The mass of substance is monitored as a function of temperature or time (Brown, 2001). Most of the TGA instruments are dynamic TGA, in which the temperature continuously

increases at a constant rate and TGA monitors sample mass changes. The weight change versus temperature is plotted and it is known as a thermogravimetric curve or thermogram. This is a useful technique for testing the sample purity, thermal stability and chemical dehydration, decomposition analysis (Earnest, 1988). A differential scanning calorimetry (DSC) measures the heat flows of a sample as a function of temperature or time. DSC measurements provide information about physical and chemical changes of processes (exothermic or endothermic) and the heat capacity.

The thermal stability tests of BN samples were performed using thermal gravimetric analysis (TG-DSC), ultra-micro balance, Mettler Toledo, both investigating TG and DSC profiles. The apparatus consists of three major parts of a furnace including a microgram balance, an auto sampler and a thermocouple. An alumina crucible pan was loaded with 5-10 mg of sample material and heated from room temperature to 1173 K at a rate of 10 K/min in either air or N_2 atmosphere.

3.3.7. CO_2 sorption test: thermogravimetric analysis (TGA)

CO_2 adsorption-desorption test with temperature gravimetric analyser (TGA) is considered as a better option compared to the volumetric adsorption technique as it can be applied at high temperatures (≥ ambient temperature). Both CO_2 sorption of BN samples and their cyclic stability tests were conducted with TGA/DSC 3+ micro balance, Mettler Toledo. gravimetric instrument. Figure 3.4 presents a schematic representation of CO_2 test with thermogravimetric analyser. As can be seen in Figure 3.4, the TG profile curves are recorded, using an electronic microbalance and a furnace. The samples were placed into alumina crucible from the microbalance inside the furnace. Nitrogen flow gas (99.999%, 150 mL/min) is applied in drying (at 393 K for 6 hours) and stabilisation (298 K for 15 min) processes. Finally, the CO_2 capture capacity of the sorbents were collected after switching to the pure CO_2 (99.999%, 50 mL/min) flow, followed by measuring the mass uptake of the sample. Further details of the procedure on dynamic CO_2 testing with the BN synthesised materials will be given in Chapter 7.

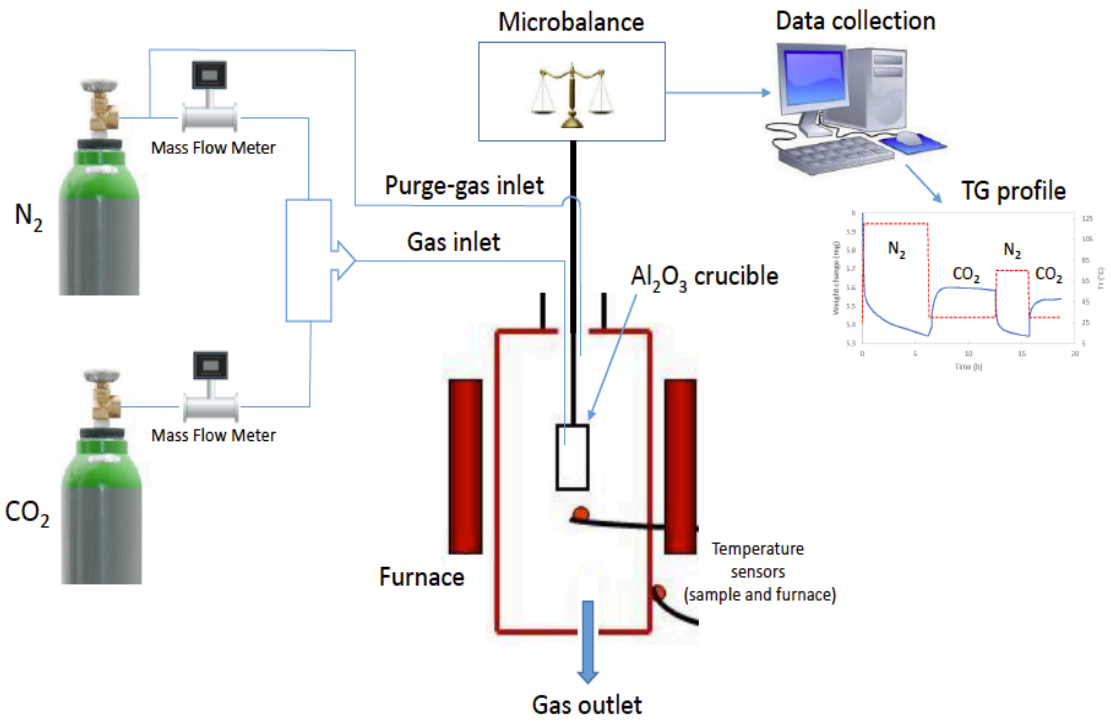

Figure 3.4 Illustration of CO_2 sorption experiment with thermogravimetric analyser

3.4. Conclusions

In summary, the methodological approach taken in this study is a mixed methodology based on building new BN adsorbents, characterisation processes and BN adsorbents screening to assess their productivity and working capacity in carbon capture applications.

Data for this study were collected using various techniques such as X-ray diffraction (XRD), Fourier transform infrared spectroscopy (FTIR), electron microscopy instruments (SEM-TEM), nitrogen adsorption-desorption isotherms and thermogravimetric analysis (TGA) to name a few. This chapter has demonstrated that each of these characterisation and process techniques are particularly useful in studying properties such as material's morphology, size, structure, chemical properties, stability and gas adsorption performance. A major advantage of using gravimetric analyser for CO_2 adsorption is that it can be applied in a wide range of temperatures above 298 K as a fixed-bed reactor in carbon capture technologies.

CHAPTER 4

PRECURSOR-MEDIATED SYNTHESIS OF POROUS BORON NITRIDE

Outline of the chapter

This chapter discusses the impact of different reactants on production of pristine porous boron nitride. Experimental procedure and samples characterisation are also considered in this chapter. The effect of urea composition ratio, with two different solvents composition and using multiple boron precursors on the structure, surface chemistry, stability and textural properties of porous boron nitride are extensively explained. The chapter is organised as follows:

4.1. Introduction

4.2. Materials and synthesis

4.3. Effect of urea proportion on porous boron nitride

4.4. Effect of solvent on Porous BN

4.5. Effect of using multiple boron precursors on porous BN

4.4. Conclusions

4. Precursor-mediated synthesis of porous boron nitride

4.1. Introduction

Both template and template-free methods can lead to porous boron nitride with variation of morphologies and structure such as nanorod (Zhang *et al.*, 2006), nanofibers (Lin *et al.*, 2016), (3D) BN foam (Maleki *et al.*, 2016) and Layered nanosheets (Wang *et al.*, 2018a) to name a few. As indicated in the literature review chapter, numerous soft (dodecyl trimethyl ammonium chloride (DTAC) cetyl-trimethyl ammonium bromide (CTAB), hard (silica, activated carbon, zeolites) and dynamic (Magnesium diboride (MgB_2) templates were commonly used as templates during production of porous BN materials (Zhang *et al.*, 2014, Ning *et al.*, 2016, Xiao *et al.*, 2016). However, these approaches have several limitations such as impurity and lower surface area obtained in final the products. Therefore, various process conditions were made based on non-template strategy in order to obtain a higher specific surface area (SSAs) and porosity with less synthetic steps and impurities compared to the template method. The majority of previous studies employed a wet chemical reaction of boron and nitrogen precursors followed by high temperature treatment (pyrolysis) under either a nitrogen, an ammonia or nitrogen/hydrogen atmosphere (Song *et al.*, 2017, Weng *et al.*, 2014, Maiti *et al.*, 2017). Despite the fact that changing the morphology and structure of porous BN are easier using the template method, using the non-template procedure can also result in diverse structural features of BN nanomaterials. This variation can be achieved by changing precursors, their molar ratio, temperature and solvent during non-template techniques. Thus, it is essential to study different synthetic conditions during the fabrication process in order to achieve well-defined porous BN for a specific purpose. So far, very little attention has been paid to investigate the role of precursors in controlling BN properties in terms of morphology, chemistry and porosity. Both boron and nitrogen precursors and their usage amount share a number of key features in creating porous structural networks of BN. Moreover, if BN is to be applied in gas adsorption applications, it is important to obtain a certain level of control over its porosity and microscale properties. Given that, the following part of this chapter moves on to describe how to select different experimental conditions, which may provide a high impact on the porosity of the final products.

In what follows, the role of using different precursors with different molar ratios will be discussed as well as solvent-mediated on the porosity, structure and chemistry of BN

via template-free method. This approach produced porous BN materials, which are practical for gas adsorption properties. Characterisation of samples is important for better understanding of their properties. To do so, a number of techniques including X-ray Diffraction Pattern (XRD), Fourier Transform Infrared Spectroscopy (FTIR), Raman, Scanning Electron Microscopy (SEM/EDX), Transition Electron Microscopy (TEM) and nitrogen adsorption/desorption isotherms were applied for each of the samples. This chapter provides a deeper understanding of pure BN formation through template-free method.

4.2. Materials and synthesis

Porous boron nitride was synthesised with a two-step method of solvent evaporation and high thermal decomposition (detail of the methodology is discussed in Chapter 3). In the first step of precursor-mediate, various amounts of urea (for synthesis, Sigma-Aldrich) and boric acid (ACS reagent, Sigma-Aldrich) in molar ratios of 15:1 and 30:1 were dissolved in a mixed solution containing 20 ml of methanol (analytical standard, Sigma-Aldrich) and 20 ml of water at 338 K (Figure 4.1). Furthermore, to evaluate the solvent's impact on the production of BN materials, porous BN was prepared with 50 ml of distilled water without using methanol under the same conditions. In the second step, multiple-B precursors were applied using boric acid (ACS reagent, Sigma-Aldrich), borax (99%, Sigma-Aldrich) and urea (for synthesis, Sigma-Aldrich). All the solutions were heated and stirred vigorously until a white powder was obtained and were further dried in an oven at 338 K for 24 hours. Finally, these powders were loaded in alumina boat crucible and heated in a tubular furnace under nitrogen flow from room temperature to 1173 K at the rate of 8 K min^{-1}. This temperature was maintained for three hours followed by cooling to the room temperature at the rate of 8 K min^{-1}. All the prepared samples are shown in Table 4.1 with different composition ratio of reactants.

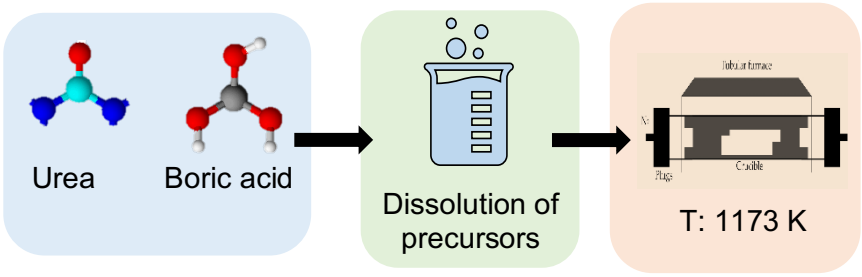

Figure 4.1 Template-free synthesis schematic of h-BN

Table 4-1 Sample notation of porous h-BN fabricated under different conditions

Sample	Urea (mol)	Boric acid (mol)	Borax (mol)	Solvent
BU_{15}	15	1	–	Methanol/Water
BU_{30}	30	1	–	Methanol/Water
BU_{30}	30	1	–	Water
$BU_{15}B_1$	15	1	1	Methanol/Water

4.3. Effect of urea proportion on porous boron nitride

This section reviews the effects of different urea molar ratios on BN structure, chemistry and porosity. The optimisation of urea proportion is essential in order to obtain high specific surface area and proper structure for the application of gas adsorbents properties.

4.3.1. Analysis of structural, chemistry and porosity features

In the first investigation of applying different urea proportions, X-ray diffraction was performed to find out the structural properties using an X-ray diffractometer in reflection mode. In typical XRD patterns, the results of both samples displayed clear peaks around 2θ ~ 26° and 42°, which are attributed to the (002) and (100) reflections corresponding to hexagonal boron nitride (Figure 4.2a) (Kurakevych and Solozhenko,

2007). The weak crystalline B_2O_3 peaks appeared around 2θ ~ 15° for the sample with lower urea molar ratio was removed by utilising a higher amount of urea. It seems possible that these peaks appeared during the dehydration of boric acid that were formed as a residual B_2O_3 (Balci *et al.*, 2012). Notably, the peaks of both samples reveal the presence of turbostratic and amorphous materials (Alkoy *et al.*, 1997). It is interesting to note that in most cases of the template free conditions, turbostartic crystalline orders were reported in the literature. We believe that if the purpose of using these materials is for adsorption properties, the low crystalline order is a more favorable option. This is due to the fact that in this type of structure, the defects appearing on porous surfaces may improve the adsorptive performance.

Moreover, the chemistry of samples was analysed using FTIR spectroscopy. As shown in Figure 4.2 (b), both peaks exhibited two main characteristic bonds of boron nitride at ~ 1360 and 800 cm^{-1} corresponding to in-plane B-N transverse optical mode and out-of-plane B-N-B bending mode, respectively (Geh *et al.*, 1966). The small peak observed around ~ 2300 cm^{-1} for the sample with lower amount of urea is due to the presence of CO_2 and can be ignored. The results show that there is not a significant difference between the two samples in this chemical feature analysis. In total, the structural and chemical results of both samples, indicating a successful preparation of BN material *via* template-free method.

The characteristic feature of pore strucure is vital and needs to be investigated for sorbent materials. Therefore, In order to find a proper sample for CO_2 adsoprtion properies, the materials were characterised by nitrogen sorption isotherm at 77 K. The isotherms and the resulting pore size distributions are shown in Figure 4.2 (c). The plot for boric acid/urea 1:30 has been moved vertically upward. Thus, the surface area increases with an increasing proportion of urea in the reaction mixture. A possible explanation of this finding is the decrease in the number of layers which previously reported by Nag *et al.*, (2010). The resultant BET SSAs were 85 and 753 m^2/g for boric acid/urea ratio of 1:15 and 1:30, respectively. Moreover, what can be clearly observed in Figure 4.2 (c) is the growth of microporosity in BU30 sample. This remarkable change in textural parameters demonstrates the influence of urea as a nitrogen precursor on BN pore structure. Therefore, with the findings in this section, one could suggest that the amount of nitrogen precursors is a practical issue to direct the material to micro porosity scale.

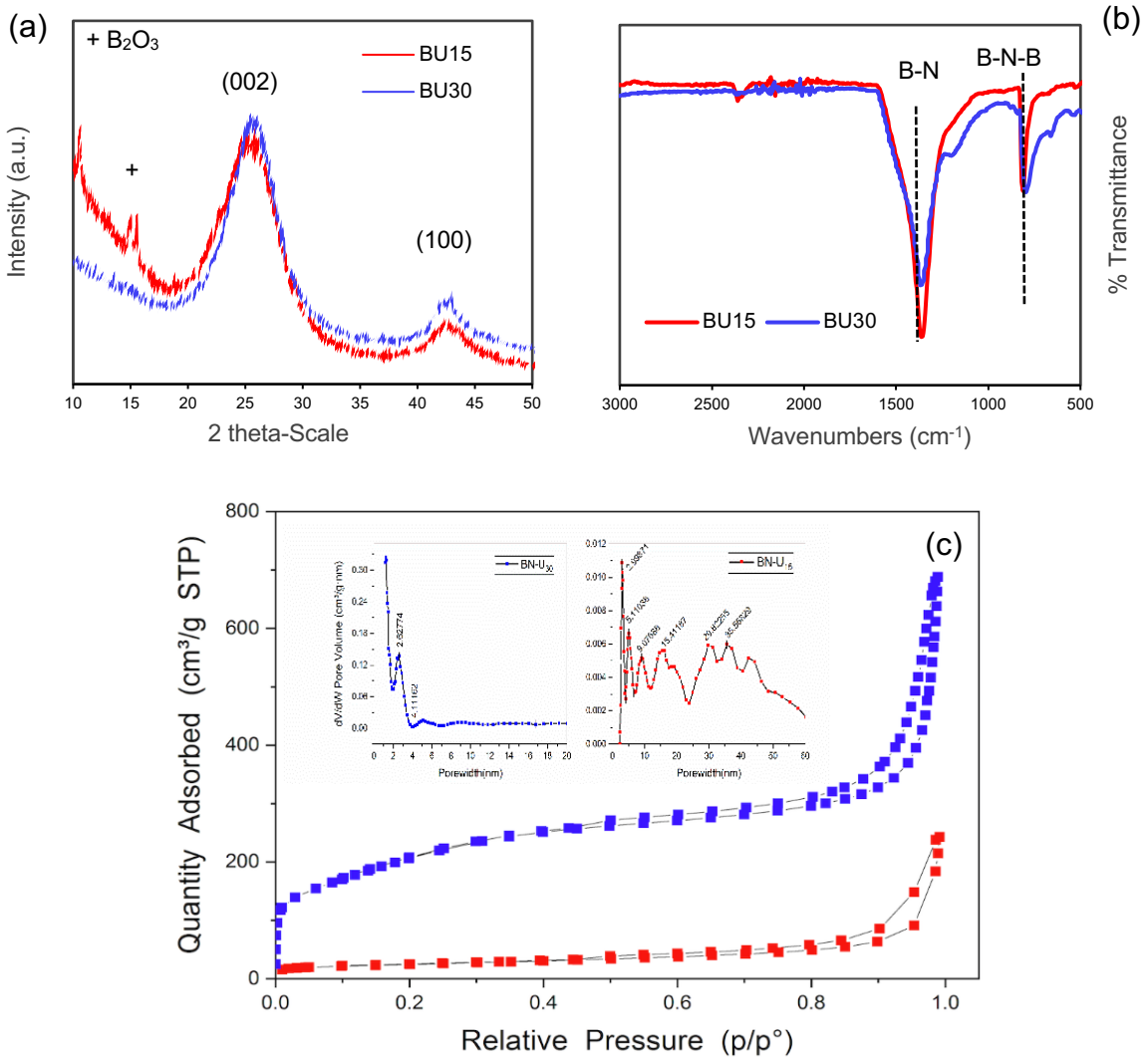

Figure 4.2 (a) XRD patterns; (b) FTIR spectra and (c) Nitrogen sorption isotherm at 77 K (insert shows pore size distribution) of BN samples using different urea proportion.

4.3.2. Analysis of morphology

SEM images for both samples are shown in Figure 4.3(a, b). Noticeably, despite the quite similar structural results found in the previous section, the samples exhibited different morphologies with regards to various levels of urea. Images in Figure 4.3(a, b) show the thin layered-like morphology for the porous BN using high urea molar ratio, whereas the rod shape with visible macropores was observed for porous BN with lower urea molar ratio. Additionally, to get a better insight into the BN micro scale, Transmission Electron Microscopy (TEM) was used for the BU_{30} sample, which showed thin layers of boron nitride that were rolled and knotted, creating an ideal substrate (Figure 4.4a-d). Micrographs were collected in bright-field (BF) mode and

with different magnifications (from 1 μm to 100 nm). Figure 4.4 (a) illustrates tiny nanoparticles with sizes less than 10 nm where homogeneously dispersed (blue dashed circles).

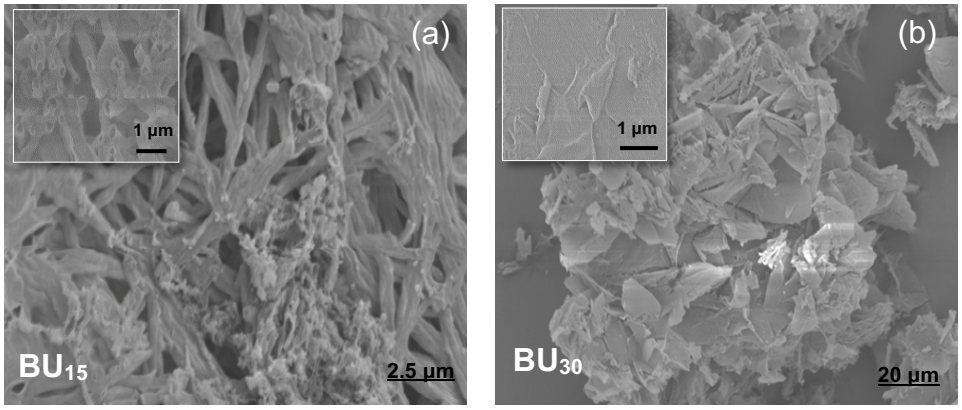

Figure 4.3 (a) SEM images of BU15 and (b) BU30

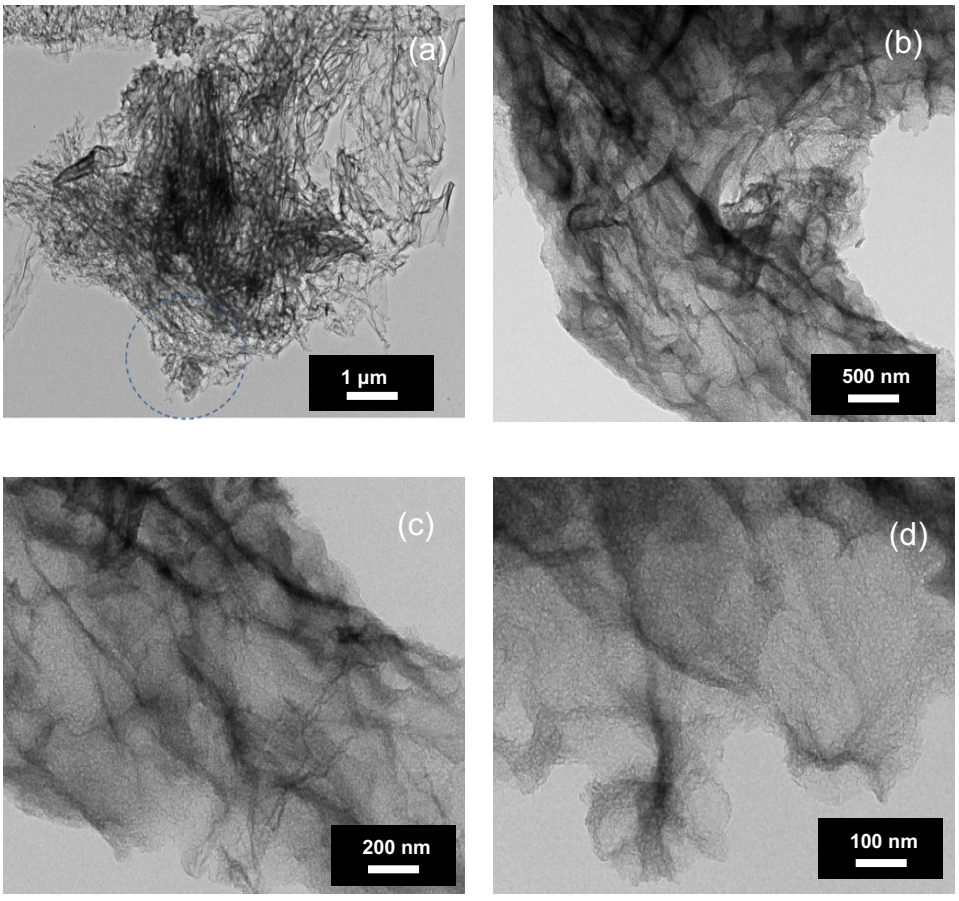

Figure 4.4 TEM images for BU30 sample (a-d)

4.4. Effect of solvent on Porous BN

This section investigates the impact of using two different types of solvent during the thermal evaporation step on the production of porous BN. As it can be seen in Table 4.1, BU_{30} was synthesised in a mixture of both water and water/methanol followed by high thermal decomposition process. The significance of this study is linked to the CO_2 adsorption result, which will be discussed in more detail in chapter 7. Potential readers should note that the importance of this aspect on catalytic activities of BN was highlighted by Wu *et al.*, (2016b) which shows that a low boiling point of solvent has the potential to accelerate the recrystallization of urea, further increasing the higher SSA of BN.

4.4.1. Analysis of chemical features and porosity

Chemical composition of both samples (boric acid and urea with a molar ratio 1:30 dissolved in distilled water and water/methanol) were characterised by EDX. As can be seen in Figure 4.5 (a, b) both samples were composed of similar boron (B), nitrogen (N) and oxygen (O) elements. This observation may specify that solvents have no major effect on the chemical compositions of porous BN. However, the thermal stability of samples indicated different degradation behaviours using TG analysis (Figure 4.5c). BN-water/methanol is stabilised and reached saturation point (plateau) around ~ 600 K, whereas the BN-water sample continuously losing weight before ~ 948 K where it becomes stabilised.

Further exploration of using different solvents was determined by N_2 adsorption at 77 K. The isotherms in Figure 4.6(a) belongs to type II /IV based on IUPAC classification and type H3 hysteresis loops indicate the presence of disordered micro and mesoporous adsorbents. What is striking in Figure 4.6(a) is the sharp rise of isotherms in low relative pressure for BN-Water/Methanol sample, which indicates presence of microporous structures. According to the non-local density functional theory (NLDFT) shown in Figure 4.6(b), BN-Water/Methanol sample underline the prominent formation of highly microporous structures, while a significantly lower microporosity (almost zero) was observed for the sample synthesised with water as a solvent. The BET surface area of BN-Water/Methanol and BN-Water are reported as 753 m^2g^{-1} and 102 m^2g^{-1} respectively. This result could be explained by the fact that the porosity of BN materials

remarkably decreases *via* dissolution of the precursors in water. Understanding the role of large surface area and the effect of using different solvents on CO_2 adsorption properties of BN are crucial and will be investigated in Chapter 7.

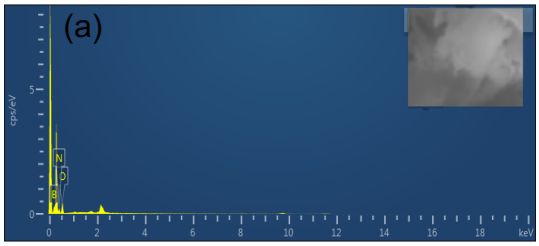

Element	Weight %	Atomic %
O	28.51	23.17
N	33.35	30.97
B	38.14	45.86
Total	100	100

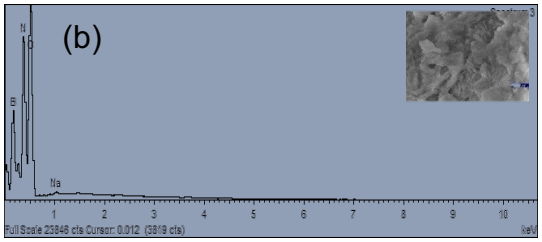

Element	Weight %	Atomic %
O	29.98	24.45
N	32.76	30.54
B	37.27	44.98
Total	100	100

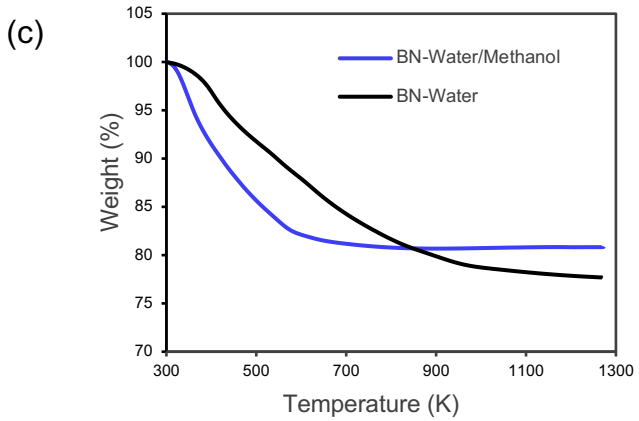

Figure 4.5 EDX spectra and corresponding atomic % of elements for BN-Water and BN-Water/Methanol samples (a, b); TG curves of the same samples (c)

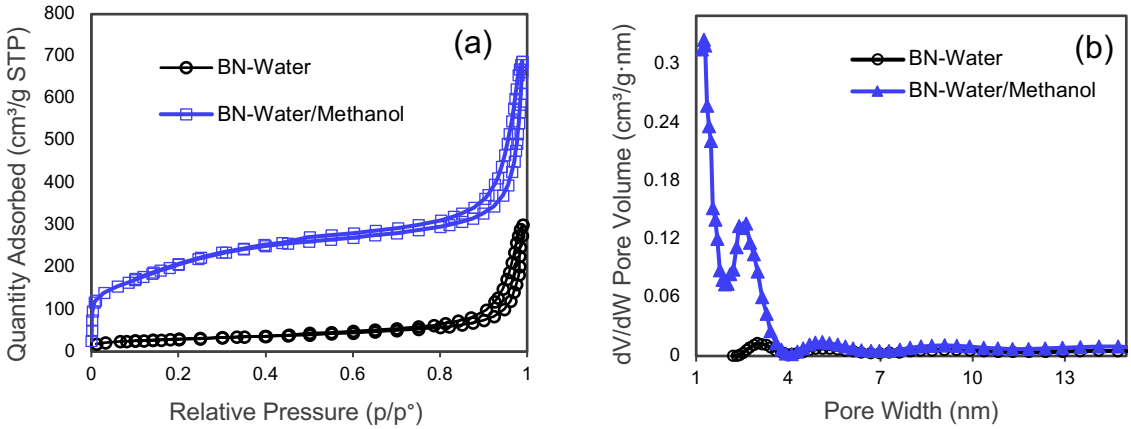

Figure 4.6 (a) Nitrogen sorption isotherm at 77 K and (b) NLDFT pore size distribution of BN sample produced using different solvents

4.5. Effect of using multiple boron precursors on porous BN

The influence of nitrogen sources and use of various solvents during the fabrication process on porous BN have been investigated so far. This section is looking at the effect of using multiple boron precursors on the structure, chemistry and porosity of BN. Moreover, after proceeding the experimental procedures of this plan, the section has argued whether using multiple boron sources can be a successful way to synthesise pure BN as it is able to be applied in gas adsorption properties.

Herein, borax was used as a secondary B-precursor together with boric acid (Table 3.1.). In this experiment, after heating, boron sources ($Na_2B_4O_7.10H_2O$ and H_3BO_3) were transformed into $Na_2O.2B_2O_3$ and B_2O_3 respectively, as governed by chemical reaction type (1) and (2) (Zhang *et al.*, 2015a). At 948 K, solid Na_2O played the role of supporting structure and H_3BO_3 helped Na_2O particles to move and rearrange themselves by pervading into the interior of the structure.

$$Na_2B_4O_7.10H_2O \longrightarrow Na_2O.2B_2O_3 + 10H_2O \quad (1)$$

$$2H_3BO_3 \longrightarrow B_2O_3 + 3H_2O \quad (2)$$

4.5.1. Analysis of structural, chemistry and porosity features

Contrary to our expectations, the XRD result of multiple boron sources indicates a significant difference to other XRD findings reported so far. As shown in Figure 4.7. (a) the d-spacing was decreased by using multiple boron source precursors and a more crystalline nature of material was formed (Figure 4.7a). It can be concluded that using borax leads to promote ordering from t-BN to h-BN (Ning *et al.*, 2016). The XRD pattern highlighted that the use of multiple boron source components had no effect on phase composition to form BN (according to the Powder Diffraction File (PDF) 00-009-0012). In order to confirm further structural analysis, the sample was analysed by Raman spectrometry. The peak at ~ 1373 cm^{-1} is detected in Figure 4.7 (b) which corresponds to the B-N vibration mode (E_2g). In addition, the chemical analysis of the sample was characterized using FTIR spectra. Peaks in Figure 4.7 (c), displayed no evident change compared to single boron used precursor. Similar to the previous FTIR results which were pointed out earlier, two broad peaks around ~ 1365 and 750 cm^1

are assigned to in-plane B-N transverse optional modes of hexagonal boron nitride and N-B stretching vibration modes respectively.

It could conceivably be hypothesised that the observed difference in crystallinity between single and multiple B precursors could influence the particle size as well as morphology aspects of materials. To investigate this, the N_2 adsorption-desorption isotherms were carried out for two samples (BU_{15} and $BU_{15}B_1$) with similar proportions of urea to boric acid (1:15 molar ratio boric acid/urea) with two types of boron sources, being single and multiple boron sources (Figure 4.8a). The most important result of this section is that the BET surface area obtained for the $BU_{15}B_1$ sample ($BU_{15}B_{1SSA}$ = 34 m^2/g) which is the lowest specific surface area (SSA) among the pristine BN samples. This finding, while preliminary, suggests that the use of borax leads to creation of materials with lower surface area and porosity for multiple B-precursors. Moreover, the sample, as shown in Figure 4.8 (b, c), exhibited plate-shaped morphology in SEM images. Comparison of the findings with those of other reported in this chapter confirms that the current sample is not a proper candidate for adsorptive application. To get a better view of the material properties of this sample, its performance has been investigated and will be explained in detail in Chapter 7.

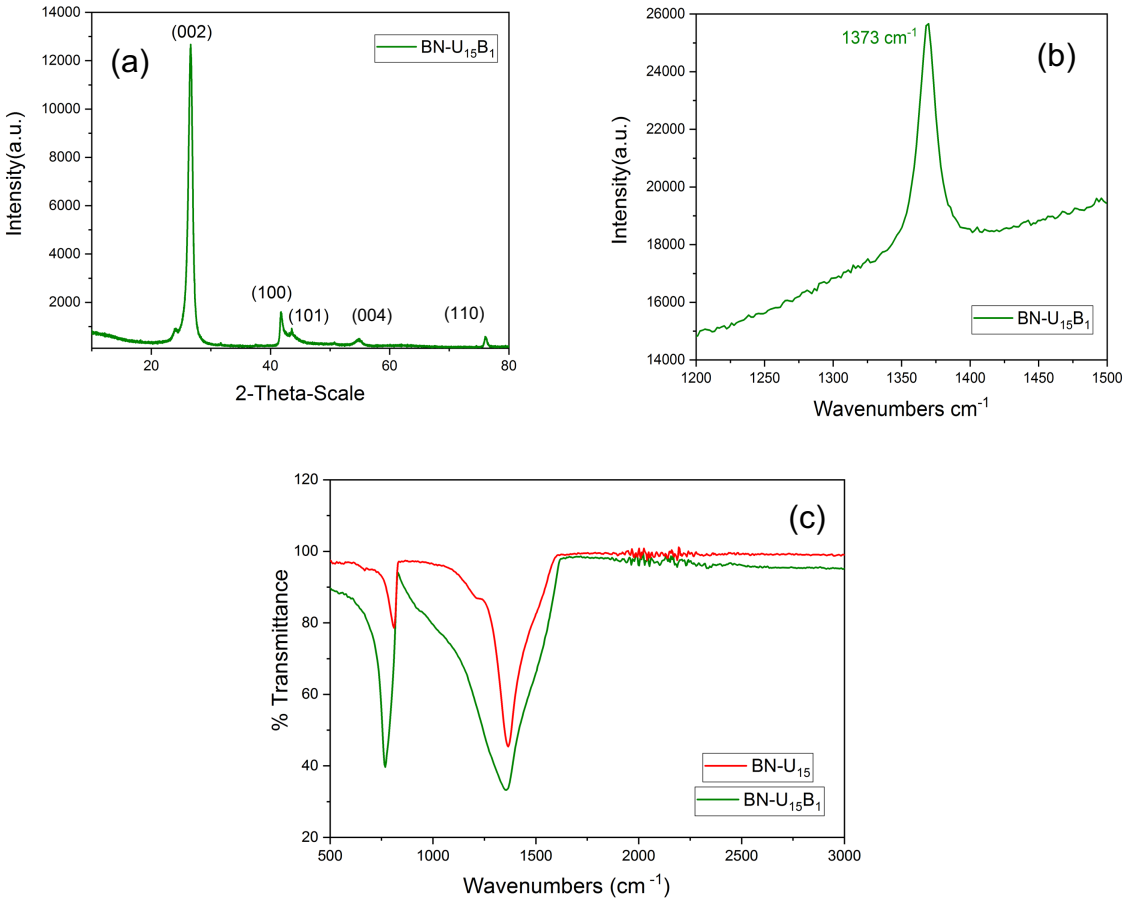

Figure 4.7 (a) XRD; (b) Raman spectra and (c) FTIR analysis for sample $BU_{15}B_1$

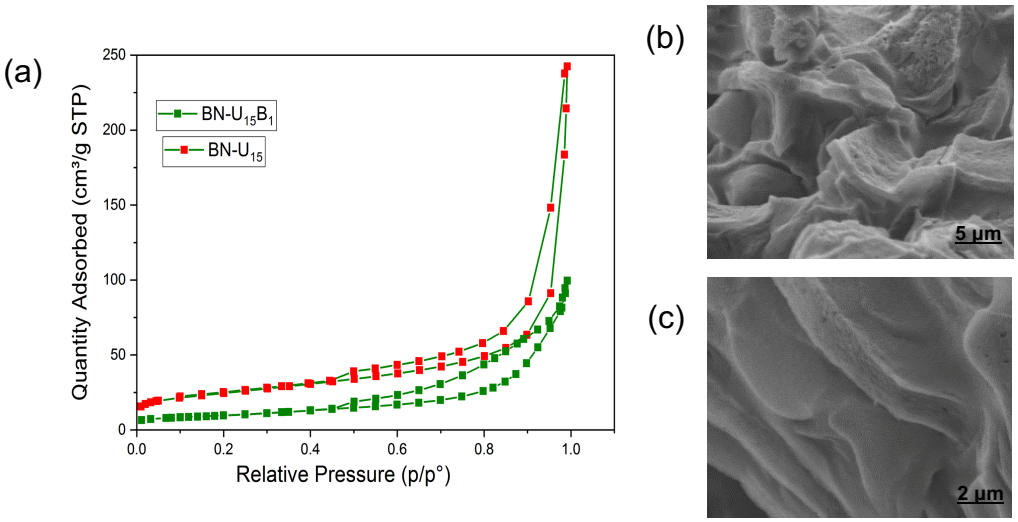

Figure 4.8 (a) Nitrogen sorption isotherm at 77 K for BU_{15} and $BU_{15}B_1$ and (b, c) SEM images of $BU_{15}B_1$

4.6. Conclusions

An initial objective of the project was to synthesise pure porous BN materials (without using modification steps) and to identify some practical samples for modification steps and consequently, conduct CO_2 adsorption tests (which will be discussed in the following chapters). To this end, an overview of research on precursor-mediate synthesis of boron nitride in terms of synthesis, structure and properties has been presented in this chapter. The first set of experiments in section 4.3 established that using an excess of urea as a nitrogen source is essential to create a higher porosity, which is one of the criteria for adsorptive applications. Therefore, the highest specific surface area, which is recognised in this chapter, belongs to the BU_{30} methanol/water sample of about 753 m^2/g. According to SEM results, a difference was observed in morphology between samples with higher and lower use of urea proportion. While the layered structure obtained with lower proportion of urea, the rod-like morphology observed for the sample with lower consumption of urea. It is difficult to explain this result in detail; however, it would suggest that it is related to thermal decomposition of urea during the pyrolysis step, which might lead to obtaining various shapes. Other characteristics in terms of structure and chemistry features of these two samples are shown to be relatively the same.

Furthermore, dissolution of precursors in the mixture of methanol/water had significant impact on obtaining the high SSA as discussed in section 4.4. There were also slight changes detected in the thermal analysis of samples with two different procedures of solvents usage. In particular, the analysis of thermal stability was performed to show the thermal stability of pristine BN.

In section 4.5, the preparation of BN with multiple boron sources turned to an enhanced hexagonal structure of these materials with clean plate shape, while the SSA sharply diminished. The main disadvantage of the experimental method is that the production of pristine BN has a relatively low porosity and surface area when borax is used as a second sources of boron precursors.

Overall, the studies presented thus far considered possible influences of using different precursors on porous BN structure, chemistry and porosity networks. Owing to the essential properties of solid sorbent materials, it is postulated that the formation of BN with higher porosity and SSA is more favorable for CO_2 adsorption.

CHAPTER 5

METAL-FREE MODIFICATION OF POROUS BORON NITRIDE

Outline of the chapter

This chapter focuses on metal-free modification strategy to achieve highly porous BN with tuneable porosity, which is useful in carbon capture applications. Moreover, experimental methods and sample characterisation are considered in this chapter. The effect of adding Pluronic P123 triblock copolymers surfactant as an extra reactant on porous BN materials properties is discussed. The chapter is organised as follows:

5.1. Introduction

5.2. Materials and synthesis of porous BN using structure directing agent

5.3. Results and discussion

5.4. Conclusions

5. Metal-free modification of porous boron nitride

5.1. Introduction

Carbon capture based on dry sorbent materials requires development of robust and reusable solids for a long-term deployment. Recently, porous boron nitride materials have gained renewed interest to be applied for carbon capture due to their cost-effectiveness, high chemical stability and ease of production. Despite these properties, most of the researchers on this topic take extra attempts to control BN material properties to develop its performance. The relatively low efficiency of pure BN (without taking surface functionalisation/modification steps) to CO_2 molecules is likely to be related to its pore size and surface area properties. However, from a theoretical perspective, there are evidences suggesting weak interaction of Lewis acidic molecules and electron deficiency of boron atoms in B-N bonds (Choi *et al.*, 2011; Sun *et al.*, 2013; Paura *et al.*, 2014; Tan *et al.*, 2016).

The characterisation results of the designed pristine porous BN samples in the previous chapter suggested potential of BN as a good candidate for CO_2 capture/release with high chemical and thermal stability. Now, a key issue is to take a further challenge to promote a better porous BN adsorbent. In this case, one of the main objectives is designing porous BNs to achieve a material with a high surface area and porosity for CO_2 adsorption, which is discussed in the current chapter. Evidences in Chapter 4 indicate that precursor is among the most important synthetic factors for creating pores. It can therefore be assumed that adding an extra precursor into boron and nitrogen sources may change porous BN construction. Some approaches have deliberated the impact of tri-block copolymers on creation of porosity during the decomposition process of BN materials (Li *et al.*, 2013; Xiong *et al.*, 2016; Xiong *et al.*, 2017). Although the above studies utilised surfactant directing-agents to develop activated porous BN with outstanding porosity, a debated question is whether this strategy (metal-free modification of BN) is beneficial for the CO_2 adsorption process.

To address this question, in this chapter, we selected Pluronic P123 triblock copolymers to tune the pristine BN samples, aiming at enhancing the adsorption performance. Metal-free modification of porous boron nitride (BN) was carried out by simple heat treatment procedure under N_2 flow. This synthetic procedure relies on using triblock copolymer P123 during the precursors evaporation step of BN and does not show major impurities (Xiong *et al.*, 2016).

The following section (section 5.2.) is a brief description of the method and the raw materials, which were used during the process. Then the characterisation results on urea-based and melamine-based BN modified sample are described in section 5.3 in terms of structure, morphology, chemistry, optical and textural analysis. The characterisation results of these two modified samples will be compared and discussed by pure BN sample (without applying modification step). This chapter aims to contribute to this growing area of research by exploring the new formation of porous BN.

5.2. Materials and synthesis of porous BN using structure directing agent

Metal-free modified BN was synthesised with a two-step method of solvent evaporation and high thermal decomposition. Boric acid (ACS reagent, Sigma-Aldrich), urea (for synthesis, Sigma-Aldrich) or melamine (99%, Sigma-Aldrich) and Pluronic P123 triblock copolymers ($M_n \approx 5800$, Sigma-Aldrich) based on poly (ethylene glycol)-poly (propylene glycol)-poly (ethylene glycol) were used as raw materials. In detail, urea: boric acid and urea: melamine with molar ratios of 30 and 4 were mixed and dissolved with deionised water. The urea ratio was chosen based on previous results in Chapter 4 as it is more effective for adsorptive performance. Then, 0.5 g of P123 was introduced into the mixture solution and heated up at 338 K under vigorous stirring. A white precipitate was obtained after complete evaporation of water at that temperature. Afterwards, the precursor was dried in the oven for 24 hours and annealed at 1173 K under N_2 gas (the flow rate was 150 mL/min) for three hours. The heat treatment step is vital to achieve the porous samples, as discussed in Chapter 4. Finally, modified porous BN were collected with two different nitrogen precursors. For comparison, pristine BN was also prepared following the same procedure without adding any surfactant.

5.3. Results and discussion

In this section, we considered modified urea-based BN sample first which was named BN-P123. A number of techniques were employed to determine the influence of using

structure-directing agent over porous BN structure, chemistry and textural properties. In order to get a better understanding of the role of P123, all these results were also associated with pristine BN. Furthermore, the effect of P123 on the chemistry, morphology and pore structure of melamine-based BN sample was discussed. This sample was performed to estimate the different features of BN using various nitrogen sources.

5.2.1. Morphology and chemical features of modified urea-based BN

The morphology of the samples was studied using scanning electron microscopy (SEM). The pristine BN exhibited an ultrathin flake-like morphology, as displayed in Figures 5.1(a, b). Two SEM images as well as the insert of BN-P123 presented a similar shape to pristine BN with a cloud-like sheet structure and interconnected network of porous structures (Figures 5.1c, d). To compare samples chemical properties, the formations of pristine BN and BN-P123 were studied by EDX and elemental mapping (Figures 5.2 a, b). From the results, it is obvious that the product is mainly comprised of boron (B), nitrogen (N) and oxygen (O). The EDX results in Figure 5.2b shows a slight increase in the BN-P123 sample in terms of oxygen content compared to pristine BN. The observed increase in oxygen may be due to the introduction of P123 into BN formation.

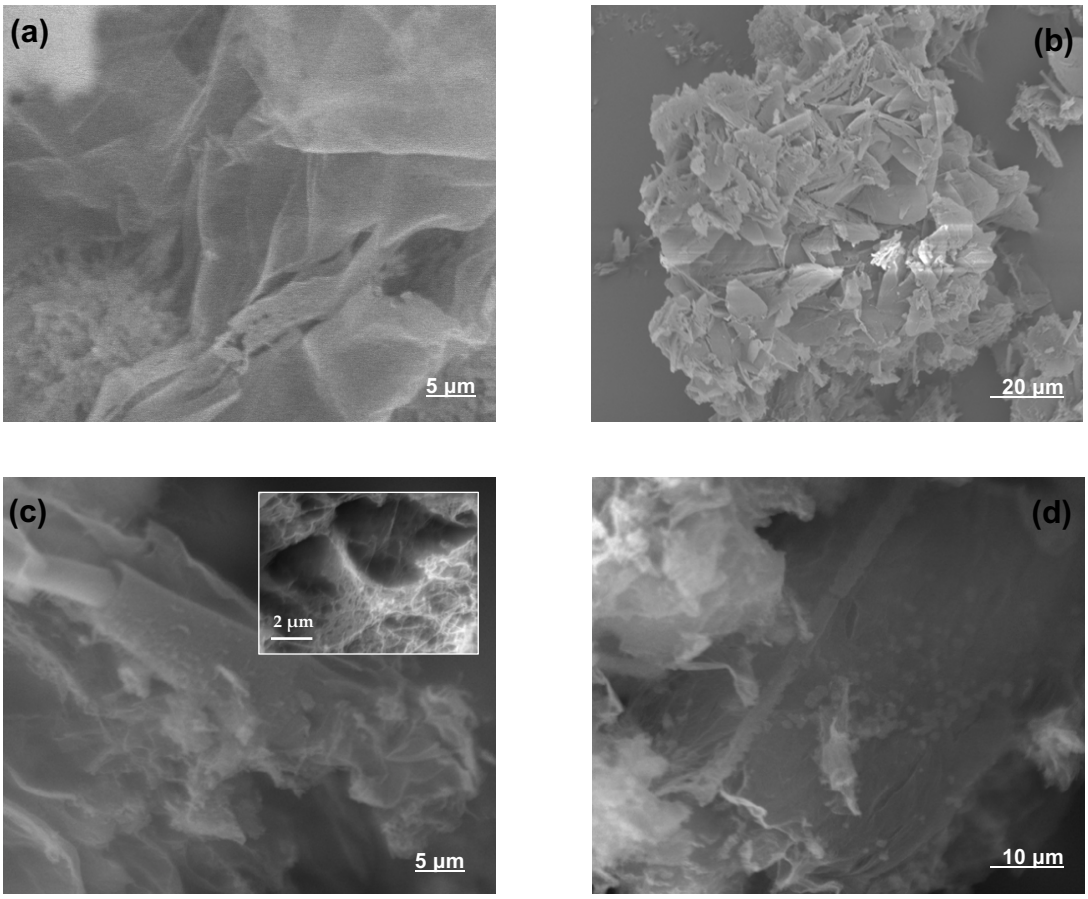

Figure 5.1 SEM images of (a, b) pristine BN; (c, d) BN-P123.The insert shows the interconnected porous structure

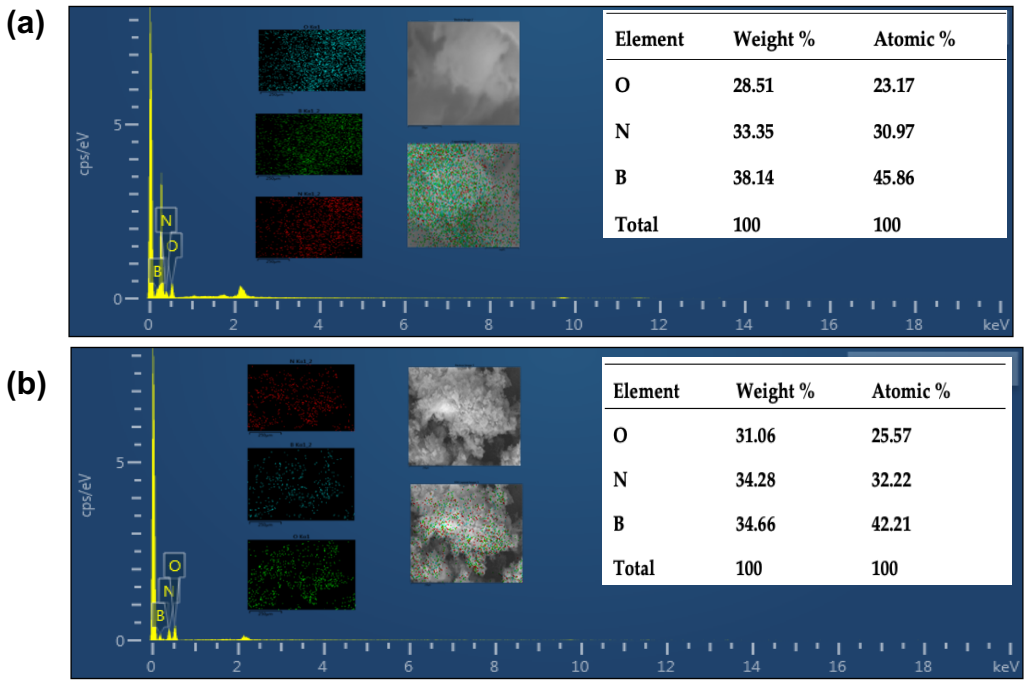

Figure 5.2 EDX spectra of (a) pristine BN; (b) BN-P123 and the insert show the elemental mapping and corresponding atomic % of elements.

5.2.2. Structural and optical analysis of urea-based BN

The structures of both samples were analysed using the outputs given in Figure 5.3a which depicts the XRD patterns of the prepared samples. No structural differences were found in the modified sample after utilising surfactant. Similar to the hexagonal structure of BN, two characteristic peaks around were observed ~25° and ~42° which are ascribed to the (002) and (100) crystal planes, respectively (Kurakevych and Solozhenko, 2007). Additionally, the peaks of both samples confirmed the poor crystallization with the presence of turbostratic material. Compared with the pristine BN, the (002) diffraction peaks of BN-P123 shifted to a lower angle, which promotes a more disordered hexagonal boron nitride (h-BN) structure. Moreover, the optical properties of samples were examined, using UV-vis absorption. The peaks in Figure 5.3b indicates a highly transparent form visible to UV wavelength (Ba *et al.*, 2017) . The maximum absorption peak around 209 nm is attributed to intrinsic excitation absorption band of h-BN. Besides, small humps around 265 and 352 nm were detected in BN-P123, corresponding to impurities which were negligible.

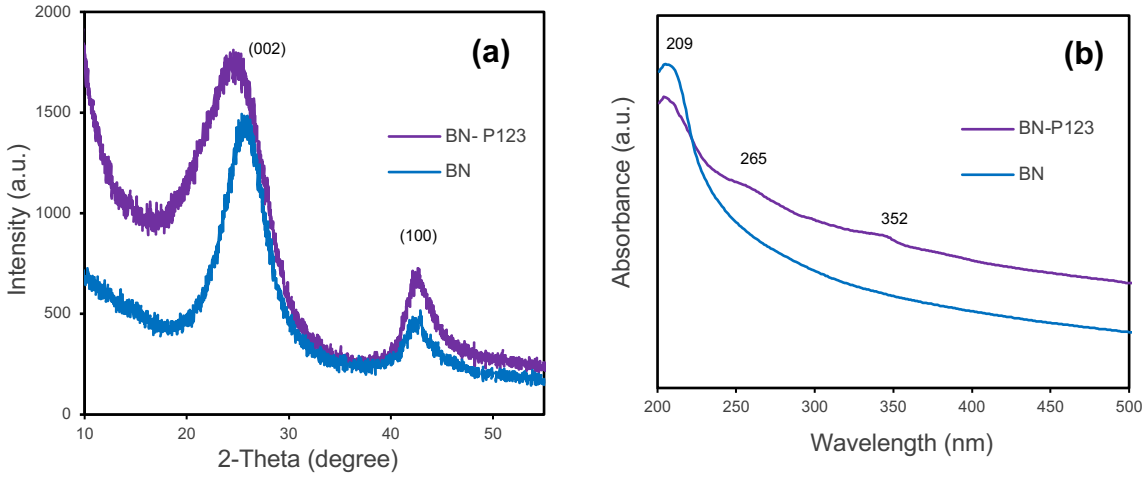

Figure 5.3 (a) XRD patterns; (b) UV-Vis of prepared samples

5.2.3. Chemical and thermal decomposition properties of urea-based BN

Having discussed the formation of pristine BN and BN-P123 with EDX elemental mapping, this section addresses the chemical features which were supported by Fourier transform infrared (FTIR) spectroscopy. There are no additional functional groups shown in Figure 5.4.a for the BN-P123 sample. Both peaks exhibited two main characteristic bands of boron nitride at ≈1300 and 800 cm^{-1} corresponding to in-plane

B-N transverse optical mode and out-of-plane B-N-B bending mode, respectively (Liu *et al.*, 2015). According to this finding, we can suggest that P123 was eliminated from the as-prepared BN during the decomposition process and did not affect the surface functional bonding.

Additionally, to check the thermal stability of samples, a thermal gravimetric analyser (TGA) test was performed in air atmosphere (rate = 10 K/min) and the results are shown in Figure 5.4b. The TG thermograms reflected the weight loss of 19% for both samples, representing the removal of moisture adsorbed on the material surface. After 573 K, the lines show the thermal stability nature of BN at a high temperature and that there was no significant weight loss up to 1273 K. So far, above all characteristic results of both samples, it was found that the structure and chemical nature of BN has not changed after modifying BN with the surfactant compound and both samples revealed almost similar features. We assumed that the utilisation of block copolymer (P123) can affect the textural properties of pristine BN.

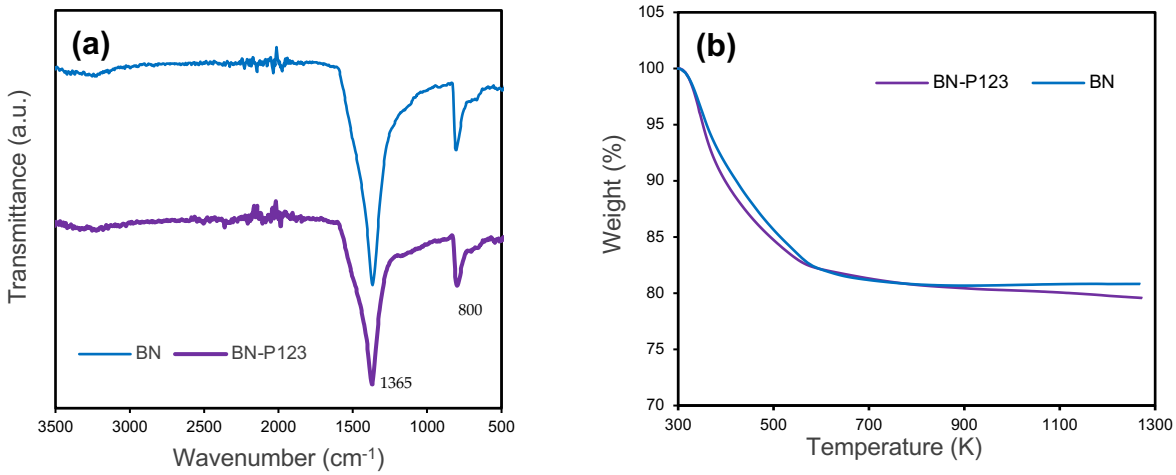

Figure 5.4 (a) FTIR spectra; (b) TGA thermal decomposition curves in an inert nitrogen atmosphere of both samples.

5.2.4. Analysis of modified melamine-based BN

Porous BN shows different morphologies using melamine as a nitrogen source since different structures of precursors were used for the formation of BN. Therefore, one of the interesting issues that emerges from BM4-P123 is its morphology results, which are depicted in Figures (5.5a, b). What can be determined from figures (5.5a, b) is that

when melamine was employed, porous BN showed a whisker-like structure, which is previously mentioned in the literature (Li *et al.*, 2016). In contrast, a typical FTIR spectra of melamine-based BN exhibits similar bands like urea-based BN for boron nitride B-N in-plane transverse stretching mode at ~1346 cm^{-1} and B-N-B out-of-plane bending mode at 779 cm^{-1} (Figures 5.5c). However, the broad peak of ~3359 cm^{-1} and the small peak at ~1095 cm^{-1} were also observed which could be attributed to O–H and C–O chemical structures respectively.

In order to further understand the chemistry of BM4-P123, the decomposition profile of melamine-based BN was analysed by TGA. Two main stages of degradation can be found in Figures 5.5(d), which ~ 12 wt% of mass loss for the first stage. The second step of degradation occurs over a broad temperature starting from 870 K, which corresponds, to decomposition of remaining products. Additionally, melamine precursors begins to decompose at a higher temperature than urea between 473 K and 761 K (Hoffendahl *et al.*, 2014). To better investigate the effect of using melamine as a nitrogen precursor in the formation of BN, the sample was analysed with EDX (Figure 5.6). Results showed that the atomic composition of elements is oxygen (O), nitrogen (N), boron (B) and carbon (C). The Si peak appears from Si dead layer of Si (Li) detector. Taken together, it should be underlined that the use of melamine in porous BN leads to presence of carbon content which brings about an increase of the impurities.

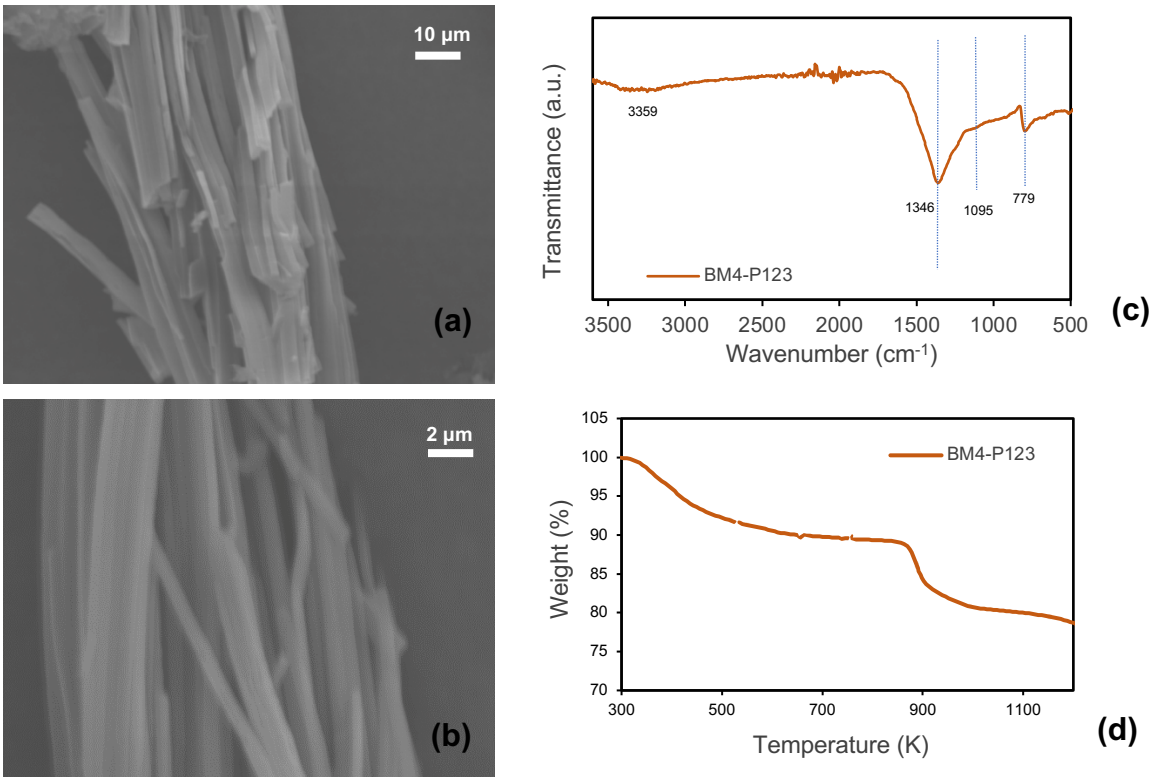

Figure 5.5 (a, b) SEM images; (c) FTIR Spectra; (d) TG curve of BM4-P123

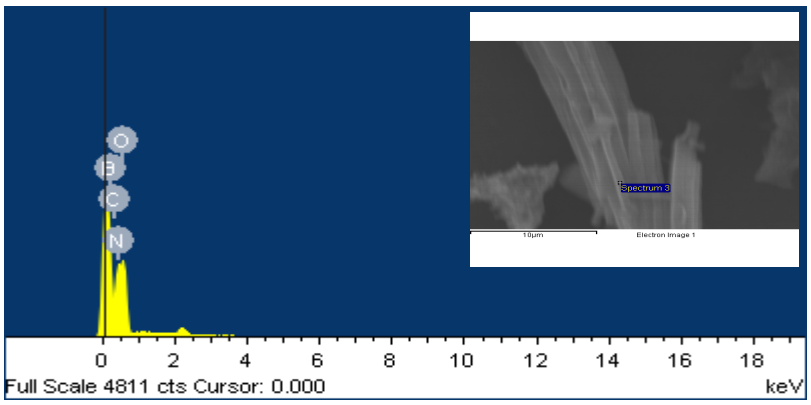

Element	Weight%	Atomic%
B K	9.67	13.65
C K	12.84	16.31
N K	33.64	36.64
O K	23.35	22.27
Si	20.50	11.13
Totals	100.00	

Figure 5.6 EDX spectra and corresponding atomic % of elements of BM4-P123

5.2.5. Textural analysis of modified BN

So far, the possible impacts of using structure directing-agent on porous BN construction and stability has been investigated. Now, the textural properties of the samples are considered which are expected to improve. Porosity analysis of all

samples which was derived from nitrogen adsorption/desorption isotherm at 77 K are summarised in Table 1. The isotherm results display a typical type IV curve based on IUPAC classification and type H3 hysteresis loop in the partial pressure range 0.4–1.0, which indicates presence of mesopores and slit shape pores (Pang *et al.*, 2018) (Figure 5.7a). More importantly, there is a trivial rise in N_2 adsorption-desorption isotherm of BU30-P123 at lower pressure ($P/P_0 < 0.25$), which is caused by presence of micropores (Bi *et al.*, 2018). The BJH adsorption theory was used to calculate pore size distributions. As expected, the d*V*/d*D* pore volume of BN-P123 increases dramatically with abundance of micropores (Figure 5.7b). Meanwhile, using the Brunauer-Emmett-Teller (BET) method (Brunauer *et al.*, 1938), the specific surface areas are calculated showing that the BET surface area of samples with P123 are higher than pristine BN and the highest SSA referred to BU30-P123 (Table 5.1). This result allows us to conclude that urea as a nitrogen precursor has greater impact on surface area as opposed to melamine. Besides, it is clear from the above measurements that the P123 introduced into precursors during the fabrication process is highly effective on the microscale structure of porous BN and improves surface area and pore volume of the sample.

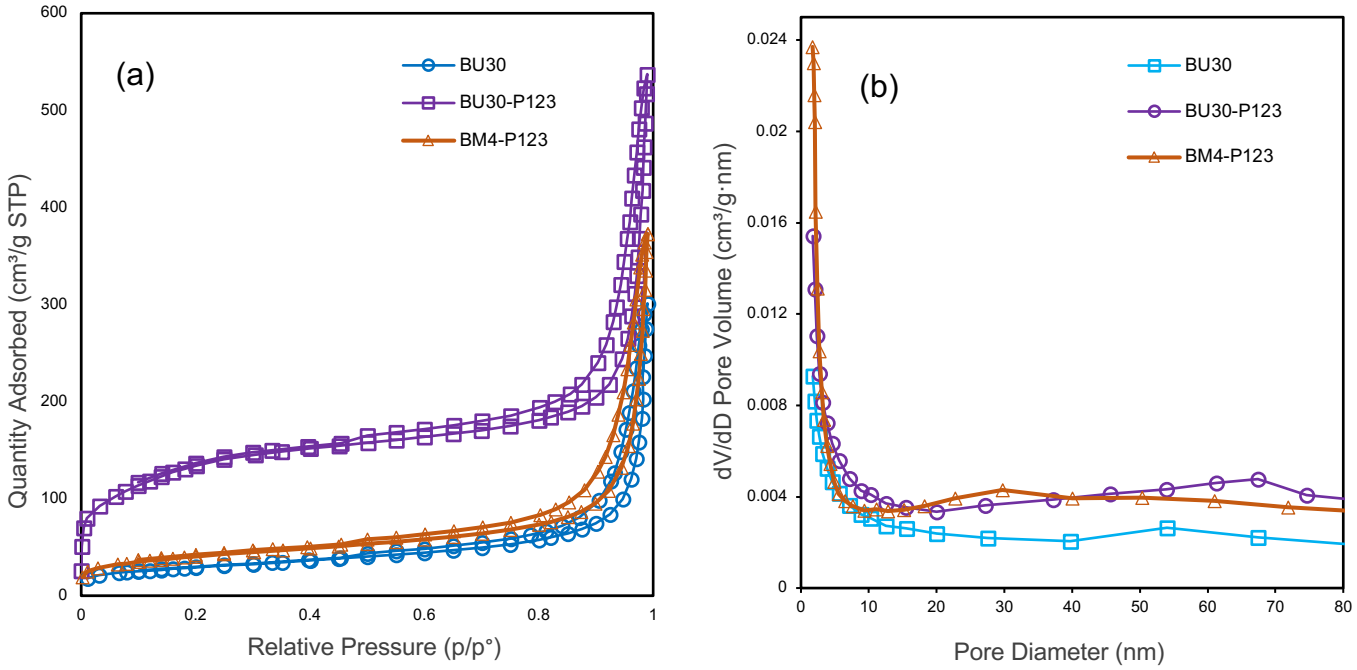

Figure 5.7 (**a**) Nitrogen adsorption-desorption isotherm of pristine BN and modified BN; (**b**) BJH adsorption dV/dD Pore Volume of the same samples.

Table 5-1.Textural properties of prepared materials.

Sample	S_{BET} [1] (m^2/g)	V_{total} [2] (cm^3/g)
BN	102	0.46
BN-P123	476	0.83
BM4-P123	143	0.57

[1] Specific surface area (m^2/g) obtained by Brunauer-Emmett-Teller (BET) method. [2] Total pore volume (cm^3/g) calculated at P/P_0 = 0.99.

5.3. Conclusions

This chapter highlights one of the modification strategies based on controlling the porosity parameters of porous BN formation. The porosity of boron nitride has been successfully tuned by introducing the triblock copolymer surfactant (P123) during the preparation process of BN precursors.

This approach is tested on two different types of pristine BN. While urea-boric acid was used for pristine BN type one, the second type of pristine BN was formed using melamine-boric acid. A thorough comparison of these two forms enables us to discover the influences of the interaction between P123 with chemical formation of the precursors. In general, we found that utilising P123 into boron and nitrogen precursors leads to improving the porosity of samples. Particularly, in the urea-based BN modified sample (BN-P123), the surface area and total pore volume revealed a remarkable change (SSA = 476 m^2/g and V_{total} = 0.83 cm^3/g). To be more precise, the textual properties results were virtually quadrupled as a result of the modification. This significant change is attributed to the formation of more gases during the decomposition process, thereby P123 acts as a porogen agent which gives rise to tailor the pore chemistry of BN. However, this outcome is contrary to the BM4-P123 sample, which observed a slight growth in textural pore properties (SSA = 143 m^2/g and V_{total} = 0.57 cm^3/g) after tuning the sample with surfactant template. These differences are likely related to the urea proportion and its decomposition reaction, which have relatively good impact on porosity parameters. Given the findings on the presence of carbon impurity, which is confirmed in the BM4-P123 sample by EDX

elemental mapping analyser, the addition in melamine proportion is not a good idea to achieve a more tuneable porous structure of BN. Another important change by means of applying melamine instead of urea is the shape of BN, which is transformed from flake layered structure to whisker-like morphology.

Furthermore, based on the other characterisation results obtained in this work, all samples share almost similar chemical features. Therefore, it can be concluded that this synthetic condition (the addition of P123 surfactant) is less likely to change BN chemical bonding.

All in all, a key outcome of this chapter is modifying the pore morphology of the BN productions without significant impurities. With this method, a greater understanding of the formation of porous BN with high levels of porosity is reached. It is believed that these findings make a significant contribution to the field of novel adsorbents when they are used for application in carbon capture.

CHAPTER 6

METAL MODIFICATION OF POROUS BORON NITIRDE

Outline of the chapter

This chapter focuses on the metal modification strategy of porous BN to improve the interaction between the BN sample and CO_2 molecules in carbon capture applications. Furthermore, experimental method and sample characterisation are considered in this chapter. The influence of Ni impregnation of porous BN surface on chemistry, structure and porosity of sample is discussed. The chapter is organised as follows:

6.1. Introduction

6.2. Materials and synthesis of Ni loading on porous boron nitride

6.3. Results and discussion

6.4. Conclusions

6. Metal modification of porous boron nitride

6.1. Introduction

Following the strengths of solid sorbents, porous materials are commonly used in numerous adsorptive applications, in particular for CO_2 adsorption. Recent investigation of the literature has confirmed the fundamental features of porous materials for carbon capture processes. These factors include tuneable porosity (Rehman and Park, 2018), surface polarity (Singh *et al.*, 2017, Ren *et al.*, 2017) and tolerance against water to name a few (Yoo *et al.*, 2016). Porous BN materials with partly ionic structure and their unique pore structure have been popular candidates for CO_2 adsorption applications. However, much of the research up to now has reported that the poor interaction of pristine boron nitride with CO_2 molecules causes a decline in boron nitride's carbon capture performance. As mentioned in the literature review, the modification strategy is considered as an effective way to promote the BN affinity to adsorb more CO_2. The most obvious finding to emerge from the BN analysis is that BN's textural and chemical properties are correlated to increase its efficiency through CO_2 capture. A series of experimental demonstrations of BN textural effects were carried out in the previous chapter with the aim of assessing the use of structural directing agent in improving BN porosity/pore size and surface area. The second question in this area sought to determine the impact of metal modification approach on CO_2's total adsorption by changing the surface chemistry of BN. Hence, according to the Lewis acidic molecules of CO_2, we now consider providing polar active site groups, which are favourable to interact with CO_2. This chapter describes the synthesis and characterisation of loading Ni (II) compounds by simple impregnation and calcination methods to modify basicity of the BN surface. The facial synthesis was carried out using boron and nitrogen precursors for the production of porous BN. Consequently, Ni $(NO_3)_2.6H_2O$ was loaded before the heat treatment step. The details of the synthesis are described in section 6.2. The material characteristics of all the samples are discussed in section 6.3 by using various techniques. This section analysed the structure, morphology, chemistry, optical and porosity aspects before and after metal modification of BN surface. All these properties are important to figure out the main effect of Ni loading on porous BN for its CO_2 uptake behaviour. To find this, the next chapter will provide CO_2 sorption tests using a gravimetric technique at

a low (<1 bar) pressure for all the relevant results discussed in this chapter. Overall, a summary of the main results of four samples is provided in this chapter.

6.2. Materials and synthesis of Ni loading on porous boron nitride

Porous BN with different levels of Ni (II) were prepared through a template-free heat-treatment approach. In a typical experiment, firstly boric acid (ACS reagent, Aldrich), urea (synthesis grade, Aldrich) with a molar ratio 1:30 were dissolved in deionised water (50 ml). Then a certain amount of Ni $(NO_3)_2.6H_2O$ (Aldrich, 99%) was added into the mixture followed by heating and stirring to completely evaporate the excess water before the sample was dried overnight at 348 K. The light green powders were then transferred into alumina crucibles and annealed in a tube furnace at 1173 K for three hours under N_2 atmosphere (oxygen free cylinder, BOC Ltd). Further calcination was applied where the samples were placed in a muffle furnace at 673 K for an hour to obtain a nickel oxide phase. The resulting samples are referred to as: BN-(X) Ni where X was 0.1%, 0.5%, 1% molar percentage. For the sake of comparison, pristine BN prepared based on the same procedure without adding Ni $(NO_3)_2$ $6H_2O$. Samples with various composition ratio of Ni are presented in Figure 6.1.

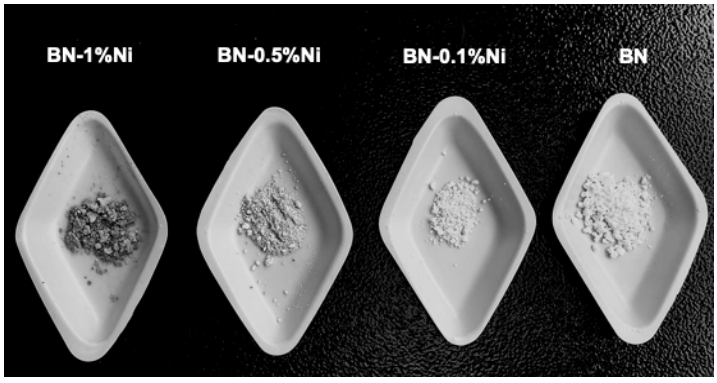

Figure 6.1 BN, BN-0.1%Ni, BN-0.5%Ni, BN-1%Ni powders

6.3. Results and discussion

This section has reviewed fundamental aspects of Ni@BN material properties of the prepared samples. Firstly, to investigate how certain amounts of Ni $(NO_3)_2.6H_2O$ were distributed on the surface of porous BN, various material techniques were used to

characterise the structural, morphology and chemical properties of all samples. These techniques include XRD to find the crystallographic order, FTIR to identify functional chemical bonding, SEM/TEM and EDX/LIBS to explore shape and elemental composition of the samples respectively. Secondly, due to the intrinsic electronic properties of Ni as a transition metal, could have important effects on the optical properties of porous BN. Therefore, UV-vis absoption and fluorescence spectroscopy were applied to describe the influence of loading nickel on luminescence properties of BN. Moreover, it is hypothesied that introduction of Ni (II) into porous BN might control the pore size and consequently impact on textural properties (surface area and pore vulume) of BN. Thus, nitrogen adsorption/desorption isotherms were obtained using a porosity analyser (Micromeritics ASAP2060) at 77 K. The thermal stability of samples was also performed using thermal gravimetric analysis (TG-DSC), Ultra micro balance, Mettler Toledo, both investigating TG and DSC profiles.

6.3.1. Structural and chemical analysis of Ni loading on porous BN

The evaluation of the crystalline phases of samples was carried out through Powder X-ray diffraction (PXRD) measurements. As indicated previously in Chapter 4, the wide-angle diffraction pattern reveals two broad peaks at 2Theta approximately 25° and 42° for pristine BN (refer to Figure 6.2 (a)), corresponding to the (002) and (100) reflections of hexagonal BN lowly organised turbostratic phase (Kurakevych and Solozhenko, 2007). In the BN-1%Ni sample, it is also possible to identify the Ni-containing phase (inset of Figure 2) as metallic Ni (PDF Card 4-0850). Owing to the low Ni content in the BN-0.1%Ni sample, no evidence of any Ni-containing phase can be revealed. Surprisingly, for the BN-0.5%Ni sample, the same treatment leads to the formation of a polymorph of ammonium borate phase with orthorhombic crystal structure (PDF Card 31-0043) accompanied by the presence of NiO (PDF Card 47-1049) as shown in the inset of Figure 6.2 (a)). Actually, NiO is the expected phase from the $Ni(NO_3)_2.6H_2O$ decomposition by calcination and the BN phase evolution towards the orthorhombic phase is the most feasible as reported by other authors (Alkoy *et al.*, 1997). The reduction of Ni (II) to Ni (0) during the calcination treatment of the BN-1%Ni sample could be the reason of the formation of the enigmatic phase (PDF Card 19-0072) with unknown crystal structure.

Furthermore, the characteristic of chemical functional groups of BN-0.5%Ni and BN-1%Ni samples is determined by Fourier transform infrared (FTIR) spectroscopy (refer to Figure 6.2 (b)). As can be seen from Figure 6.2 (b), all peaks exhibited two main characteristic bonds of in-plane B–N transverse optical mode and out-of-plane B–N–B bending mode (Liu *et al.*, 2015). As expected, the stretching vibration mode of NiO bond was detected in the BN-0.5%Ni sample after calcination step.

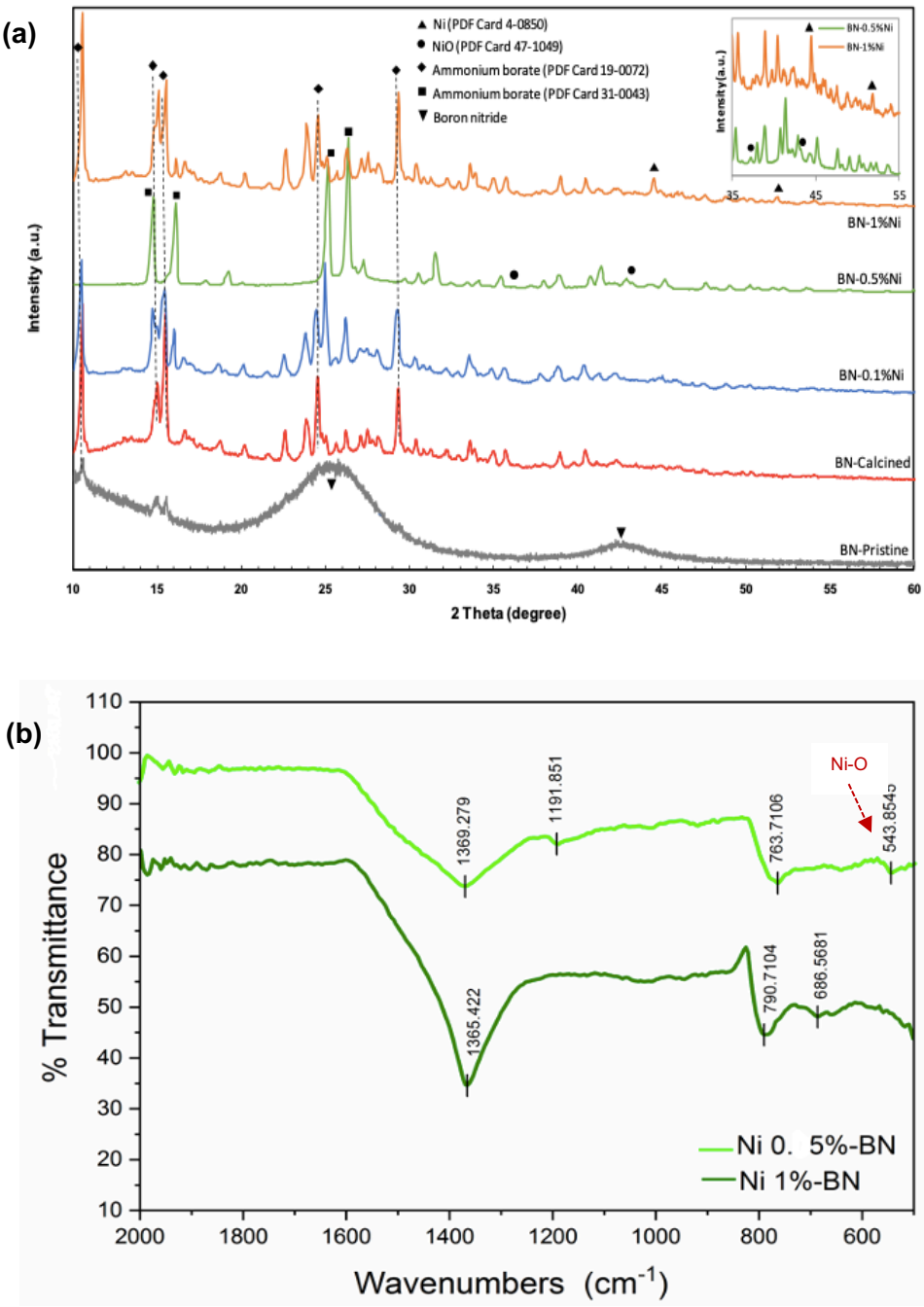

Figure 6.2 (a) XRD pattern; (b) and FTIR spectra of different amount of Ni loaded BN

Elemental analysis techniques were also employed in order to confirm homogenous impregnation of Ni (II) into BN frameworks. To do so, Laser-induced breakdown spectroscopy (LIBS) provided elemental analysis on BN-0.5% Ni sample. As it is shown in Figure 6.3 (a), Nickel was detected in the UV scan range. The LIBS signals of nickel target within the wavelength range of 300 nm-350 nm were observed under pulse laser ablation. Further investigation of elemental analysis on BN-(0.5%) Ni was subjected to EDX analyser. It is evident that the sample is mainly contained of boron (B), nitrogen (N) and oxygen (O) and very low amount of nickel (Ni) elements (refer to Figure 6.3 (b)). Similar to the discussion in Zhu *et al.* (2016), the outputs of the experiments show that the amount of oxygen mainly resulted from the nickel oxide and slight surface oxidation of the material under ambient condition. This result has also been confirmed in this study through XRD results as discussed in the previous section.

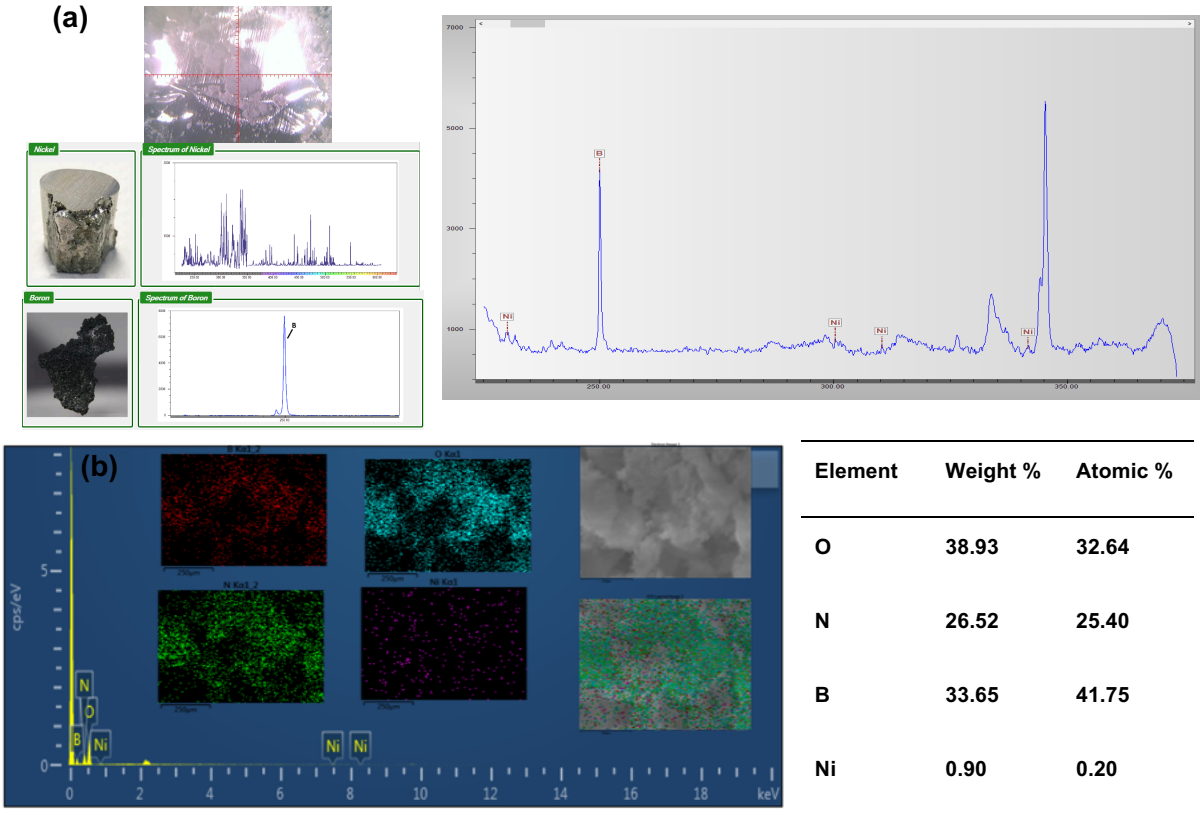

Element	Weight %	Atomic %
O	38.93	32.64
N	26.52	25.40
B	33.65	41.75
Ni	0.90	0.20

Figure 6.3 (a) LIBS; (b) Elemental mapping by EDX spectroscopy for BN-(0.5%) Ni and the atomic % of elements

6.3.2. Morphology

Scanning Electron Microscopy (SEM) along with Transmission Electron Microscopy (TEM) were further employed to visualise the morphology of samples and to determine whether metal particles were embedded within the BN sheets. SEM imaging of pristine BN shows a layered-like morphology as previously stated in Chapter 4 (Figure 6.4a). These sheets were clustered and shaped to a fluffy structure in the BN-0.5% Ni sample (Figure 6.4b). This may lead to more disordered formation of the structure.

Additionally, TEM analysis of BN-0.5% Ni showed a different nano-scale morphology. It can be observed from the TEM images that the size of metal-base particles varies from 50 to 200 nm. Moreover, a component constituted by thin layers was rolled and clustered (refer to Figure 6.5 (a, b)). The tubular structures with diameters from 100 to 200 nm and length no less than 2 micrometers also detected as given in Figure 6.5 (c, d). These structures seem to be constituted by empty cylinders with a smaller size that put together to form the final tube of micrometric size. Dark-field (DF) images show crystalline walls of 5-7 nm related to the tubular structures. The micrograph of BN-0.5%Ni sample homogeneously distribution of metal oxide nanoparticles evidenced by darker spots due to highest Z-contrast as provided in Figure 6.5 (e, f).

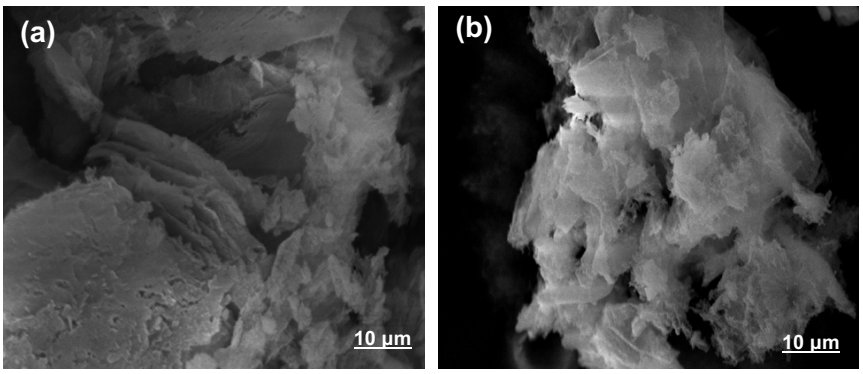

Figure 6.4.SEM images of (a) BN and (b) BN-0.5%Ni

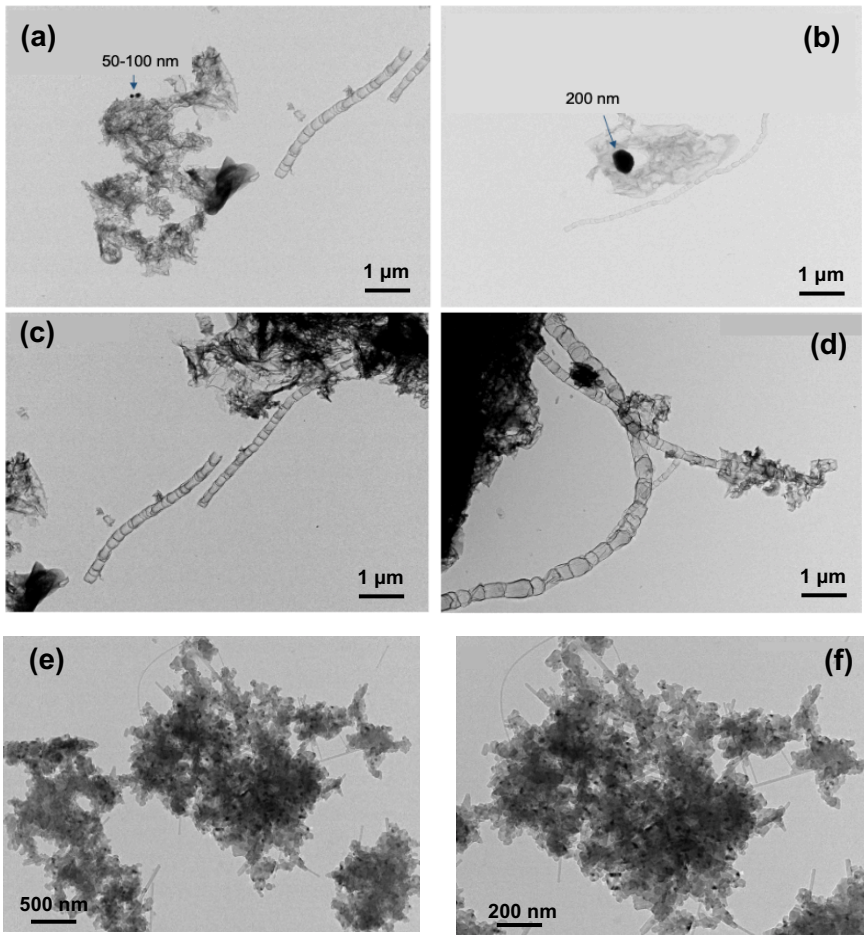

Figure 6.5 (a – f) TEM images BN-0.5%Ni

6.3.3. Optical and photoluminescence analysis

Another crucial composition effect of Ni(II) impregnation of BN is determined by optical techniques. To this end, the optical properties of all the samples were charaterised by UV-vis absorption and fluorescence spectra. UV-vis results indicate the absorpation peaks before 250 nm which is ascribed to intrinsic excitation absorption band of h-BN (Kumar *et al.*, 2016). In addition, the intensity of absorption in the visible range was improved for the Ni-doped samples (refer to Figure 6.6(a)). This can be brought about by the slight shift of optical band gap to the lower energy with incorporation of Ni into the BN lattice (Ge *et al.*, 2011). The changes in fluorescence emissions of BN samples are reported in Figure 6.6(b). The maximum fluorescence intensity was achieved at 487 nm with an excitation wavenumebr of 240 nm and no significant shift difference was observed. A decrease in fluorescence emission of samples is detected with an increase in nickel concentration (Thangaraj *et al.* 2016). This observation could be

justified by the fact that Ni loading causes the recombination of photoinduced electron-holes pair in which hindering the charge-seperation efficiency occurs as emphasised in Tonda *et al.*, (2014).

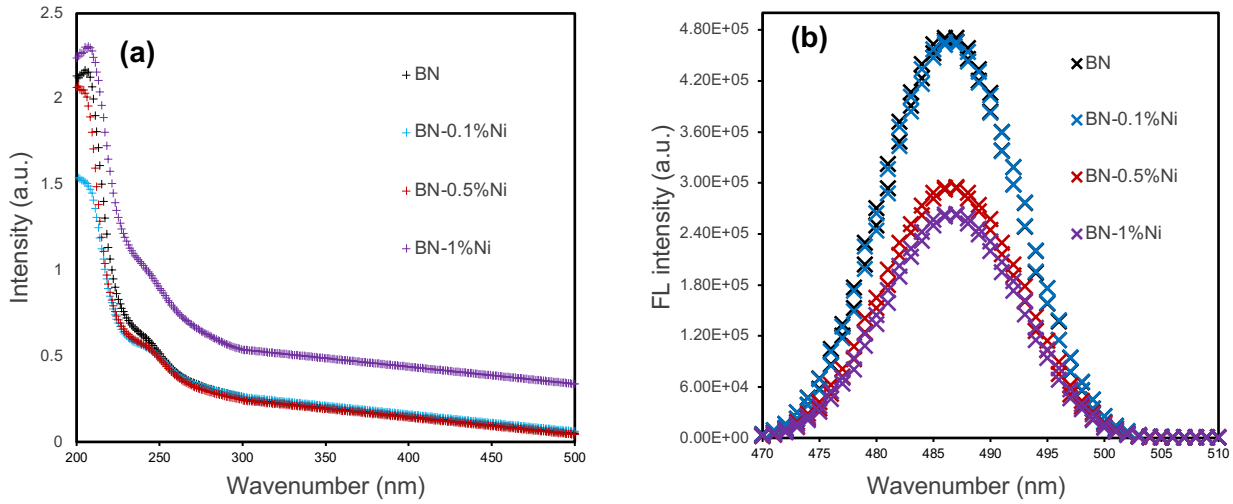

Figure 6.6 (a) UV-vis absorption; (b) Fluorescence emission spectra of all samples (λ_{ex}= 240 nm).

6.3.2. Thermal decomposition and textural analysis

The thermal stability of samples is one of the significant properties, which needs to be considered prior to the gas sorption test in order to be commercially used as a solid sorbent. Hence, the thermogravimetric (TG) analysis was carried out in N_2 (rate = 10 K/min) from room temperatures up to 1173 K. The thermal decomposition of samples could be observed at the beginning of the TG process, which was linked to the removal of physically adsorbed water and other impurities as shown in Figure 6.7(a). As shown in Figure 6.7(a), the pure BN and the modified BN with very low amount of Ni (0.1%) are more stable than the higher doped ones. Besides, the total weight loss of samples has been increased with growing Ni particles. However, the pristine BN shows higher weight loss (19%) compared to BN-0.1% Ni, presumably because of the high moisture content. It may be the case therefore that these variations are observed. In the case of BN-1% Ni sample, the thermal analysis indicates the highest weight loss. Moreover, it showed that the sample is stabilised at a higher temperature of 666 K as a result of incorporation of metallic concentration of Ni ions into BN structure (Das *et al.*, 2018).

Accordingly, the DSC curves display an exothermic peak that reaches the temperature about 640 K followed by prominent endothermic drop occurring near 1140 K due to the complete degradation as can be seen in Figure 6.7(b).

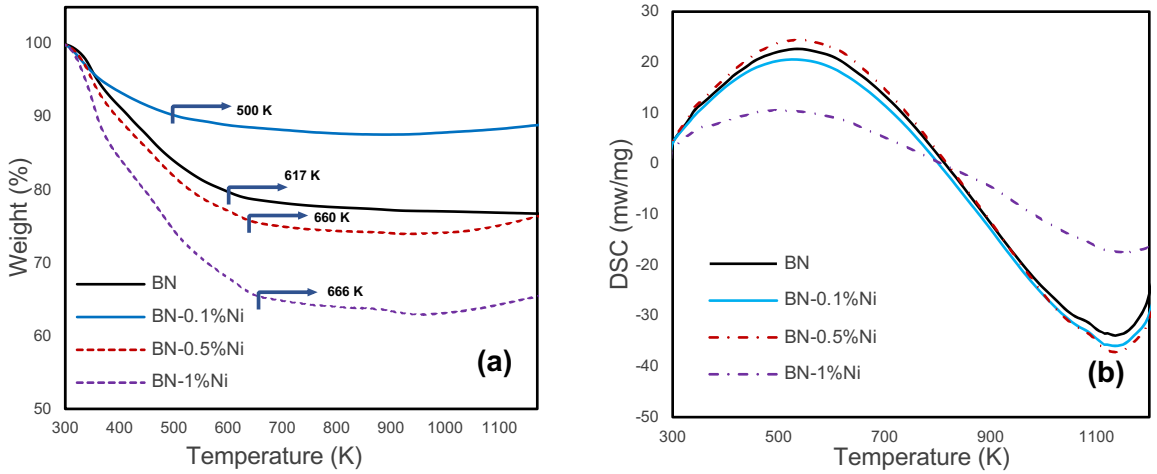

Figure 6.7 (a)TG; (b) DSC curves of prepared samples

The textural properties of samples are vital to gain a better understanding of textural influences of Ni with different concentration ratios of loading. Hence, the nitrogen sorption was measured using a porosity analyser at 77 K. According to the IUPAC classification, N_2 adsorption-desorption isotherms of all samples belong to type IV and type H3 hysteresis loop, which indicates the disordered pore networks (Figure 6.8a) (Cychosz *et al.*, 2017b). Additionally, the pore size distributions were reported by the BJH method as given in Figure 6.9(a- d). It can be observed that the proportion of microporosity (d < 2 nm) and *dV/dD* pore volume increased with loading a small ratio of Ni. The BET surface area and total pore volume of porous BN and prepared BN-Ni samples were reported in Figure 6.8(b). As expected, the BET surface area and volume of pores have shown an increase in BN-Ni and it reached 660 m^2/g in BN-0.1%Ni sample with small amount of nickel loading. However, one important finding is that further increasing the Ni loading in BN-1% Ni sample leads to dropping the value of S_{BET} as well as pore volume to 63.02 (m^2/g) and 0.37 (cm^3/g) respectively. This inconsistency may be attributed to the aggregation of Ni nanoparticles, which weakens the pore structure. It is also interesting to notice that though the surface area diminished with the excess in Ni content, the total pore volume in BN-0.5% Ni displays the highest value of 0.61 (cm^3/g) compared to other samples. All above measurements

demonstrate that metal modification of BN had a fundamental effect on the microscale structure of pristine BN and improves the adsorption properties of BN materials. To have further insight on gas sorption properties, as the final step of this dissertation, we investigated whether in-cooperation of Ni into the matrix of BN could enhance the CO_2 adsorption.

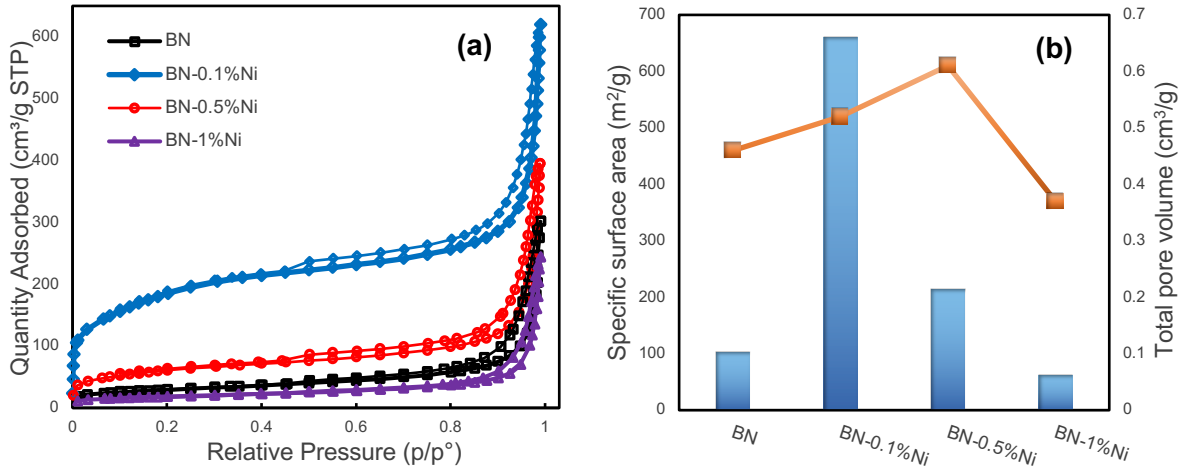

Figure 6.8 (a) N_2 sorption isotherms measured at 77K; (b) Bar plots showing the BET equivalent surface areas, total volume of pores

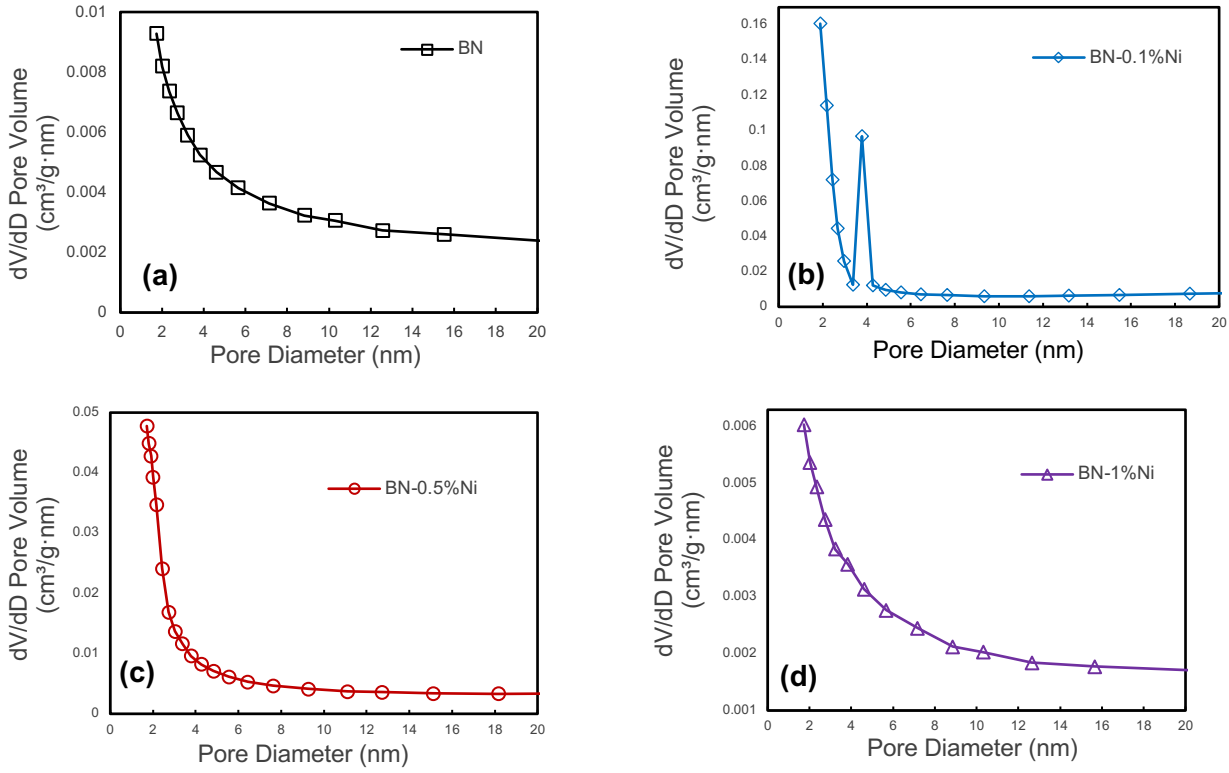

Figure 6.9 Pore size distribution of BN (a); BN-0.1%Ni (b); BN-0.5%Ni (c); BN-1%Ni (d)

6.4. Conclusions

This chapter has identified a facial synthesis of porous boron nitride based on the metal modification method. Porous boron nitride was doped successfully with varying levels of Ni concentration by following a simple yet effective high thermal treatment procedure.

The presence of Ni species was confirmed by structural and elemental characterisation. The XRD analysis is highlighted the partial oxidation of BN to ammonium borate (BON) as a consequence of calcination treatment needed for the NiO formation. The homogenous dispersion of Ni on BN surface was also confirmed by the TEM results. Notably, there is not a significant variation observed in morphology and shape of the samples. The SEM images revealed the flake and layered structure. Moreover, the results of photoluminescence analysis indicated that the optical absorption behaviour is highly dependent on the Ni concentration on porous BN. The highest absorption intensity in visible light belonged to the sample with 1% Ni loading. To establish whether the prepared samples have high stability to heat, thermal analysis was carried out in a range of temperatures from room temperature to 1173 K. The TG results confirmed that all samples are thermally stable.

One unanticipated finding was that the Ni modification procedure had a significant effect on the pore structure of porous BN. Basically by changing the molar ratio of the Ni precursor, a porous BN with varied BET surface area (from 102 to 660 m^2/g) was obtained. Porous BN with low amount of Ni led to a high micropore volume and surface area, making it a desirable candidate in adsorptive performance, particularly in carbon capture. The highest surface area belonged to the BN-0.1% Ni sample, while the maximum pore volume (0.61 cm^3/g) is reported to be for that of the BN-0.5% Ni. Overall, the findings of this chapter have several important implications for future of the solid sorbents practice, which have been discussed in Chapter 7.

CHAPTER 7

EVALUATION OF POROUS BORON NITRIDE FOR CARBON DIOXIDE CAPTURE

Outline of the chapter

This chapter describes CO_2 sorption procedure on prepared and designed porous BN samples. It includes a dynamic CO_2 sorption test *via* gravimetric technique at low pressure. The chapter is organised as follows:

7.1. Introduction

7.2. Materials and Dynamic CO_2 testing

7.3. CO_2 sorption on non-metal modified porous BN

7.4. Effect of Ni loading porous BN on CO_2 adsorption

7.5. Cycle tests on pristine BN at 303 K

7.6. Conclusions

7. Evaluation of porous boron nitride for carbon dioxide capture

7.1. Introduction

The recent surge in fossil fuels consumption such as coal, oil and natural gas has brought about a massive increase in the amount of CO_2 emissions worldwide. To tackle these issues, the Paris agreement of the United Nations Framework Convention on Climate Change (United Nations Climate Change, 2016) was set up in 2015 to keep the temperature rise below 1.5 degrees Celsius above pre-industrial levels. As part of this agreement, accelerating the rate of deployment of carbon capture and storage (CCS) is essential and there is a need to improve technologies, particularly in the area of carbon capture.

As mentioned in the literature review, to date, chemical absorption technology (e.g. using advanced amines), which has been used to remove CO_2 from natural gas reached a commercial phase (Akinpelumi *et al.*, 2019, Mantripragada *et al.*, 2019). However, it is clear that using traditional solvent-based processes for CO_2 capture calls for a relatively high-energy penalty, whereas using dry sorbents reduces the energy requirement owing to their feasibility in a wide range of temperatures and pressures. Returning (briefly) to the subject of various dry solid sorbents, porous materials are commonly considered as highly robust adsorbents for CO_2 adsorption. This group of materials includes porous carbon (Sevilla and Fuertes, 2011; Ello *et al.*, 2013), zeolite and silica materials (Yang *et al.*, 2013), metal-organic frameworks (MOFs) (Cota and Martinez, 2017; Zhang, 2013; Wu *et al.*, 2012; Yazaydın *et al.*, 2009) as well as porous boron nitride (BN) (Wang *et al.*, 2019; Liang *et al.*, 2019) to name a few. For the last two decades, the research on boron nitride nanostructure has been a matter of interest for CO_2 capture. The literature in this area supports the hypothesis that pure porous BN without functionalisation treatment shows weak affinity to interact with CO_2 molecules. From thermodynamic and kinetics perspectives, some strategies in view of tuning the structure/defects, pore size and chemistry of the BN are capable to deal with BN disadvantages. The presence of ultramicroporosity and functional groups such as -NH_2 and -OH are shown to affect CO_2 sorption capacity (Kutty *et al.*, 2018; Chen *et al.*, 2018d). Therefore, the main challenge in adsorbents development is to optimise BN pore geometry and surface chemistry for a large enhancement of BN for CO_2 sorption capacity.

Before proceeding to control BN properties with modification techniques, it is important to synthesise pristine BN, which is known to be a good candidate in CO_2 adsorption applications. Thus, in Chapter 4 of this study, pristine BNs were prepared by a template-free approach under different conditions. The main objective of this method was to examine the effect of boron, nitrogen and solvent precursors during the thermal evaporation step on structure and chemistry of pure BN. After carrying out several techniques on each of the obtained samples, those samples with a fine structure, high porosity and relatively good thermal and chemical stability were proposed to be tested for carbon dioxide capture. Furthermore, the same samples were used for modification purposes in Chapters 5 and 6. Tuning the porosity of pristine BN with organic copolymer surfactants is another important objective, which is considered in Chapter 5. Results of modified BN with surfactant directing agents have emerged as being of higher pore volume and surface area compared to pristine BN. It can thus be suggested that the metal-free modification of BN has a pivotal role in the improvement of BN CO_2 adsorption capacity. What follows is an account of capability of developed porous BN with surfactant agents toward CO_2 sorption test at an ambient condition.

In the literature on CO_2 sorption mechanisms, different physical and chemical interactions between CO_2 and BN materials were proposed including in-plane van der Waals interaction, H-bond with OH, and NH_3 functional groups and acid base interaction (Chen *et al.*, 2018d ; Liang *et al.*, 2019; Yang *et al.*, 2019). In addition, the theory of BN construction (Sun *et al.*, 2013; Paura *et al.*, 2014) provides a useful account of how modification and doping provoke significant changes in its electronic and surface chemistry. Considering this approach, the prepared pure porous BN was doped with nickel transition metal compound as was explained in Chapter 6. As previously stated, three different concentration levels of Ni were considered during the fabrication process. The results, which were presented in Chapter 6, imply that a higher CO_2 uptake is obtained with metal-modification samples due to having a better control over BN pore structure and chemistry. Figure 7.1 illustrates two possible mechanisms for the samples. It can be explained that a combination of van der Waals interaction and Lewis acid-base interaction takes place during the sorption process for the Ni-modified BN samples.

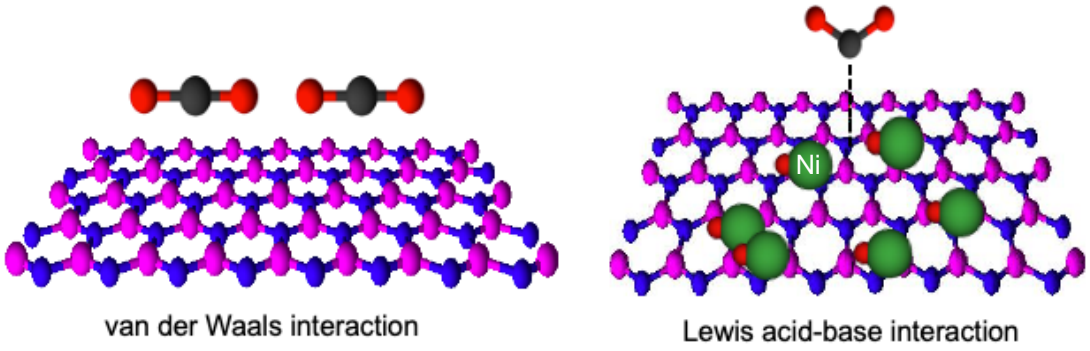

Figure 7.1 Schematic of the interaction between BN and CO_2 molecules.

So far, this dissertation has focused on synthesis, design and characterisation of novel BN materials to obtain a better understanding of their properties and to link those properties with their potential applications in the carbon capture process. The following section will show limited sorption capacities on pristine BN and discuss how modification steps, which were applied, on pristine BN enhanced its adsorption/desorption CO_2 performance.

This chapter began by describing the dynamic breakthrough curve and explaining that gravimetric sorption technique drives by breakthrough experiment in section 7.2. It proceeds to suggest that the thermal gravimetric sorption analyser is a valuable process for assessing adsorbents working capacity in a wide range of temperatures. This chapter considers the non-metal modification of obtained samples for CO_2 sorption at a low (<1 bar) pressure and room temperature and compares the results with pure porous BN at the same conditions in section 7.3. In section 7.4, the results of testing pure CO_2 adsorption at three different temperatures (298, 345, 393 K) and low pressures (<1 bar) on porous BN samples with Ni loading has been discussed. It attempts to show the implementation of each sample at different temperatures and investigates the factors that determine their adsorption behaviours. The experimental work presented here provides one of the first explorations into how Ni incorporation of BN causes a higher CO_2 uptake compared to the pure BN results.

Additionally, we turn our attention to explore the effect of using different solvents in synthetic procedure for BN@Ni samples for CO_2 adsorption. Therefore, the TGA analyser was run for the BN-0.1%Ni and BN-0.5%Ni samples which were prepared with solvents in diverse polarity at two different temperatures (298 and 345 K). As far

as reusability of adsorbents is concerned, the final section of this chapter (section 7.5) provides cycle tests based on the temperature swing CO_2 adsorption/desorption technology for three types of pristine BN, which were prepared for different objectives. All cycle tests were carried out at ambient conditions and the findings were discussed after eight continuous cycles.

7.2. Materials and Dynamic CO_2 testing

The well-defined porous BN based on metal and non-metal modification as well as different fabrication process were selected for application in carbon capture. A summary of BN adsorbents along with their fabrication targets described below.

Sample	Synthesis' Targets
BU30-P123	Metal-free modification of urea-based BN
BM4-P123	Metal-free modification of melamine-based BN
Ni-BN/water	Effect of loading Ni on CO_2 adsorption
Ni-BN/various solvents	Effect of polar solvent on CO_2 adsorption
BU30	Cycle performance on high urea concentration
BU15	Cycle performance on low urea concentration
BU15B1	Cycle performance on multiple B-containing precursors

The objectives on modification process exhibited different chemistry and pore structure as indicated previously in the introduction section. Furthermore, to understand the significance of the solvents used during synthesis, in particular Ni (II) impregnation of BN, the procedure was carried out in water and water/methanol mixture for immobilisation. The influence of all synthesis' targets was assessed in this chapter for carbon dioxide adsorption applications. The cycle test on pristine BN samples with various adsorbents property (as mentioned in Chapter 4) are investigated to assess their reusability performance. Here, urea-based BN materials

with high and low proportion of urea as well as boron rich BN materials were selected for the regenerability process.

Determination of CO_2 uptake and the breakthrough curve (theory)

In this study, thermogravimetric curves of CO_2 adsorption can be considered as "breakthrough curves" due to the crucible examined as a fixed-bed reactor. Therefore, CO_2 adsorption of the sorbents has been determined by studying the "breakthrough curves" first. A breakthrough experiment is an S-shaped plot measuring the adsorption in the adsorbent bed, which takes place due to mass change concentration (a sample breakthrough curve is given in Figure 7.2). This process provides an explanation of the mechanism that adsorbate (CO_2) is distributed within a fixed bed reactor when gas flows containing a certain amount of carbon dioxide feed through a fixed bed until the adsorbate is removed in the exit. In both post and pre combustion capture stages of this process, the capture capacity of sorbents decreases steadily with the process of carbonation. To repeat the reverse process, the used sorbents follow the regeneration step by decarbonisation under cycle process (Ji *et al.*, 2020).

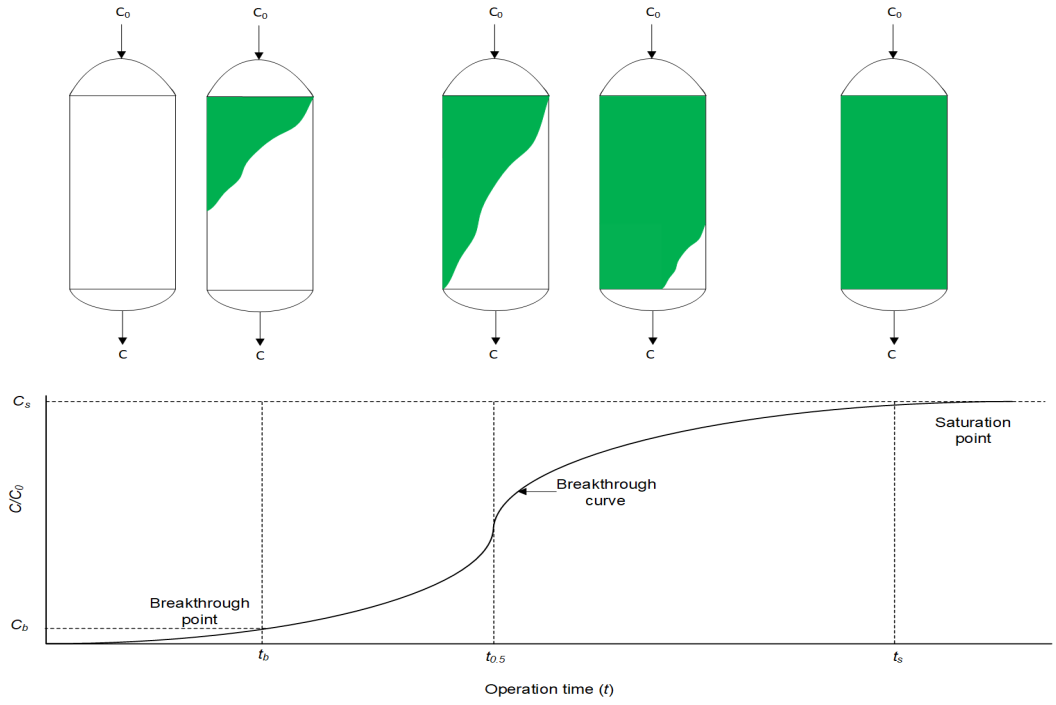

Figure 7.2 Typical breakthrough profile in a fixed-bed adsorption process (Adapted from (Nassar, 2012)).

In a typical breakthrough experiment, the gas flow passes into a defined dynamic bed and then the adsorbate is adsorbed. This continues as long as the sorbent has adequate available sites (e.g., the green area in fixed-bed columns are illustrated in Figure 7.2). When the saturation point is reached, the CO_2 capture rate declines slowly until no further adsorption takes place. The breakthrough curve is determined from the temperature of adsorption and the kinetics rate. A shorter breakthrough occurs as the temperatures of adsorption process increases. Furthermore, at lower rates of flow, the breakthrough curves become steeper (Marsh and Rodríguez-Reinoso, 2006). In order to maximise the sorption process, optimising the operating conditions with minimum mass transfer is needed. This can be associated with microporosity or particle size of adsorbents, temperature and flow rates in the fixed-bed column.

Gravimetric sorption technique at low pressure

The adsorption performance of pure CO_2 was carried out at low pressure (up to 1 bar) TGA/DSC 3+ micro balance, Mettler Toledo. First of all, samples were dried at 393 K with a heating rate of 10 K/min from 298 K under flowing N_2 (150 ml/min) for 6 hours to ensure a complete removal of moisture. Then the process was allowed to reach to the sorption temperature in which the test is to be carried out. When the sorption temperature was reached, samples were stabilized under flowing N_2 (99.999%,150 ml/min) for 15 min and then N_2 flow was switched to pure CO_2 (99,999%, 50 ml/min) flow for 6 hours. The mass uptake during this stage was interpreted as the CO_2 capture capacity.

Cycle test based on temperature swing adsorption

Temperature swing CO_2 adsorption/desorption tests were conducted with a TGA/DSC 3+ micro balance, Mettler Toledo using N_2 as the purge gas and CO_2 gas as the reactive gas. Firstly, samples were degassed at 393 K for 6 hours at atmospheric pressure. Adsorption was performed at 303 K by flowing CO_2 (50 mL/min) for 3 hours. Desorption was performed by increasing the temperature to 75 ºC (10 C/min) under N_2 gas flow (100 mL/min) for 3 hours. CO_2 adsorption/desorption capacities were calculated by the change in mass of the samples.

7.3. CO_2 sorption on non-metal modified porous BN

Due to the relatively large porosity of modified samples by introducing the triblock copolymer surfactant (P123), the materials were assessed for CO_2 capture under ambient conditions. The adsorption capacities of pure CO_2 on pristine BN and metal-free modified BN-P123 based on both using urea and melamine precursors were determined by thermogravimetric analysis. The mass uptake during this stage was interpreted as the CO_2 capture capacity. Figures7.3. illustrates the TG profiles of CO_2 uptake along with weight change results of all samples.

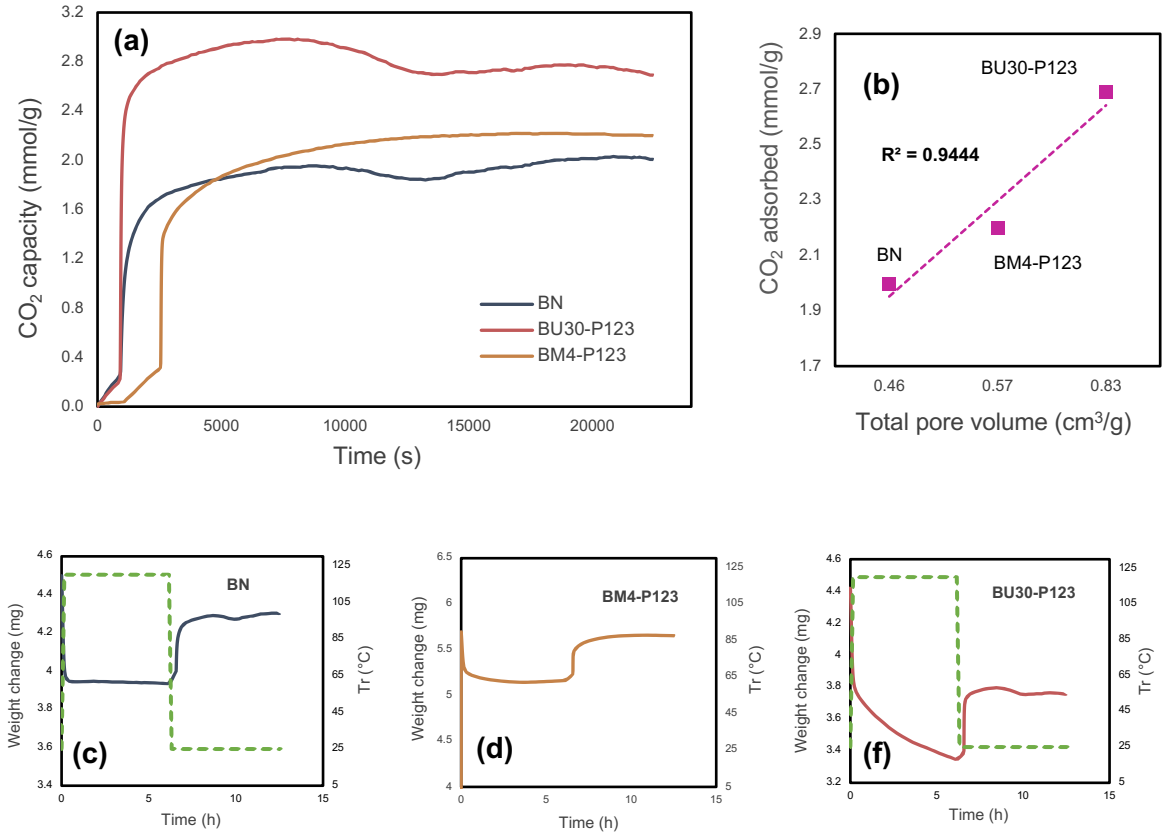

Figure 7.3 TG profiles of CO_2 adsorption on pristine BN, BM4-P123 and BU30-P123 at 298 K (a); (b) CO_2 sorption capacity *vs* V_{total} for all samples; (c, d, f).TG profiles of weight change on the same samples.

The experiments revealed that pristine BN from urea-based precursor shows a CO_2 capacity of 2 mmol/g at 298 K, which was enhanced by about 34.5% with the addition of P123 copolymer (2.69 mmol/g for BU30-P123 at 298 K). This improvement also appeared in the BM4-P123 sample (2.2 mmol/g), which indicates relatively lower capacity than BU30-P123. The augmented CO_2 adsorption on non-metal modified

samples is undoubtedly as a result of the pore network structure of prepared BN, whereas pristine BN exhibits lower porosity. Given that the CO_2 sorption capacity did not directly associate with BN surface area, the total pore volume of corresponding samples was plotted in Figure 7.3 (b). It can be observed in Figure 7.3 (b) that the CO_2 sorption capacity indicates a relatively high correlation between pore volume and CO_2 sorption capacity of the samples. The porous boron nitride prepared by urea as a nitrogen source and Pluronic P123 indicates the highest value of pore volume compared with other two samples. On the question of nitrogen sources, this study found that use of high proportion of urea induces major changes in cumulative pore structure of BN, whereas melamine did not significantly affect porosity in this measure. Accordingly, based on the kinetic principle, the BU30-P123 sample with optimal pore size detected a great physisorption CO_2 uptake as given in Figure 7.3(a). The TG profiles of weight change on all samples in Figure 7.3(c, d, f) provides the gravimetric sorption procedure at low pressure. In the first step, the observed inconsistency of weight changes among samples depends on moisture content of each sample that needs to be eliminated through N_2 purge gas.

The existing literature on this area highlights that higher microporosity provides more active sites and storage space to boost the adsorption performances (Li *et al.*, 2013a, Xiong *et al.*, 2017, Liu *et al.*, 2018). To the best of our knowledge, the result of this synthetic method is superior to other modification methods such as (3D) BCNO structure (1.8 mmol/g) at 298 K as reported by López-Salas *et al.*, (2018) and closer to porous BCN (2.49 mmol/g) at 298 K and porous BN fiber (2.85 mmol/g) at 273 K (Florent and Bandosz, 2018, Wang *et al.*, 2019). However, the use of melamine in porous BCN as well as BN fiber leads to presence of carbon content and consequently decreases the stability upon exposure to ambient air. In another major study, the effect of high-temperature treatment in different gases was studied in Liang *et al.*, (2019), where porous BN fibers treated in NH_3 gas at 1673–1773 K enhanced CO_2 adsorption capacity (from 0.45 mmol/g to 1.6 mmol/g). Nonetheless, this outcome is not a satisfactory result. One possible insight of this finding is that pyrolysis temperature and carrier gas does not lead to a remarkable change in CO_2 uptake.

Interestingly, directing triblock co-polymer was also used to design a hierarchical carbon sorbent (To *et al.*, 2016). This hierarchical structure is desirable for CO_2 capture as it shows superior capacity (4.5 mmol/g) under ambient conditions. It is

noteworthy that at lower pressures (bar ≤ 1), the density of pore volume, especially the micropores volume plays a critical role in capturing CO_2 (Li *et al.*, 2013e). Therefore, high surface area and porosity of BN-P123 has brought about a positive adsorption interaction.

What is surprising is that for the pristine BN (without adding surfactant), the CO_2 adsorption capacity on the sample exceeds those materials reported by Marchesini *et al.*, (2017b), Marchesini *et al.*, (2017a). Although they accomplished highly porous boron nitride with a high surface area (>1900 m^2/g), the CO_2 adsorption capacity of their sample was up to 1.6 mmol/g under the ambient condition. Given the results of this approach, one can conclude that though the specific surface area (SSA) is one of the main factors to increase the CO_2 capacity, obtaining a high SSA (e.g. >1000 m^2/g) does not lend itself to an increased CO_2 capacity. Hence, the unique characteristics of the modified boron nitride opens up new routes for designing porous BN, which could be employed for optimising CO_2 adsorption.

7.4. Effect of Ni loading porous BN on CO_2 adsorption

As part of our study, we found a correlation between the adsorption capacity of BN and its textural properties (surface area and pore size/shape) (Hojatisaeidi *et al.*, 2020). This section now moves on to consider another specific objective of this study to examine CO_2 adsoption test on a new plan of metal-modification of pristine BN. To this end, Ni transition metal compound has been doped on porous BN and the characterisation results have been given in Chapter 6. In this section, BN@Ni samples have been tested for CO_2 adsorption test in order to reflect the influence of chemistry and microscale properties of BN in adsorption performance. The adsorption performance of pure CO_2 was carried out at different temperatures by thermogravimetric analysis (TG). The CO_2 breakthrough curves may be classified into three main sections: pre-breakthrough, active-breakthrough and post-breakthrough. The pre-breakthrough portion is the initial part of the adsorption. During the pre-breakthrough portion, the CO_2 gas is initially absorbed into the sorbent, and the product gas contains low levels of CO_2. In the first stage of the active-breakthrough region, the CO_2 adsorption reaches the exit of the sorbent bed where the CO_2 concentration begins to increase with time. During the process of post-breakthrough,

the sorbent bed approaches complete conversion and all of the CO_2 in the feed gas passes through the sorbent bed. The effluent CO_2 concentration in this region matches the CO_2 concentration in the feed gas (99.999% by volume). To help to ensure clarity, the post-breakthrough has been taken into account to evaluate the CO_2 capacity of each sorbent considering different adsorption temperatures and Ni concentration.

Figure 7.4(a-c) illustrates the TG profiles of CO_2 capacity of Ni-loaded and Ni-non-loaded samples under different operational conditions. Based on all experimental results, it can be found that 0.5% proportion of Ni on BN exhibited the highest adsorption capacity (2.63 mmol/g) at 298 K. Moreover, the variation of CO_2 capacity with Ni loading at different temperature is summarised in Figure 7.5. It is observed that the increase in the metal content of BN strongly affects the CO_2 adsorption capacity of pure BN. For instance, at the room temperature (298 K), the capacity was gradually enhanced up to 2.4 mmol/g and 2.6 mmol/g when loaded with 0.1% and 0.5% of Ni respectively. However, it was reduced significantly and reached 1.59 mmol/g for the sample with 1% Ni loaded. This finding supports the idea that no simple correlation exists between the accessibility parameters (S_{BET} and V_p) and the sorbent performance, which should be governed by some other features of the solid. Such a behaviour is explained by two factors: firstly, increasing the Ni loading provides more active sites due to the basic feature (electron donors) of transition metal oxide particles which is favourable for the adsorption of CO_2 (Jang and Park, 2012 ; Schott *et al.*, 2017). Secondly, higher loading of Ni may cause aggregation of metal particles and consequently hinders the diffusion of CO_2. Nevertheless, the lowest capacity of CO_2 is for BN-0.1% Ni which was obtained at high temperatures (T= 345–393 K). The BN sample with high molar ratio of Ni (1%) showed a higher capacity (up to 1.92 mmol/g at 345 K) compared to the other two samples with lower concentration of Ni (Figure 7.4). This combination of findings provides some support for the conceptual premise that surface chemistry and polarizability of BN influence an association with the CO_2 adsoprtion process. As comparison, some preliminary studies suggest that functionalised BN with nitrogen groups may promote BN capability towards CO_2 capture (Huang *et al.* 2017; Owuor *et al.*, 2017; Chen *et al.*, 2018b). As pointed out in the literature review chapter, the presence of nitrogen groups may not only tune the pore size and increase the BN surface area to physically capture CO_2 with van der Waals interaction, but also provides a negative charged surface for acid-base

interaction. However, there is no unanimous agreement yet on the role of nitrogen groups in porous materails and how it leads to enhance CO_2 capture through acid-base interaction (Qi *et al.*, 2019).

Aditionally, several reports have proved the significant effect of transition metal oxide modification of porous materials (e.g. porous carbon) on CO_2 adsorption behaviour due to their basic features, high stability and low-cost (Jang and Park, 2012; Schott *et al.*, 2017; Yang *et al.*, 2019). For instance, in a similar study to this research, Yang *et al.* (2019) emphasised that chemical adsorption of CO_2 with basic sites in functionalised 3D BN nanosheets/ZnO is the main contributor of adsorption capacity. The main weakness of this method is that the highest CO_2 uptake at ambient condition was about 40 cm^3/g, i.e., 1.78 mmol/g, which is a relatively low value. This can be attributed to the low porosity of the sample and therefore, it leads to reduction in the physical adsorption of CO_2. In summary, from the discussions so far, one could conclude that the designed materials exhibit a higher CO_2 capture capacity at 298 K as well as 345 K which makes them good candidates to use in practice as the flue gas temperature is above 298 K. Notably, as far as we are concerned, this approach is the first in the literature presenting CO_2 adsorption tests on Ni-doped porous boron nitride validating the applicability of transition metal modified BN for improved capacity of pure CO_2.

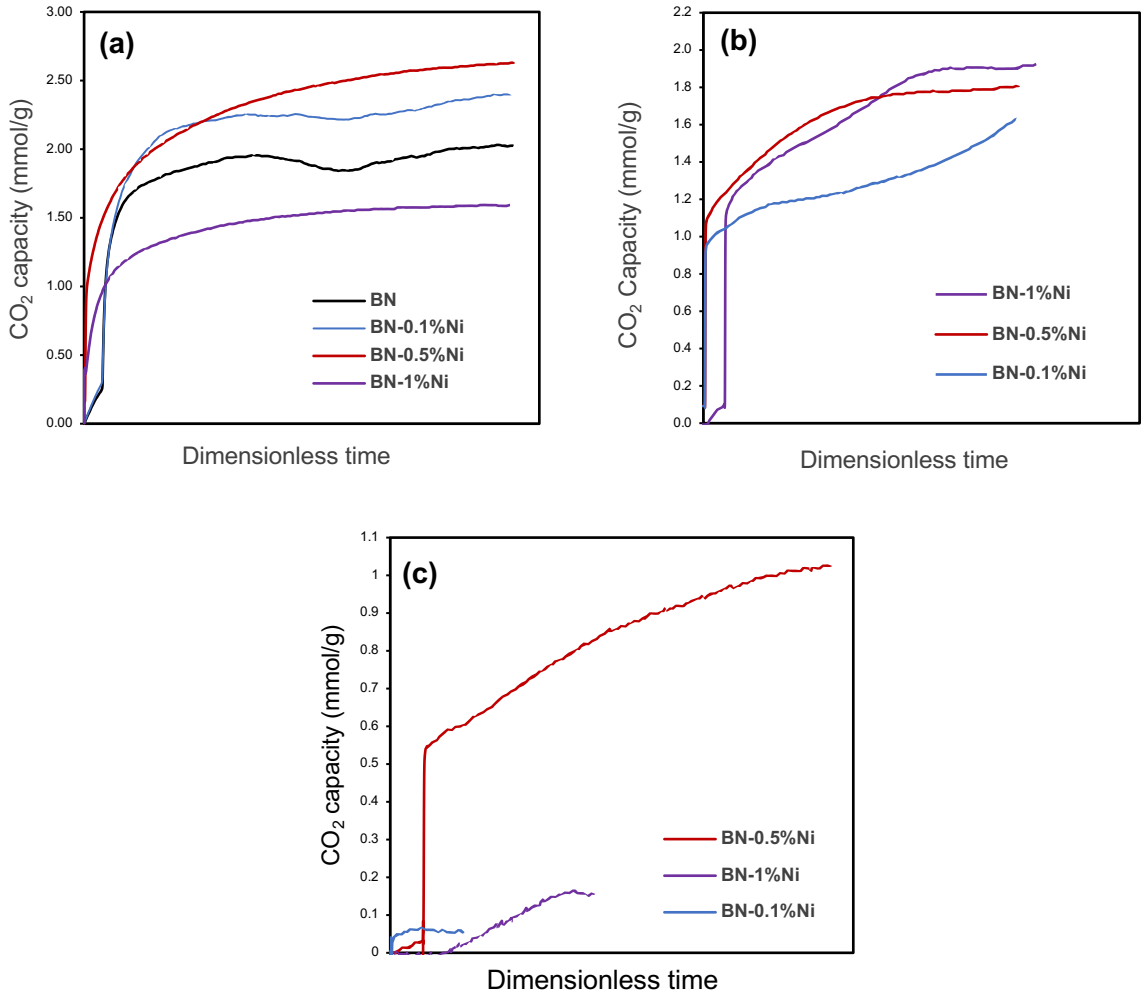

Figure 7.4 TG profiles of CO_2 adsorption on BN and BN-Ni samples at 298 K (a); 345 K (b); 393 K (c)

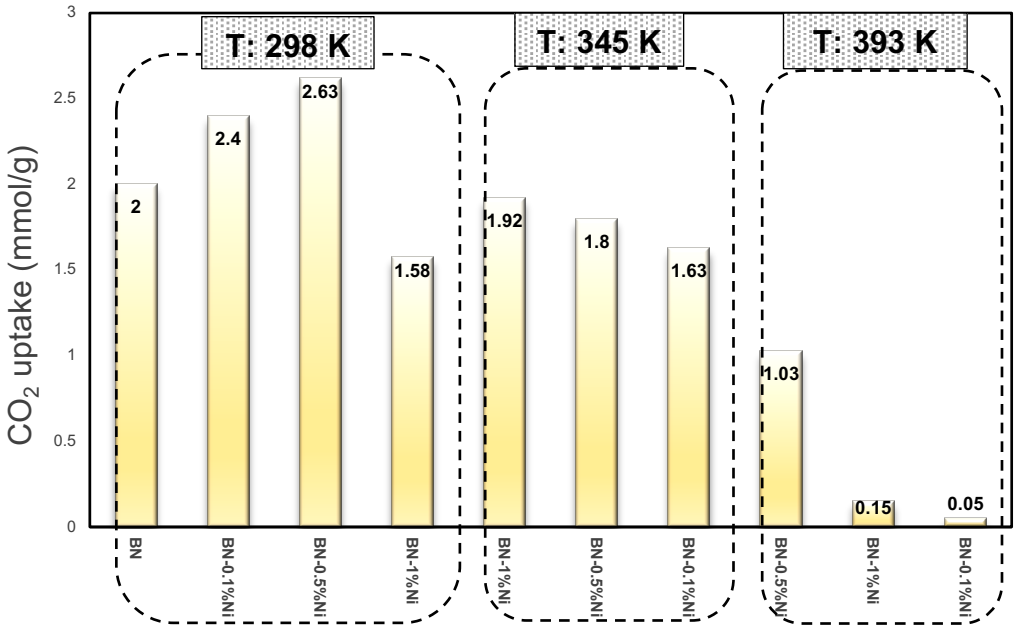

Figure 7.5 Bar plots showing CO_2 uptake adsorbents at different conditions

Effect of solvent-assisted metal modification of porous BN on the CO_2 sorption

Comprehensive study into solvent-assisted BN-Ni during the synthesis are significantly important to control the crystal structure, size and shape of the adsorbent materials. In this context, the discussion in Chapter 4 showed that the production of pristine BN in water/methanol solvents has a higher specific surface area (SSA) and pore volume than in water solvent. Considering the dominant role of SSA and total pore volume in the CO_2 adsorption performance, previous studies investigated the correlation between solvents and material's porosity in order to strengthen the quantity of adsorption (Hong *et al.*, 2013; Mohd Daud *et al.*, 2016). However, one should note that the aforementioned observation does not apply to Ni (II) modified BN and that using water/methanol solutions has failed to enhance the capturing values.

Here, the modification of Ni doped porous BN was carried out both in aqueous and alcohol solutions *via* impregnation and calcination treatment and the CO_2 adsorption performance was studied using TGA analysis. Typical TG curves at 298 K and 345 K for BN-0.5% Ni in water and BN-0.5 Ni in water/methanol are plotted in Figure7.6. (a, b). What is worthwhile to note is that at both temperatures, there is a remarkable change in CO_2 uptake between the two samples using various solvents during the fabrication process. As shown in Figure 7.6.(a, b) the BN-0.5% Ni in water has a higher affinity to CO_2 than BN-0.5% Ni in the water/methanol sample. Furthermore, a similar approach was also confirmed by lower percentage of Ni compound for BN-0.1% Ni samples under ambient conditions (see Figure 7.6c). It seems possible that these results are due to the good dispersion of nickel particles in water polar solutions, which derive much higher CO_2 uptake in BN-water sample than BN-water/methanol. Additionally, one possible implication of this is that the lower polarity of alcohol to water leads to reduction in solubility. Accordingly, the choice of solvents depends on its polarity enrichment (Ho and Van Zee, 2000). Details regarding the influence of solvent as a function of polarity on CO_2 capacity of BN-Ni samples are summarised in Figure 7.6 (d), which clearly indicates that the higher-polar solvent (pure water) group recorded by far a higher quantity of CO_2 adsorbent than the lower-polar solvent (mix water/methanol). The results of this study are fundamental to design the fabrication process for future research. A further study with more focus on solvents is therefore suggested.

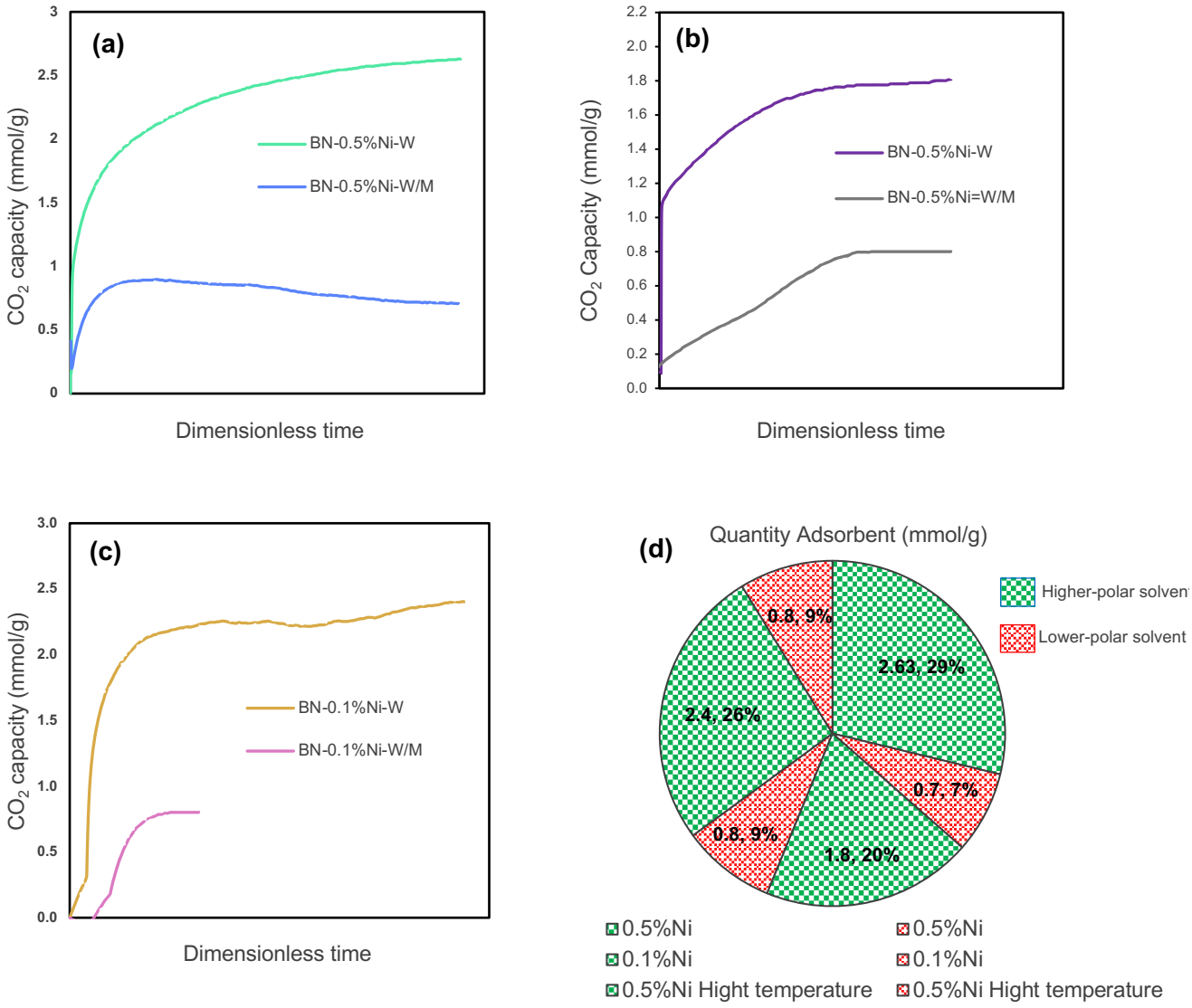

Figure 7.6 TG profiles of CO_2 adsorption on BN-0.5%Ni-W and BN-0.5%Ni-W/M at 298K (a); 345 K (b); BN-0.1%Ni-W and BN-0.1%Ni-W/M at 298 K(c); Summarise of the quantity of adsorbent for the same samples (d)

So far, this Chapter has evaluated the CO_2 adsorption isotherms for the first cycle based on different synthesised materials. To obtain a better view of current data, the results for all samples with various synthetic conditions have been reported in Table 7.1.

Table 7-1 Summary of CO_2 adsorption of all the samples reported in this study at 1 atm

Materials and methods	S_{BET} (m^2/g) / V_{total} (cm^3/g)	Adsorption temperatures T (k)	CO_2 Capacity (mmol/g)
BN - Template-free synthesis form boric acid/urea precursors followed by pyrolysis at 900 ºC in N_2	102 – 0.46	298	2.00
BU30-P123 - Metal-free modification of urea-based BN using Pluronic P123 surfactant	476 – 0.83	298	2.68
BM4-P123 - Metal-free modification of melamine-based BN using Pluronic P123 surfactant	143 – 0.57	298	2.2
BN-0.1%Ni - Metal modification of BN with Ni loading through impregnation and calcination steps	660 – 0.52	298 345 393	2.4 1.63 0.05
BN-0.5%Ni	213 – 0.61	298 345 393	2.63 1.8 1.03
BN-1%Ni	63 – 0.37	298 345 393	1.58 1.92 0.15
BN-0.5%Ni-W/M - Using mixture of water/methanol solvent	-	298 345	0.7 0.8
BN-0.5%Ni-W/M	-	298	0.8

7.5. Cycle tests on pristine BN at 303 K

The stability of sorbents throughout consecutive cycles is of utmost importance for their long-term reusability. Herein, the CO_2 sorption and desorption cyclability was calculated *via* temperature swing adsorption/desorption using TGA analysis. The cycle test was carried out at 303 K on different types of BN production (BN-U15, BN-U30 and $BU_{15}B$) as shown is Table 7.2.

The stable reusability of the BN sorbent for CO_2 capture for up to eight consecutive cycles can be observed in Figure 7.7 (a-d). The graphs present that BN material with higher proportion of urea indicates the highest capacity and the use of an additional B-containing precursors suppress the performance. This is attributed to the vital role of the BN pore chemistry in CO_2 capture performance. Figure 7.7 (a-c) shows the

thermogram referred to CO_2 adsorption/desorption cycles of the corresponding samples. During the adsorption steps at 303 K, there is an increase in weight until the saturation is achieved for each sample. The CO_2 desorption steps occur through the nitrogen flow at 348 K, which leads to decrease in weight of the samples. One of the issues that emerge from these findings is the weight loss that appeared with a combination of N_2 as the protective gas and CO_2 as reactive gas as Mettler-Toledo measurement could not provide an adequate explanation for this phenomenon.

Overall, the prepared pristine BN samples reveal to be potential CO_2 capture materials, showing a good stability throughout several cycles. It is widely accepted that CO_2 adsorption/desorption cycles is a substantial aspect to reuse sorbents for the subsequent separation of the captured CO_2 through different chemical processes. However, there is a need for an optimisation plan with considerable variations in order to perform a better cyclic process. Hence, further studies considering these variables should be undertaken.

Table 7-2 CO_2 uptake values for various samples following the cyclic adsorption test

			CO_2 uptake (mmol/g)								
NO	**Samples**	**CO_2 T_{ads} (K)**	**1st cycle**	**2nd cycle**	**3rd cycle**	**4th cycle**	**5th cycle**	**6th cycle**	**7th cycle**	**8th cycle**	**Average**
1	BU30-W/M	303	0.833	0.85	0.935	0.575	1.246	0.712	0.949	0.558	0.832
2	BU15-W/M	303	0.653	0.432	0.534	0.406	0.502	0.412	0.463	0.364	0.470
3	BU15B1-W/M	303	0.468	0.483	0.161	0.164	0.412	0.146	0.391	0.147	0.296

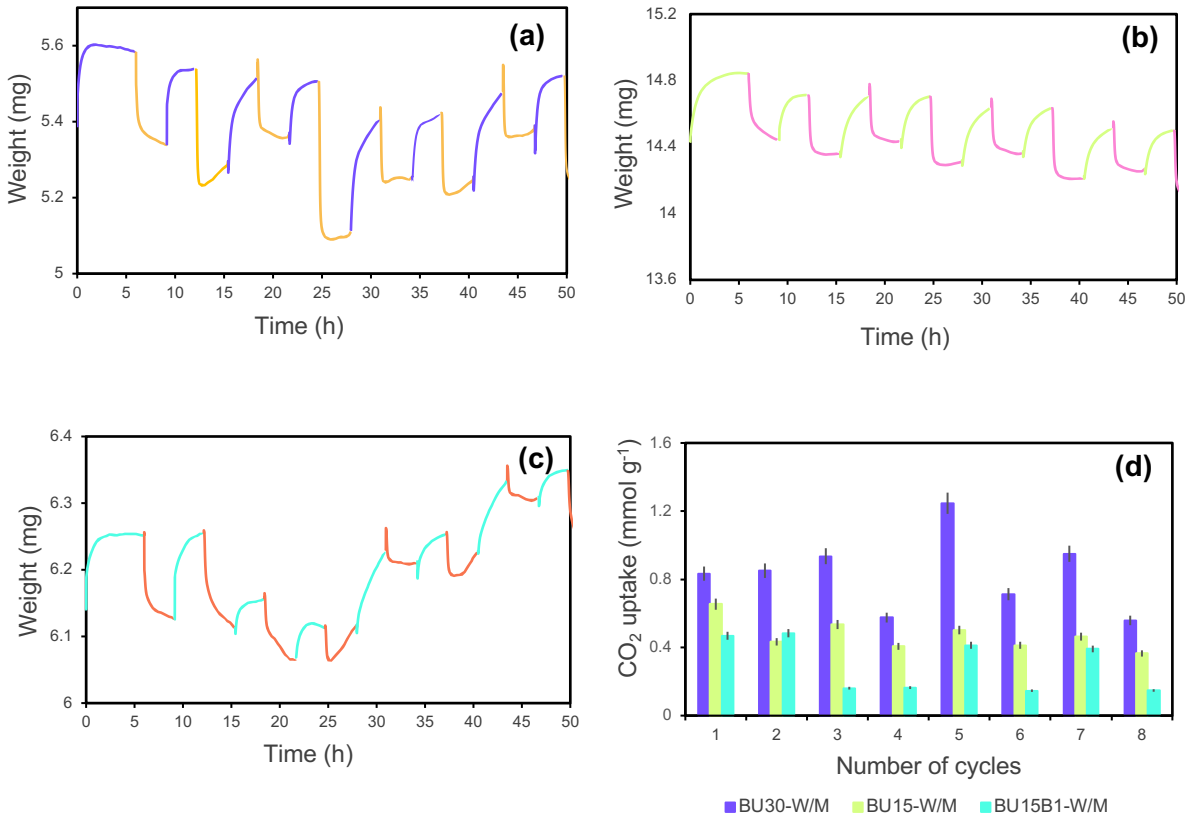

Figure 7.7 Gravimetric CO_2 adsorption- desorption cycles with temperature swing desorption between 303 K and 348 K on (a) BU30-W/M; (b) BU15-W/M; (c) BU15B1-W/M; (d) Gas sorption at low pressure for the corresponding samples.

7.6. Conclusions

In this chapter, a range of favourable porous born nitrides were selected for a dynamic CO_2 adsorption test. These samples were classified as pristine BN (prepared by different synthetic approaches), non-metal modification of pristine BN with surfactant agents and metal-modification of pristine BN with Ni (II) loading in section 7.2.

In section 7.3, it was found that utilising P123 into boron and nitrogen precursors leads to improved CO_2 adsorption capacity up to 2.69 mmol/g, as compared with pristine porous BN, which was found 2.00 mmol/g. This significant change is attributed to the creation of high porosity levels by introducing the triblock copolymer surfactant. A natural progression of this work is to describe how textural property parameters of BN lead to higher interaction between BN and CO_2 molecules.

Metal modification approach using Ni (II) impregnation procedure of porous BN was also performed for CO_2 sorption with different temperatures in section 7.4. The results

indicate that BN-Ni has stronger affinity for CO_2, whereas at 298 K the capacity of pure CO_2 was enhanced by about 31% compared to pristine BN (2.62 mmol/g for BN-0.5% Ni *vs* 2.00 mmol/gr for BN). We observed that the adsorption of CO_2 dropped when the temperature increased. Additionally, the most optimised sample in each temperature (which is BN-0.5% Ni for 298 K and 393 K and BN-1% Ni in 393 K) revealed a promising outcome in terms of capacity. Taken together, this approach confirmed the influence of total pores volume and chemistry properties of BN on van der Waals and Lewis acid-base interaction respectively. Notably, Ni (II) impregnation of BN procedure not only contributes to the tuning of total porosity, but also increases the number of basic sites and consequently improves its adsorption capacity.

Moreover, another significant challenge of BN's performance toward CO_2 capture is the effect of solvent properties on porous BN. The findings of this study are also discussed in this section. According to the CO_2 sorption tests, the results revealed a stronger affinity in solvents with a higher level of polarity due to solubility behaviour of the products. Though the findings of this study are persuasive, a more comprehensive study needs to be carried out.

In the final part of sorption experiments (section 7.5), the CO_2 cyclability was measured by temperature swing desorption over the eight adsorption-desorption cycles. This finding has important implications for developing BN materials for commercial benchmarks. However, the results were not encouraging enough as a result of possible back-pressure phenomena. This study would emphasise the importance of undertaking further work in order to optimise each operating cycle.

The present work could be extended by exploring other parameters (e.g., electronic features or surface chemistry of BN), which could influence BN to capture more CO_2. Overall, the analyses of this chapter demonstrate applicability of modification strategy of BN for enhanced capacity of pure CO_2. These findings suggest that there is an optimisation challenge between surface modification strategy and the BN materials properties, which needs to be deliberated.

CHAPTER 8

CONCLUSIONS AND RECOMMENDATIONS FOR FUTURE WORK

Outline of the chapter

This chapter provides some concluding remarks of the dissertation and discusses a summary of the level of success with each of the dissertation objectives. In addition, it offers some avenues for future research, which could be followed either to improve this work or to take a new direction towards carbon capture. The chapter is organised as follows:

8.1. Conclusions

8.2. Challenges and recommendations for future work

8. Conclusions and recommendations for future work

8.1. Conclusions

The present research has investigated the synthesis of porous boron nitride and attempted to design new porous BN materials as effective adsorbents for carbon capture. Pristine porous BN materials were synthesised based on a bottom-up approach, using the template-free strategy. Two main modification strategies were studied to determine the effect of porosity and surface chemistry of BN CO_2 adsorption. Experimental design, characterisation techniques and adsorbents screening have been implemented for different approaches. The dynamic CO_2 adsorption process at a low pressure has been employed under laboratory gravimetric experiment conditions. Regeneration process based on heat operation (temperature swing adsorption) has been applied to evaluate porous BN reusability and stability for future industrial operation where the real gas mixture exists in cyclic conditions.

In this investigation, the aim was to develop a highly performing porous BN adsorbent to enhance capacity of pure CO_2. This aim has been achieved by meeting the following objectives on each chapter as follows:

Review the previous carbon capture technologies and highlight adsorption method based on dry-sorbent materials

Recent carbon capture development and methods for separation and capture of CO_2 has been reviewed in the second chapter with a focus on using porous materials as a future carbon capture and sequestration technology with high impact on the cost-optimum deployment of CCS strategies. This could fit to this research aim considering the low-cost porous BN for future application in carbon capture.

Highlight the advantage of using porous BN for carbon capture application with investigation of its properties, experimental synthetic and modification methods

After reviewing the current solid adsorbents, which have been implemented in CO_2 physisorption studies to date, this research discussed the reasons for focusing on BN materials due to the advantages mentioned in the literature review chapter. The structural and morphology properties of boron nitride nanomaterials have been

reviewed to show the diversity of microscopic structure of BN nanomaterials that can be obtained on a laboratory scale. The fabrication procedure of porous BN has been divided into template and non-template methods. Much of the current literature on synthesising porous BN pays particular attention to template free approach, which resulted in porous BN materials with high porosity and fewer steps. The impact of various conditions including the nature of precursors, solvents, carrier gas and temperature of synthesis in non-template fabrication of porous BN has been reviewed in chapter two. The review of chemical modification strategies of porous BN is also given in chapter two due to the popularity in the literature. Taken together, this section enabled us to find the research gaps in the formation of pure BN as well as exploration of novel modification strategies to achieve a better result compared to pristine BN materials.

Investigate the precursors effect on pristine BN production

Synthesising and characterising pure porous BN nanomaterials is often considered as a critical step which can be tailored as an alternative to other successful porous adsorbents for carbon capture applications. A non-template method with various synthesis conditions including boric acid: urea molar ratio of 1:30, use of second boron sources (borax), solvothermal evaporation (methanol/water) and hydrothermal evaporation (pure water) have been carried out in Chapter 4. The highest porosity levels have been achieved for pristine BN production at boric acid: urea molar ratio of 1:30, in methanol/water mixture and decomposition temperature of 1173 K under N_2 flow gas. However, fine textural and structural properties for CO_2 adsorption test have been also observed in other samples named as BU_{15} (methanol/water), BU_{30} (pure water) and multiple boron precursors $BU_{15}B_1$ (methanol/water).

In conclusion, precursors with a variety of molar ratios and solvents mixture are key factors in obtaining highly porous BN with micro- and meso- porosity levels. High thermal stability was observed among those samples with less impurity in comparison to carbon-based materials. Samples with high purity obtained as templated were not used in this investigation. The insights gained from this study will be of assistance to control porous BN properties for operating in CO_2 adsorption process.

Design of a highly porous BN with metal-free modification strategy

Thus far, one of the main adsorption challenges that have been argued in the academic literature is the low CO_2 capture capacity of porous BN materials. Therefore, achieving high levels of porosity a significant aspect to improve porous BN CO_2 capture capacity has been considered in this study. The triblock copolymer surfactant (P123) has been introduced for both boric acid-urea and boric acid-melamine precursors (as discussed in Chapter 5). The use of additional structure directed agent served as a porogen during the decomposition step. The improvement of specific surface area and total pore volume has been achieved in both the modified samples. The overall structural, chemistry and stability properties of samples remained unchanged to pure porous BN without adding surfactant. Hereby, we would like to emphasise that the contribution of this study is to confirm the positive impact of P123 surfactant on porous BN materials, which acts as an adsorbent to capture a higher level of CO_2. This new approach has been published in the *Energies* journal and interested readers are referred to for further information (Hojatisaeidi *et al.*, 2020).

Investigate the effect of Ni loading on porous BN chemistry and porosity properties

A novel exploration of metal modification of porous BN has been examined in Chapter 6. Varying molar ratio of Ni concentration have been impregnated with boric acid and urea mixture before the heat treatment process. Solvent-assisted procedure has been considered by dissolving reactants in pure water or mix water/methanol solvents. The empirical findings in this procedure provide a better understanding of the correlation between the polarizability of solvents into formation of BN-Ni samples and their CO_2 adsorption performance.

A narrow distribution and small size (10-15 nm) of Ni nanoparticles has been observed by transmission electron microscopy (TEM) analysis. The Laser-induced breakdown spectroscopy (LIBS) and elemental mapping spectroscopy findings have defined the presence of Ni into porous BN framework. This research proved that the presence of Ni metal sites has clearly affected the optical and photoluminescence properties of porous BN. The intensity of absorption in visible light has been increased with high concentration of Ni compund. Dissimilar behaviour among samples has been also observed in fluorescence spectra data as a result of porous BN surface

fuctionalisation. The basic sites of porous BN has been confirmed by XRD analyser, which is favorable for acid-base interaction between samples and acidic CO_2 molecules. The textural properties of samples have been calculated, an enhancement was found in specefic surface area and pore volume results for samples with lower proportion of Ni doped.

Overall, this work contributes to the existing knowledge on how evaluating influences and their optimisation can enhance the CO_2 uptake of porous BN by incorporation of Ni (II) into pristine BN samples. Prior to this study, evidence of the role of Ni sites on the surface of porous BN was purely anecdotal. To the best of our knowledge, this work is the first comprehensive investigation in the published literature, which examines the association between Ni (II) basic sites of porous BN, its porosity/pore size, and chemistry which results in a high CO_2 sorption of BN. A manuscript of this approach is currently in preparation to be submitted to a high impact journal.

Study of CO_2 sorption test on pure and modified porous boron nitride samples at different temperatures

In Chapter 7, preliminary dynamic CO_2 sorption tests were conducted on a range of produced porous BNs at a low (<1 bar) pressure and different temperatures. The adsorption performance of pure CO_2 flow (99,999%, 50 ml/min) at 298 K has been analysed on modified porous BN (BM4-P123 and BU30-P123) and was compared to pure BN. The CO_2 uptake of both samples has been relatively enhanced and the highest adsorption capacity was about 2.69 mmol/g for BU30-P123. This new understanding could help to improve predictions of the impact of each textural property parameter (specific surface area, total pore volume and pore size) on porous BN CO_2 uptake. In general, therefore, we found that the total pore volume and the volume of microporosity distributions play significant roles compared to the surface area of sorbents. The findings of this investigation complement those of earlier studies.

The CO_2 adsorption performance for BN-Ni samples has been carried out at a low (<1 bar) pressure and three targets of temperatures (298 K, 345 K and 393 K) in Chapter 7. This set out experiments that confirmed the designed BN-Ni materials can be assessed even above the ambient temperature. It has been demonstrated that the highest uptake of CO_2 is for BN-0.5% Ni (2.63 mmol/g) at 298 K. For the sake of

comparison, the data at 298 K on four samples indicated that the metal modification strategy has been accomplished and the capacity of pristine BN has been gradually improved when loaded with 0.1% and 0.5% of Ni. The findings from this objective contribute to the current literature. First, this approach will prove useful in justifying the impact of the key variables (e.g. tuning porous and chemical structure of BN) involved in reaching a higher CO_2 uptake. Second, the present study has gone some way towards enhancing the understanding on the behaviour of CO_2 adsorption mechanism. Another major investigation of the metal modification plan was to determine the CO_2 adsorption behaviour on samples, which dissolve in pure water and water/methanol solvents. The CO_2 uptake has remarkably decreased with BN-Ni water/methanol samples at 273 K and 345 K. As far as we are aware, this analysis is one of the first attempts to examine the impact of composition of different solvents on Ni modification of porous BN CO_2 adsorptive performance.

Study of cyclic CO_2 adsorption performance on porous BN

The regenerability and stability of pristine porous BN has been conducted on eight cycles through temperature swing adsorption/desorption at 303 K. The findings on cyclic tests have proved the feasibility of porous BN adsorbent for the carbon capture application. Overall, porous BN can be taken into the next generation of porous materials with lower regeneration energy requirements.

8.2. Challenges and recommendations for future work

The choice of using porous BN materials as a potential and alternative dry-sorbent technology for carbon capture is enormous in comparison with the conventional solvent-based absorption processes or other solid sorbents. This could be justified in terms of their low-cost, mechanical and thermal stability and tunability properties. However, challenges in adsorbent materials development remain and need to be solved before being integrated in CCS large scale projects. The following section provides insights for future research for enhancing the process.

Apply Response Surface Methodology (RSM) technique to model and optimise the metal modification process

It was previously demonstrated that by changing the structure, porosity and chemistry of porous BN, the materials CO_2 uptake could be influenced. Therefore, one could extend the present work to find out the optimal condition to make porous BN with Ni composition. RSM is a useful technique to design and optimise the experiments to identify a number of independent variables. With regards to the approach taken in this study, these variables can be examined as reactant composition ratio, solvents and temperature of adsorption. The yield of CO_2 capture capacity can be characterised as a response. Developing a quadratic regression model is recommended for such applications to evaluate a relationship with process variables.

Performance evaluation of selectivity

Selectivity has an instrumental role in evaluation of how porous BN materials separate. One future research area is to investigate if the developed material has desirable characteristics with regards to its selectivity and working capacity. Hence, one recommendation is to perform a thorough study for investigating the selectivity of porous BN for different gases (pure CO_2 and N_2) in adsorption measurements.

Cycle design for a breakthrough experiment

One potential avenue for future research is to optimise the cycle process in order to select the best operating conditions and incorporate the materials in actual conditions. More broadly, further research is required to determine all potential cycles for each porous BN adsorbent with different material properties. In particular, we strongly believe that by combining a simulation approach and experimentation, promising porous BN sorbent recovery can be achieved *via* cyclic test. Given that the adsorption screening is crucial, this would be a useful area for further work.

9. References

Abd, A. A., Naji, S. Z., Hashim, A. S. and Othman, M. R. (2020) Carbon dioxide removal through physical adsorption using carbonaceous and non-carbonaceous adsorbents: A review, *Journal of Environmental Chemical Engineering*, 8 (5), pp. 104142. DOI:10.1016/j.jece.2020.104142.

Akinpelumi, K., Saha, C. and Rochelle, G. T. (2019) Piperazine aerosol mitigation for post-combustion carbon capture, *International Journal of Greenhouse Gas Control*, 91, pp.102845. DOI:10.1016/j.ijggc.2019.102845.

Alkoy, S., Toy, C., Gönül, T. and Tekin, A. (1997) Crystallization behavior and characterization of turbostratic boron nitride, *Journal of the European Ceramic Society*, 17 (12), pp. 1415–1422. DOI:10.1016/S0955-2219(97)00040-X.

Andrew, R. C., Mapasha, R. E., Ukpong, A. M. and Chetty, N. (2012) Mechanical properties of graphene and boronitrene, *Physical Review B*, 85 (12), pp. 125428.

Ansaloni, L. M. S. and de Sousa, E. M. B. (2013) Boron Nitride Nanostructured: Synthesis, Characterization and Potential Use in Cosmetics, *Materials Sciences and Applications*, 04 (01), pp. 22–28. DOI:10.4236/msa.2013.41004.

Asif, Q. ul A., Hussain, A., Rafique, H. M. and Tayyab, M. (2020) Computational study of Be-doped hexagonal boron nitride (h-BN): Structural and electronic properties, *Computational Condensed Matter*, 23. DOI:10.1016/j.cocom.2020.e00474.

Ba, K., Jiang, W., Cheng, J., Bao, J., Xuan, N., Sun, Y., *et al.* (2017) Chemical and bandgap engineering in monolayer hexagonal boron nitride, *Scientific Reports*, 7, pp. 45584.

Balci, S., Sezgi, N. A. and Eren, E. (2012) Boron oxide production kinetics using boric acid as raw material, *Industrial and Engineering Chemistry Research*, 51 (34), pp. 11091–11096. DOI:10.1021/ie300685x.

BEISC (2019) *Carbon capture usage and storage: third time lucky?* Available from: https://publications.parliament.uk/pa/cm201719/cmselect/cmbeis/1094/1094.pdf. [Accessed 7 October 2020].

Belmabkhout, Y., Serna-Guerrero, R. and Sayari, A. (2009) Adsorption of CO_2 from

dry gases on MCM-41 silica at ambient temperature and high pressure. 1: Pure CO_2 adsorption, *Chemical Engineering Science*, 64 (17), pp. 3721–3728.

Ben Belgacem, A., Hinkov, I., Yahia, S. Ben, Brinza, O. and Farhat, S. (2016) Arc discharge boron nitrogen doping of carbon nanotubes, *Materials Today Communications*, 8, pp. 183–195. DOI:https://doi.org/10.1016/j.mtcomm.2016.08.001.

Bhowmick, S., Singh, A. K. and Yakobson, B. I. (2011) Quantum dots and nanoroads of graphene embedded in hexagonal boron nitride, *The Journal of Physical Chemistry C*, 115 (20), pp. 9889–9893.

Bi, W., Hu, Y., Li, W., Jiang, H. and Li, C. (2018) Construction of Nanoreactors Combining Two-Dimensional Hexagonal Boron Nitride (h-BN) Coating with Pt/Al_2O_3 Catalyst toward Efficient Catalysis for CO Oxidation, *Industrial & Engineering Chemistry Research*, 57 (40), pp. 13353–13361.

Boldrin, L., Scarpa, F., Chowdhury, R. and Adhikari, S. (2011) Effective mechanical properties of hexagonal boron nitride nanosheets, *Nanotechnology*, 22 (50), pp. 505702.

Broom, D. P. and Thomas, K. M. (2013) Gas adsorption by nanoporous materials: Future applications and experimental challenges, *MRS Bulletin*, 38 (5), pp. 412–421. DOI:10.1557/mrs.2013.105.

Brown, M. E. (2001) *Introduction to thermal analysis: techniques and applications*. Vol. 1. Springer Science & Business Media.

Brunauer, S., Emmett, P. H. and Teller, E. (1938) Adsorption of gases in multimolecular layers, *Journal of the American Chemical Society*, 60 (2), pp. 309–319.

Budinis, S., Krevor, S., Dowell, N. Mac, Brandon, N. and Hawkes, A. (2018) An assessment of CCS costs, barriers and potential, *Energy Strategy Reviews*, 22 (May), pp. 61–81. DOI:10.1016/j.esr.2018.08.003.

Bui, M., Adjiman, C. S., Bardow, A., Anthony, E. J., Boston, A., Brown, S., *et al.* (2018) Carbon capture and storage (CCS): the way forward, *Energy & Environmental Science*.

Butler, J. and Montzka, S. A. (2013) The NOAA annual greenhouse gas index (AGGI),

NOAA Earth System Research Laboratory, Global Monitoring Division, Available from: https://*Esrl. Noaa. Gov/Gmd/Aggi/Aggi. Html,* [Accessed 7 October 2020].

Cao, Y., Maitarad, P., Gao, M., Taketsugu, T., Li, H., Yan, T., Shi, L. and Zhang, D. (2018) Defect-induced efficient dry reforming of methane over two-dimensional Ni/h-boron nitride nanosheet catalysts, *Applied Catalysis B: Environmental*, 238 (May), pp. 51–60. DOI:10.1016/j.apcatb.2018.07.001.

Chang, H., Chao, Y., Pang, J., Li, H., Lu, L., He, M., Chen, G., Zhu, W. and Li, H. (2018) Advanced Overlap Adsorption Model of Few-Layer Boron Nitride for Aromatic Organic Pollutants, *Industrial & Engineering Chemistry Research*, 57 (11), pp. 4045–4051.

Chen, D., Huang, Y., Hu, X., Li, R., Qian, Y. and Li, D. (2018a) Green Synthesis of Boron Carbonitride with High Capacitance, *Materials*, 11 (3), pp. 387. DOI:10.3390/ma11030387.

Chen, D., Huang, Y., Hu, X., Li, R., Qian, Y. and Li, D. (2018b) Synthesis and characterization of 'ravine-like' BCN compounds with high capacitance, *Materials*, 11 (2), pp. 1–9. DOI:10.3390/ma11020209.

Chen, L., Zhou, M., Luo, Z., Wakeel, M., Asiri, A. M. and Wang, X. (2019) Template-free synthesis of carbon-doped boron nitride nanosheets for enhanced photocatalytic hydrogen evolution, *Applied Catalysis B: Environmental*, 241, pp. 246–255. DOI:https://doi.org/10.1016/j.apcatb.2018.09.034.

Chen, S., Li, P., Xu, S., Pan, X., Fu, Q. and Bao, X. (2018c) Carbon doping of hexagonal boron nitride porous materials toward CO_2 capture, *Journal of Materials Chemistry A*, 6(4), 1832–1839.

Chen, S., Yang, H., Chen, Q., Liu, L., Hou, X., Luo, L., Lin, C., Li, C. and Chen, Y. (2020) Synthesis of BCN nanoribbons from coconut shells using as high-performance anode materials for lithium-ion batteries, *Electrochimica Acta*, 346, pp. 136239. DOI:https://doi.org/10.1016/j.electacta.2020.136239.

Chen, Y. J., Zhang, H. Z. and Chen, Y. (2006) Pure boron nitride nanowires produced from boron triiodide, *Nanotechnology*, 17 (3), pp. 786.

Chen, Y., Wang, J., Chen, Y., Liu, D., Huang, S. and Lei, W. (2018d) One-step

template-free synthesis of 3D functionalized flower-like boron nitride nanosheets for NH3 and CO_2 adsorption, *Nanoscale*.

Chen, Y., Zou, J., Campbell, S. J. and Le Caer, G. (2004) Boron nitride nanotubes: pronounced resistance to oxidation, *Applied Physics Letters*, 84 (13), pp. 2430–2432.

Ciofani, G., Genchi, G. G., Liakos, I., Athanassiou, A., Dinucci, D., Chiellini, F. and Mattoli, V. (2012) A simple approach to covalent functionalization of boron nitride nanotubes, *Journal of Colloid and Interface Science*, 374 (1), pp. 308–314.

Committee on Climate Change (2019) *Net Zero: The UK's contribution to stopping global warming*, *Committe on Climate Change*. Available from: https:// tinyurl.com/yybbpnzf [Accessed 7 October 2020].

Corso, M., Auwärter, W., Muntwiler, M., Tamai, A., Greber, T. and Osterwalder, J. (2004) Boron nitride nanomesh, *Science*, 303 (5655), pp. 217–220.

Cota, I. and Martinez, F. F. (2017) Recent advances in the synthesis and applications of metal organic frameworks doped with ionic liquids for CO_2 adsorption, *Coordination Chemistry Reviews*, 351, pp. 189-204.

Coutris, C., Macken, A. L., Collins, A. R., El Yamani, N. and Brooks, S. J. (2015) Marine ecotoxicity of nitramines, transformation products of amine-based carbon capture technology, *Science of The Total Environment*, 527–528, pp. 211–219. DOI:https://doi.org/10.1016/j.scitotenv.2015.04.119.

Cychosz, K. A., Guillet-Nicolas, R., García-Martínez, J. and Thommes, M. (2017a) Recent advances in the textural characterization of hierarchically structured nanoporous materials, *Chemical Society Reviews*, 46 (2), pp. 389–414. DOI:10.1039/c6cs00391e.

Cychosz, K. A., Guillet-Nicolas, R., García-Martínez, J. and Thommes, M. (2017b) Recent advances in the textural characterization of hierarchically structured nanoporous materials, *Chemical Society Reviews*, 46 (2), pp. 389–414. DOI:10.1039/c6cs00391e.

Das, D., Banerjee, D., Mondal, M., Shett, A., Das, B., Das, N. S., Ghorai, U. K. and Chattopadhyay, K. K. (2018) Nickel doped graphitic carbon nitride nanosheets and its application for dye degradation by chemical catalysis, *Materials Research Bulletin*. 101, pp. 291–304. DOI:10.1016/j.materresbull.2018.02.004.

Delgado, J. A., Uguina, M. A., Sotelo, J. L., Ruíz, B. and Rosário, M. (2007) Separation of carbon dioxide/methane mixtures by adsorption on a basic resin, *Adsorption*, 13 (3–4), pp. 373–383.

Department for Business, Energy, I. S. (2019) *UK's largest carbon capture project to prevent equivalent of 22,000 cars' emissions from polluting the atmosphere from 2021*. Available from: https://tinyurl.com/yys3xpvy [Accessed 7 October 2020].

Dibandjo, P., Chassagneux, F., Bois, L., Sigala, C. and Miele, P. (2005) Comparison between SBA-15 silica and CMK-3 carbon nanocasting for mesoporous boron nitride synthesis, *Journal of Materials Chemistry*, 15 (19), pp. 1917–1923.

Dijkstra, J. W., Walspurger, S., Elzinga, G. D., Pieterse, J. A. Z., Boon, J. and Haije, W. G. (2018) Evaluation of postcombustion CO2 capture by a solid sorbent with process modeling using experimental CO_2 and H2O adsorption characteristics, *Industrial & Engineering Chemistry Research*, 57 (4), pp. 1245–1261.

Du, M., Liu, Q., Huang, C. and Qiu, X. (2017) One-step synthesis of magnetically recyclable Co@BN core-shell nanocatalysts for catalytic reduction of nitroarenes, *RSC Advances*, 7 (56), pp. 35451–35459. DOI:10.1039/c7ra04907b.

Duan, J., Jin, W. and Kitagawa, S. (2017) Water-resistant porous coordination polymers for gas separation, *Coordination Chemistry Reviews*, 332, pp. 48–74.

Earnest, C. M. (1988) *Compositional analysis by thermogravimetry*. Vol. 997. ASTM International.

Ello, A. S., de Souza, L. K. C., Trokourey, A. and Jaroniec, M. (2013) Coconut shell-based microporous carbons for CO_2 capture, *Microporous and Mesoporous Materials*, 180, pp. 280–283.

Figueroa, J. D., Fout, T., Plasynski, S., McIlvried, H. and Srivastava, R. D. (2008) Advances in CO_2 capture technology—the US Department of Energy's Carbon Sequestration Program, *International Journal of Greenhouse Gas Control*, 2 (1), pp. 9–20.

Florent, M. and Bandosz, T. J. (2018) Irreversible water mediated transformation of BCN from a 3D highly porous form to its nonporous hydrolyzed counterpart, *Journal of Materials Chemistry A*, 6 (8), pp. 3510–3521.

Fu, L., Chen, G., Jiang, N., Yu, J., Lin, C. Te and Yu, A. (2016) In situ growth of metal nanoparticles on boron nitride nanosheets as highly efficient catalysts, *Journal of Materials Chemistry A*, 4 (48), pp. 19107–19115. DOI:10.1039/c6ta06409d.

Galey, P. (2019) Climate impacts 'to cost world $7.9 trillion' by 2050, *Phys Org*, (November), pp. 9–11. Available from: https://phys.org/news/2019-11-climate-impacts-world-trillion.html [Accessed 7 October 2020].

Gao, G., Mathkar, A., Martins, E. P., Galvão, D. S., Gao, D., Alves Da Silva Autreto, P., Sun, C., Cai, L. and Ajayan, P. M. (2014) Designing nanoscaled hybrids from atomic layered boron nitride with silver nanoparticle deposition, *Journal of Materials Chemistry A*, 2 (9), pp. 3148–3154. DOI:10.1039/c3ta12892j.

Gao, R., Yin, L., Wang, C., Qi, Y., Lun, N., Zhang, L., Liu, Y.-X., Kang, L. and Wang, X. (2009) High-yield synthesis of boron nitride nanosheets with strong ultraviolet cathodoluminescence emission, *The Journal of Physical Chemistry C*, 113 (34), pp. 15160–15165.

Gautam, C., Tiwary, C. S., Jose, S., Brunetto, G., Ozden, S., Vinod, S., Raghavan, P., Biradar, S. and Galvao, D. S. (2015) Hexagonal Boron Nitride Solids, *ACS Nano*, (12), pp. 12088–12095. DOI:10.1016/j.physb.2009.08.318.

Gautam, C., Tiwary, C. S., Machado, L. D., Jose, S., Ozden, S., Biradar, S., *et al.* (2016) Synthesis and porous h-BN 3D architectures for effective humidity and gas sensors, *RSC Advances*, 6 (91), pp. 87888–87896. DOI:10.1039/c6ra18833h.

GCCSI (2020) The value of carbon capture and storage, Global CCS Institute. Available from: https:// tinyurl.com/yxdapogg [Accessed 7 October 2020].

Ge, L., Han, C., Liu, J. and Li, Y. (2011) Enhanced visible light photocatalytic activity of novel polymeric g-C 3N4 loaded with Ag nanoparticles, *Applied Catalysis A: General*. DOI:10.1016/j.apcata.2011.10.006.

Geick, R., Perry, C. H. and Rupprecht, G. (1966) Nornral Modes in Hexagonal Boron Nitride, *Physical Review*, 146 (2), pp. 543.

Global Carbon Capture & Storage Institute (2018) *CCS: A solution to climate change right beneath our feet*. Available from: https://unfccc.int/sites/default/files/resource/40_UNFCCC_Submission_Global_CCS

Institute.pdf. [Accessed 7 October 2020].

Global Carbon Project (2017) Global Carbon Budget. Available from: https:// https://www.globalcarbonproject.org/carbonbudget/archive/2017/GCP_CarbonBudget_2017.pdf. [Accessed 7 October 2020].

Golberg, D., Bando, Y., Huang, Y., Terao, T., Mitome, M., Tang, C. and Zhi, C. (2010) Boron nitride nanotubes and nanosheets, *ACS Nano*, 4 (6), pp. 2979–2993. DOI:10.1021/nn1006495.

Gómez Díaz, J., Ding, Y., Koitz, R., Seitsonen, A. P., Iannuzzi, M. and Hutter, J. (2013) Hexagonal boron nitride on transition metal surfaces, *Theoretical Chemistry Accounts*, 132 (4), pp. 1–17. DOI:10.1007/s00214-013-1350-z.

Gou, G., Pan, B. and Shi, L. (2009) The nature of radiative transitions in O-doped boron nitride nanotubes, *Journal of the American Chemical Society*, 131 (13), pp. 4839–4845.

Grad, B., Blaha, P., Schwarz, K., Auwärter, W. and Greber, T. (2003) Density functional theory investigation of the geometric and spintronic structure of h-BN/Ni(111) in view of photoemission and STM experiments, *Physical Review B - Condensed Matter and Materials Physics*, 68 (8). DOI:10.1103/PhysRevB.68.085404.

Guo, H., Zhang, W., Lu, N., Zhuo, Z., Zeng, X. C., Wu, X. and Yang, J. (2015) CO2 capture on h-BN sheet with high selectivity controlled by external electric field, *The Journal of Physical Chemistry C*, 119 (12), pp. 6912–6917.

Hagio, Tsuyoshi and Nonaka, Kazuhiro and Sato, T. et al. (1997) Microstructural development with crystallization of hexagonal boron nitride, *Journal of Materials Science Letters*, 16 (10), pp. 795–798.

Han, M. and Yu, J. (2018) Pressure-induced vapor synthesis, formation mechanism, and thermal stability of well-dispersed boron nitride spheres, *Diamond and Related Materials*, 87 (March), pp. 10–17. DOI:10.1016/j.diamond.2018.04.029.

Han, W.-Q., Brutchey, R., Tilley, T. D. and Zettl, A. (2004) Activated boron nitride derived from activated carbon, *Nano Letters*, 4 (1), pp. 173–176.

Han, W., Ge, C., Zhang, R. and Zhang, X. (2019) Synthesis of boron nitride microrods with fish-scale-like structures for enhanced thermal conductivity of water, *International*

Journal of Heat and Mass Transfer, 132, pp. 1284–1295. DOI:10.1016/j.ijheatmasstransfer.2018.12.101.

Han, W., Wang, J., Liu, S., Ge, C., Cao, S., Song, B., Wang, J. and Zhang, X. (2017) Spectral properties of spherical boron nitride prepared using carbon spheres as template, *Ceramics International*, 43 (4), pp. 3569–3575.

Hannah Ritchie and Max Roser (2017) CO_2 and Greenhouse Gas Emissions, *Our World in Data*. Available from: https://ourworldindata.org/co2-and-other-greenhouse-gas-emissions [Accessed 7 October 2020].

Hao, J., Wang, J., Qin, S., Liu, D., Li, Y. and Lei, W. (2018) B/N co-doped carbon nanosphere frameworks as high-performance electrodes for supercapacitors, *Journal of Materials Chemistry A*, 6 (17), pp. 8053–8058. DOI:10.1039/c8ta00683k.

Hao, L., Gong, L., Chen, L., Guan, M., Zhou, H., Qiu, S., *et al.* (2020) Composite pesticide nanocarriers involving functionalized boron nitride nanoplatelets for pH-responsive release and enhanced UV stability, *Chemical Engineering Journal*, pp. 125233.

He, Y., Xu, N., Junior, L. B., Hao, X., Yao, B., Yang, Q., Liu, D. and Ma, Z. (2020) Construction of AuNPs/h-BN nanocomposites by using gold as interfacial electron transfer mediator with highly efficient degradation for levofloxacin hydrochloride and hydrogen generation, *Applied Surface Science*, 520 (April). DOI:10.1016/j.apsusc.2020.146336.

Ho, C. H. and Van Zee, J. W. (2000) Effect of ethanol and temperature on the hydrolysis of a nickel(II) ion in ethanol-water solutions, *Industrial and Engineering Chemistry Research*, 39 (3), pp. 752–758. DOI:10.1021/ie9702789.

Hoffendahl, C., Duquesne, S., Fontaine, G. and Bourbigot, S. (2014) Decomposition mechanism of melamine borate in pyrolytic and thermo-oxidative conditions, *Thermochimica Acta*, 590, pp. 73–83. DOI:10.1016/j.tca.2014.06.016.

Hojatisaeidi, F., Mureddu, M., Dessì, F., Durand, G. and Saha, B. (2020) Metal-Free Modified Boron Nitride for Enhanced CO_2 Capture, *Energies*, 13 (3), pp. 549. DOI:10.3390/en13030549.

Hong, S. M., Kim, S. H. and Lee, K. B. (2013) Adsorption of carbon dioxide on 3-

aminopropyl-triethoxysilane modified graphite oxide, *Energy and Fuels*, 27 (6), pp. 3358–3363. DOI:10.1021/ef400467w.

Huang, C., Chen, C., Zhang, M., Lin, L., Ye, X., Lin, S., Antonietti, M. and Wang, X. (2015) Carbon-doped BN nanosheets for metal-free photoredox catalysis, *Nature Communications*, 6, pp. 1–7. DOI:10.1038/ncomms8698.

Huang, K., Liang, L., Chai, S., Tumuluri, U., Li, M., Wu, Z., Sumpter, B. G. and Dai, S. (2017) Aminopolymer functionalization of boron nitride nanosheets for highly efficient capture of carbon dioxide, *Journal of Materials Chemistry A*, 5 (31), pp. 16241–16248.

Huang, X., Zhi, C., Jiang, P., Golberg, D., Bando, Y. and Tanaka, T. (2013) Polyhedral oligosilsesquioxane-modified boron nitride nanotube based epoxy nanocomposites: an ideal dielectric material with high thermal conductivity, *Advanced Functional Materials*, 23 (14), pp. 1824–1831.

Idem, R., Wilson, M., Tontiwachwuthikul, P., Chakma, A., Veawab, A., Aroonwilas, A. and Gelowitz, D. (2006) Pilot plant studies of the CO_2 capture performance of aqueous MEA and mixed MEA/MDEA solvents at the University of Regina CO_2 capture technology development plant and the boundary dam CO_2 capture demonstration plant, *Industrial & Engineering Chemistry Research*, 45 (8), pp. 2414–2420.

IEA/UNIDO (2011) CCS in Industry Technology Roadmap. Available from: https://www.iea.org/reports/technology-roadmap-carbon-capture-and-storage-in-industrial-applications [Accessed 7 October 2020].

Ikuno, T., Sainsbury, T., Okawa, D., Fréchet, J. M. J. and Zettl, A. (2007) Amine-functionalized boron nitride nanotubes, *Solid State Communications*, 142 (11), pp. 643–646.

In, I., Metz, B., Davidson, O., de Coninck, H. C., Loos, M. and Meyer, L. A. (2005) IPCC Special Report on Carbon Dioxide Capture and Storage: Prepared by Working Group III of the Intergovernmental Panel on Climate Change. Metz, B., Davidson, O., de Conink, H., Loos, M., Meyer, L., Eds.

IPCC (2014) *Climate Change 2014 Synthesis Report Summary Chapter for Policymakers*, *Intergovernmental Panel on Climate Change*. DOI:10.1017/CBO9781107415324.

Iqbal, J. and Ayub, K. (2016) Enhanced electronic and non-linear optical properties of alkali metal (Li, Na, K) doped boron nitride nano-cages, *Journal of Alloys and Compounds*, 687, pp. 976–983.

Ishibashi, M., Ota, H., Akutsu, N., Umeda, S., Tajika, M., Izumi, J., Yasutake, A., Kabata, T. and Kageyama, Y. (1996) Technology for removing carbon dioxide from power plant flue gas by the physical adsorption method, *Energy Conversion and Management*, 37 (6–8), pp. 929–933.

Jang, D. Il and Park, S. J. (2012) Influence of nickel oxide on carbon dioxide adsorption behaviors of activated carbons, *Fuel*, (102), pp. 439–444. DOI:10.1016/j.fuel.2012.03.052.

Janik, J. F., Ackerman, W. C., Paine, R. T., Hua, D.-W., Maskara, A. and Smith, D. M. (1994) Boron nitride as a selective gas adsorbent, *Langmuir*, 10 (2), pp. 514–518.

Ji, G., Yang, H., Memon, M. Z., Gao, Y., Qu, B., Fu, W., Olguin, G., Zhao, M. and Li, A. (2020) Recent advances on kinetics of carbon dioxide capture using solid sorbents at elevated temperatures, *Applied Energy*, 267 (March). DOI:10.1016/j.apenergy.2020.114874.

Ji, H., Sun, J., Wu, P., Dai, B., Chao, Y., Zhang, M., Jiang, W., Zhu, W. and Li, H. (2016) Deep oxidative desulfurization with a microporous hexagonal boron nitride confining phosphotungstic acid catalyst, *Journal of Molecular Catalysis A: Chemical*, 423, pp. 207–215. DOI:10.1016/j.molcata.2016.06.019.

Jiang, X. F., Weng, Q., Wang, X. Bin, Li, X., Zhang, J., Golberg, D. and Bando, Y. (2015) Recent Progress on Fabrications and Applications of Boron Nitride Nanomaterials: A Review, *Journal of Materials Science and Technology*, 31 (6), pp. 589–598. DOI:10.1016/j.jmst.2014.12.008.

Jiang, Z., Zhu, W., Xu, G., Xu, X., Wang, M., Chen, H., Huang, W., Ge, X. and Lin, M. (2020) Ni-nanoparticle-bound boron nitride nanosheets prepared by a radiation-induced reduction-exfoliation method and their catalytic performance, *Journal of Materials Chemistry A*, 8 (18), pp. 9109–9120. DOI:10.1039/d0ta03701j.

Joffe, D., Livermore, S., Hemsley, M., Stark, C., Gault, A., Thompson, M., *et al.* (2018) Hydrogen in a Low-carbon Economy, *London: Committee on Climate Change*.

Karbhal, I., Devarapalli, R. R., Debgupta, J., Pillai, V. K., Ajayan, P. M. and Shelke, M. V (2016) Facile Green Synthesis of BCN Nanosheets as High-Performance Electrode Material for Electrochemical Energy Storage, *Chemistry–A European Journal*, 22 (21), pp. 7134–7140.

Kikkinides, E. S., Yang, R. T. and Cho, S. H. (1993) Concentration and recovery of carbon dioxide from flue gas by pressure swing adsorption, *Industrial & Engineering Chemistry Research*, 32 (11), pp. 2714–2720.

Kim, D., Nakajima, S., Sawada, T., Iwasaki, M., Kawauchi, S., Zhi, C., Bando, Y., Golberg, D. and Serizawa, T. (2015) Sonication-assisted alcoholysis of boron nitride nanotubes for their sidewalls chemical peeling, *Chemical Communications*, 51 (33), pp. 7104–7107.

Kinik, F. P., Altintas, C., Balci, V., Koyuturk, B., Uzun, A. and Keskin, S. (2016) [BMIM][PF6] Incorporation Doubles CO_2 Selectivity of ZIF-8: Elucidation of Interactions and Their Consequences on Performance, *ACS Applied Materials & Interfaces*, 8 (45), pp. 30992–31005.

Kokulnathan, T. and Wang, T.-J. (2019) Synthesis and characterization of 3D flower-like nickel oxide entrapped on boron doped carbon nitride nanocomposite: An efficient catalyst for the electrochemical detection of nitrofurantoin, *Composites Part B: Engineering*, 174, pp. 106914.

Kostoglou, N., Lukovic, J., Babic, B., Matovic, B., Photiou, D., Constantinides, G., *et al.* (2016) Few-step synthesis, thermal purification and structural characterization of porous boron nitride nanoplatelets, *Materials & Design*, 110, pp. 540–548.

Kumar, A., Malik, G., Chandra, R. and Mulik, R. S. (2020) The role of post annealing temperature on a facile synthesis of 2D h-BN nanoflowers, *Ceramics International*, (May), pp. 0–1. DOI:10.1016/j.ceramint.2020.05.213.

Kumar, N., Moses, K., Pramoda, K., Shirodkar, S. N., Mishra, A. K., Waghmare, U. V., Sundaresan, A. and Rao, C. N. R. (2013) Borocarbonitrides, BxCyNz, *Journal of Materials Chemistry A*, 1 (19), pp. 5806–5821. DOI:10.1039/c3ta01345f.

Kumar, N., Raidongia, K., Mishra, A. K., Waghmare, U. V, Sundaresan, A. and Rao, C. N. R. (2011) Synthetic approaches to borocarbonitrides, BCxN (x=1–2), *Journal of*

Solid State Chemistry, 184 (11), pp. 2902–2908. DOI:https://doi.org/10.1016/j.jssc.2011.08.034.

Kumar, V., Nikhil, K., Roy, P., Lahiri, D. and Lahiri, I. (2016) Emergence of fluorescence in boron nitride nanoflakes and its application in bioimaging, *RSC Advances*. 6(53), pp.48025 - 48032. DOI:10.1039/c6ra05288f.

Kurakevych, O. O. and Solozhenko, V. L. (2007) Rhombohedral boron subnitride, B13N2, by X-ray powder diffraction, *Acta Crystallographica Section C: Crystal Structure Communications*, 63 (9), pp. i80–i82.

Kutty, R. G., Sreejith, S., Kong, X., He, H., Wang, H., Lin, J., *et al.* (2018) A topologically substituted boron nitride hybrid aerogel for highly selective CO_2 uptake, *Nano Research*, 11 (12), pp. 6325–6335.

Lale, A., Bernard, S. and Demirci, U. B. (2018) Boron Nitride for Hydrogen Storage, *ChemPlusChem*, 83 (10), pp. 893–903. DOI:10.1002/cplu.201800168.

Le Quéré, C., Jackson, R. B., Jones, M. W., Smith, A. J. P., Abernethy, S., Andrew, R. M., *et al.* (2020) Temporary reduction in daily global CO_2 emissions during the COVID-19 forced confinement, *Nature Climate Change*, pp. 1–7.

Lee, D., Lee, B., Park, K. H., Ryu, H. J., Jeon, S. and Hong, S. H. (2015) Scalable exfoliation process for highly soluble boron nitride nanoplatelets by hydroxide-assisted ball milling, *Nano Letters*, 15 (2), pp. 1238–1244.

Lee, S.-Y. and Park, S.-J. (2015) A review on solid adsorbents for carbon dioxide capture, *Journal of Industrial and Engineering Chemistry*, 23, pp. 1–11.

Lei, W., Mochalin, V. N., Liu, D., Qin, S., Gogotsi, Y. and Chen, Y. (2015) Boron nitride colloidal solutions, ultralight aerogels and freestanding membranes through one-step exfoliation and functionalization, *Nature Communications*, 6, pp. 8849.

Lei, W., Zhang, H., Wu, Y., Zhang, B., Liu, D., Qin, S., *et al.* (2014) Oxygen-doped boron nitride nanosheets with excellent performance in hydrogen storage, *Nano Energy*, 6, pp. 219–224.

Leung, D. Y. C., Caramanna, G. and Maroto-Valer, M. M. (2014) An overview of current status of carbon dioxide capture and storage technologies, *Renewable and Sustainable Energy Reviews*, 39, pp. 426–443.

DOI:https://doi.org/10.1016/j.rser.2014.07.093.

Li, B., Duan, Y., Luebke, D. and Morreale, B. (2013a) Advances in CO_2 capture technology: A patent review, *Applied Energy*, 102, pp. 1439–1447.

Li, H., Zhu, S., Zhang, M., Wu, P., Pang, J., Zhu, W., Jiang, W. and Li, H. (2017) Tuning the Chemical Hardness of Boron Nitride Nanosheets by Doping Carbon for Enhanced Adsorption Capacity, *ACS Omega*, 2 (9), pp. 5385–5394.

Li, J., He, S., Li, R., Dai, W., Tao, J., Wang, C., Liu, J., Wu, T. and Tang, C. (2018a) Template-free synthesis of three dimensional porous boron nitride nanosheets for efficient water cleaning, *RSC Advances*, 8 (57), pp. 32886–32892. DOI:10.1039/c8ra06445h.

Li, J., Lin, J., Xu, X., Zhang, X., Xue, Y., Mi, J., *et al.* (2013b) Porous boron nitride with a high surface area: hydrogen storage and water treatment, *Nanotechnology*, 24 (15), pp. 155603.

Li, J., Xiao, X., Xu, X., Lin, J., Huang, Y., Xue, Y., Jin, P., Zou, J. and Tang, C. (2013c) Activated boron nitride as an effective adsorbent for metal ions and organic pollutants, *Scientific Reports*, 3, pp. 3208.

Li, L., Chang, K., Fang, P., Du, K., Chen, C., Zhou, S., *et al.* (2020a) Highly efficient scavenging of Ni(II) by porous hexagonal boron nitride: Kinetics, thermodynamics and mechanism aspects, *Applied Surface Science*, 521 (January). DOI:10.1016/j.apsusc.2020.146373.

Li, Q., Li, L., Yu, X., Wu, X., Xie, Z., Wang, X., *et al.* (2020b) Ultrafine platinum particles anchored on porous boron nitride enabling excellent stability and activity for oxygen reduction reaction, *Chemical Engineering Journal*, 399 (April), pp. 125827. DOI:10.1016/j.cej.2020.125827.

Li, Q., Yang, T., Yang, Q., Wang, F., Chou, K.-C. and Hou, X. (2016) Porous hexagonal boron nitride whiskers fabricated at low temperature for effective removal of organic pollutants from water, *Ceramics International*, 42 (7), pp. 8754–8762.

Li, X., Lin, B., Li, H. H. H., Yu, Q., Ge, Y., Jin, X., *et al.* (2018b) Superior performance of borocarbonitrides, BxCyNz, as stable, low-cost metal-free electrocatalysts for the hydrogen evolution reaction, *Scientific Reports*, 6 (1), pp. 1–7.

DOI:10.1039/c5ee02521d.

Li, X., Zhao, J. and Yang, J. (2013d) Semihydrogenated BN sheet: a promising visible-light driven photocatalyst for water splitting, *Scientific Reports*, 3, pp. 1858.

Li, Y., Ben, T., Zhang, B., Fu, Y. and Qiu, S. (2013e) Ultrahigh gas storage both at low and high pressures in KOH-activated carbonized porous aromatic frameworks, *Scientific Reports*, 3, pp. 2420.

Liang, J., Song, Q., Lin, J., Huang, Y., Fang, Y., Yu, C., Xue, Y., Liu, Z. and Tang, C. (2019) Pore structure regulation and carbon dioxide adsorption capacity improvement on porous BN fibers: Effects of high-temperature treatments in gaseous ambient, *Chemical Engineering Journal*, 373, pp. 616–623.

Liao, Y., Chen, Z., Connell, J. W., Fay, C. C., Park, C., Kim, J. and Lin, Y. (2014) Nanotubes: Chemical Sharpening, Shortening, and Unzipping of Boron Nitride Nanotubes (Adv. Funct. Mater. 28/2014), *Advanced Functional Materials*, 24 (28), pp. 4560.

Lim, H. S., Oh, J. W., Kim, S. Y., Yoo, M. J., Park, S. D. and Lee, W. S. (2013) Anisotropically alignable magnetic boron nitride platelets decorated with iron oxide nanoparticles, *Chemistry of Materials*. DOI:10.1021/cm401488a.

Lin, J., Xu, L., Huang, Y., Li, J., Wang, W., Feng, C., *et al.* (2016) Ultrafine porous boron nitride nanofibers synthesized via a freeze-drying and pyrolysis process and their adsorption properties, *RSC Advances*, 6 (2), pp. 1253–1259.

Lin, Y. and Connell, J. W. (2012) Advances in 2D boron nitride nanostructures: Nanosheets, nanoribbons, nanomeshes, and hybrids with graphene, *Nanoscale*, 4 (22), pp. 6908–6939. DOI:10.1039/c2nr32201c.

Lin, Y., Williams, T. V and Connell, J. W. (2010) Soluble, exfoliated hexagonal boron nitride nanosheets, *The Journal of Physical Chemistry Letters*, 1 (1), pp. 277–283.

Lin, Y., Williams, T. V, Xu, T.-B., Cao, W., Elsayed-Ali, H. E. and Connell, J. W. (2011) Aqueous dispersions of few-layered and monolayered hexagonal boron nitride nanosheets from sonication-assisted hydrolysis: critical role of water, *The Journal of Physical Chemistry C*, 115 (6), pp. 2679–2685.

Liu, F., Li, S., Yu, D., Su, Y., Shao, N. and Zhang, Z. (2018) Template-free synthesis

of oxygen-doped bundlelike porous boron nitride for highly efficient removal of heavy metals from wastewater, *ACS Sustainable Chemistry & Engineering*, 6 (12), pp. 16011–16020.

Liu, F., Yu, J., Ji, X. and Qian, M. (2015) Nanosheet-structured boron nitride spheres with a versatile adsorption capacity for water cleaning, *ACS Applied Materials & Interfaces*, 7 (3), pp. 1824–1832.

Liu, X. Y., Zhang, H. and Cheng, X. L. (2019) Tuning the electronic and magnetic properties of in-planar graphene/boron nitride heterostructure by doping 3d transition metal atom, *Journal of Physical Chemistry C*, 123 (36), pp. 22403–22412. research-article. DOI:10.1021/acs.jpcc.9b06537.

Lock, S. S. M., Lau, K. K., Ahmad, F. and Shariff, A. M. (2015) Modeling, simulation and economic analysis of CO_2 capture from natural gas using cocurrent, countercurrent and radial crossflow hollow fiber membrane, *International Journal of Greenhouse Gas Control*, 36, pp. 114–134. DOI:https://doi.org/10.1016/j.ijggc.2015.02.014.

López-Salas, N., Ferrer, M. L., Gutiérrez, M. C., Fierro, J. L. G., Cuadrado-Collados, C., Gandara-Loe, J., Silvestre-Albero, J. and del Monte, F. (2018) Hydrogen-bond supramolecular hydrogels as efficient precursors in the preparation of freestanding 3D carbonaceous architectures containing BCNO nanocrystals and exhibiting a high CO2/CH4 adsorption ratio, *Carbon*, 134, pp. 470–479.

Lowell, S., Shields, J. E., Thomas, M. A. and Thommes, M. (2004) Adsorption isotherms, in: *Characterization of Porous Solids and Powders: Surface Area, Pore Size and Density*. Springer, pp. 11–14.

Lu, J., Zhang, K., Liu, X. F., Zhang, H., Sum, T. C., Neto, A. H. C. and Loh, K. P. (2013) Order–disorder transition in a two-dimensional boron–carbon–nitride alloy, *Nature Communications*, 4 (1), pp. 1–7.

Lu, Q., Zhao, Q., Yang, T., Zhai, C., Wang, D. and Zhang, M. (2018) Preparation of Boron Nitride Nanoparticles with Oxygen Doping and a Study of Their Room-Temperature Ferromagnetism, *ACS Applied Materials and Interfaces*, 10 (15), pp. 12947–12953. DOI:10.1021/acsami.7b17932.

Luo, J., Chao, Y., Tang, Z., Hua, M., Li, X., Wei, Y., *et al.* (2019) Design of Lewis Acid Centers in Bundlelike Boron Nitride for Boosting Adsorptive Desulfurization Performance, *Industrial and Engineering Chemistry Research*, 58 (29), pp. 13303–13312. research-article. DOI:10.1021/acs.iecr.9b01745.

Maiti, K., Thanh, T. D., Sharma, K., Hui, D., Kim, N. H. and Lee, J. H. (2017) Highly efficient adsorbent based on novel cotton flower-like porous boron nitride for organic pollutant removal, *Composites Part B: Engineering*, 123, pp. 45–54. DOI:10.1016/j.compositesb.2017.05.018.

Maleki, M., Shokouhimehr, M., Karimian, H. and Beitollahi, A. (2016) Three-dimensionally interconnected porous boron nitride foam derived from polymeric foams, *RSC Advances*, 6 (56), pp. 51426–51434. DOI:10.1039/c6ra07751j.

Mantripragada, H. C., Zhai, H. and Rubin, E. S. (2019) Boundary Dam or Petra Nova – Which is a better model for CCS energy supply?, *International Journal of Greenhouse Gas Control*. DOI:10.1016/j.ijggc.2019.01.004.

Marchesini, S., McGilvery, C. M., Bailey, J. and Petit, C. (2017a) Template-Free Synthesis of Highly Porous Boron Nitride: Insights into Pore Network Design and Impact on Gas Sorption, *ACS Nano*, 11 (10), pp. 10003–10011.

Marchesini, S., Regoutz, A., Payne, D. and Petit, C. (2017b) Tunable porous boron nitride: Investigating its formation and its application for gas adsorption, *Microporous and Mesoporous Materials*, 243, pp. 154–163. DOI:10.1016/j.micromeso.2017.02.010.

Marom, N., Bernstein, J., Garel, J., Tkatchenko, A., Joselevich, E., Kronik, L. and Hod, O. (2010) Stacking and registry effects in layered materials: The case of hexagonal boron nitride, *Physical Review Letters*, 105 (4), pp. 1–4. DOI:10.1103/PhysRevLett.105.046801.

Marsh, H. and Rodríguez-Reinoso, F. (2006) CHAPTER 4 - Characterization of Activated Carbon, in: Marsh, H. and Rodríguez-Reinoso, F. B. T.-A. C. (eds.) Oxford: Elsevier Science Ltd, pp. 143–242.

Matveev, A. T., Permyakova, E. S., Kovalskii, A. M., Leibo, D., Shchetinin, I. V., Maslakov, K. I., Golberg, D. V., Shtansky, D. V. and Konopatsky, A. S. (2020) New

insights into synthesis of nanocrystalline hexagonal BN, *Ceramics International*, (May), pp. 1–7. DOI:10.1016/j.ceramint.2020.05.041.

Mishra, N. S. and Saravanan, P. (2018) A Review on the Synergistic Features of Hexagonal Boron Nitride (White Graphene) as Adsorbent-Photo Active Nanomaterial, *ChemistrySelect*, 3 (28), pp. 8023–8034.

Mohd Daud, F. D., Vignesh, K., Sreekantan, S., Mohamed, A. R., Kang, M. and Kwak, B. S. (2016) $Ca(OH)_2$ nano-pods: Investigation on the effect of solvent ratio on morphology and CO_2 adsorption capacity, *RSC Advances*, 6 (42), pp. 36031–36038. DOI:10.1039/c5ra27771j.

Naderi, M. (2015) Surface Area: Brunauer–Emmett–Teller (BET), in: *Progress in filtration and separation*. Elsevier, pp. 585–608.

Nag, A., Raidongia, K., Hembram, K. P. S. S., Datta, R., Waghmare, U. V and Rao, C. N. R. (2010) Graphene analogues of BN: novel synthesis and properties, *ACS Nano*, 4 (3), pp. 1539–1544.

Nassar, N. N. (2012) Iron oxide nanoadsorbents for removal of various pollutants from wastewater: an overview, *Application of Adsorbents for Water Pollution Control*, pp. 81–118.

Ning, Z., Huan, L., Tianwen, Z., Hongmin, K., Xiaoyang, W. and Xingyu, C. (2016) *Ceramic Processing Research Effects of boron source composition ratio on the microstructure and adsorption performance of hexagonal boron nitride prepared by template method*, *Journal of Ceramic Processing Research*. Vol. 17.

Office for National Statistics (2019) *Net zero and the different official measures of the UK ' s greenhouse gas emissions*. Available from: https://www.ons.gov.uk/economy/environmentalaccounts/articles/netzeroandthedifferentofficialmeasuresoftheuksgreenhousegasemissions/2019-07-24 [Accessed 7 October 2020].

Oh, W. Da, Wong, Z., Chen, X., Lin, K. Y. A., Veksha, A., Lisak, G., He, C. and Lim, T. T. (2020) Enhanced activation of peroxydisulfate by CuO decorated on hexagonal boron nitride for bisphenol A removal, *Chemical Engineering Journal*, 393 (December 2019), pp. 124714. DOI:10.1016/j.cej.2020.124714.

Örnek, M., Hwang, C., Reddy, K. M., Domnich, V., Miller, S. L., Akdoğan, E. K., Hemker, K. J. and Haber, R. A. (2018) Formation of BN from BCNO and the development of ordered BN structure: I. Synthesis of BCNO with various chemistries and degrees of crystallinity and reaction mechanism on BN formation, *Ceramics International*, 44 (13), pp. 14980–14989. DOI:10.1016/j.ceramint.2018.05.126.

Örnek, M., Hwang, C., Xiang, S., Xie, K. Y., Etzold, A., Yang, B. and Haber, R. A. (2019) Effect of synthesis conditions of BCNO on the formation and structural ordering of boron nitride at high temperatures, *Journal of Solid State Chemistry*, 269 (July 2018), pp. 212–219. DOI:10.1016/j.jssc.2018.09.025.

Ou, X., Lu, X., Chen, S. and Lu, Q. (2020) Thermal conductive hybrid polyimide with ultrahigh heat resistance, excellent mechanical properties and low coefficient of thermal expansion, *European Polymer Journal*, 122. DOI:10.1016/j.eurpolymj.2019.109368.

Owuor, P. S., Park, O.-K., Woellner, C. F., Jalilov, A. S., Susarla, S., Joyner, J., *et al.* (2017) Lightweight hexagonal boron nitride foam for CO_2 absorption, *ACS Nano*, 11 (9), pp. 8944–8952.

Pakdel, A., Bando, Y. and Golberg, D. (2014a) Nano boron nitride flatland, *Chemical Society Reviews*, 43 (3), pp. 934–959.

Pakdel, A., Bando, Y. and Golberg, D. (2014b) Plasma-assisted interface engineering of boron nitride nanostructure films, *Acs Nano*, 8 (10), pp. 10631–10639.

Pakdel, A., Zhi, C., Bando, Y. and Golberg, D. (2012) Low-dimensional boron nitride nanomaterials, *Materials Today*, 15 (6), pp. 256–265.

Pang, J., Chao, Y., Chang, H., Li, H., Xiong, J., Zhang, Q., *et al.* (2018) Silver Nanoparticle-Decorated Boron Nitride with Tunable Electronic Properties for Enhancement of Adsorption Performance, *ACS Sustainable Chemistry and Engineering*, 6 (4), pp. 4948–4957. DOI:10.1021/acssuschemeng.7b04481.

Paura, E. N. C., da Cunha, W. F., Martins, J. B. L., e Silva, G. M., Roncaratti, L. F. and Gargano, R. (2014) Carbon dioxide adsorption on doped boron nitride nanotubes, *Rsc Advances*, 4 (54), pp. 28249–28258.

Peng, D., Jiang, W., Li, F.-F., Zhang, L., Liang, R.-P. and Qiu, J.-D. (2018) One-pot

synthesis of boron carbon nitride nanosheets for facile and efficient heavy metal ions removal, *ACS Sustainable Chemistry & Engineering*, 6 (9), pp. 11685–11694.

Pennycook, S. J., David, B. and Williams, C. B. (2010) Transmission electron microscopy: a textbook for materials science, *Microscopy and Microanalysis*, 16 (1), pp. 111.

Primo, A., Forneli, A., Corma, A. and García, H. (2012) From biomass wastes to highly efficient CO2 adsorbents: Graphitisation of chitosan and alginate biopolymers, *ChemSusChem*, 5 (11), pp. 2207–2214. DOI:10.1002/cssc.201200366.

Qi, S. C., Wu, J. K., Lu, J., Yu, G. X., Zhu, R. R., Liu, Y., Liu, X. Q. and Sun, L. B. (2019) Underlying mechanism of CO_2 adsorption onto conjugated azacyclo-copolymers: N-doped adsorbents capture CO_2 chiefly through acid-base interaction?, *Journal of Materials Chemistry A*, 7 (30), pp. 17842–17853. DOI:10.1039/c9ta04785a.

Rehman, A. and Park, S. J. (2018) Highlighting the relative effects of surface characteristics and porosity on CO2 capture by adsorbents templated from melamine-based polyaminals, *Journal of Solid State Chemistry*, 258 (November 2017), pp. 573–581. DOI:10.1016/j.jssc.2017.11.019.

Ren, X., Li, H., Chen, J., Wei, L., Modak, A., Yang, H. and Yang, Q. (2017) N-doped porous carbons with exceptionally high CO_2 selectivity for CO_2 capture, *Carbon*, 114, pp. 473–481. DOI:10.1016/j.carbon.2016.12.056.

Rogelj, J., Shindell, D., Jiang, K., Fifita, S., Forster, P., Ginzburg, V., *et al.* (2018) Mitigation Pathways Compatible with 1.5°C in the Context of Sustainable Development. In: Global Warming of 1.5°C. An IPCC Special Report on the impacts of global warming of 1.5°C above pre-industrial levels and related global greenhouse gas emission pathw, *IPCC Special Report Global Warming of 1.5 °C*, pp. 82pp. Available from: https://www.ipcc.ch/site/assets/uploads/sites/2/2019/02/SR15_Chapter2_Low_Res.pdf [Accessed 7 October 2020].

Roger Harrabin (2019) Climate change: UK government to commit to 2050 target, *BBC environment analyst*. Available from: https://www.bbc.co.uk/news/science-environment-48596775 [Accessed 7 October 2020].

Romano, M. C., Chiesa, P. and Lozza, G. (2010) Pre-combustion CO_2 capture from natural gas power plants, with ATR and MDEA processes, *International Journal of Greenhouse Gas Control*, 4 (5), pp. 785–797. DOI:https://doi.org/10.1016/j.ijggc.2010.04.015.

Rubin, E. S., Mantripragada, H., Marks, A., Versteeg, P. and Kitchin, J. (2012) The outlook for improved carbon capture technology, *Progress in Energy and Combustion Science*, 38 (5), pp. 630–671. DOI:10.1016/j.pecs.2012.03.003.

Rushton, B. and Mokaya, R. (2008) Mesoporous boron nitride and boron-nitride-carbon materials from mesoporous silica templates, *Journal of Materials Chemistry*, 18 (2), pp. 235–241. DOI:10.1039/b713740k.

Sainsbury, T., Satti, A., May, P., Wang, Z., McGovern, I., Gun'ko, Y. K. and Coleman, J. (2012) Oxygen radical functionalization of boron nitride nanosheets, *Journal of the American Chemical Society*, 134 (45), pp. 18758–18771.

Salameh, C., Moussa, G., Bruma, A., Fantozzi, G., Malo, S., Miele, P., Demirci, U. B. and Bernard, S. (2018) Robust 3D Boron Nitride Nanoscaffolds for Remarkable Hydrogen Storage Capacity from Ammonia Borane, *Energy Technology*, 6 (3), pp. 570–577. DOI:10.1002/ente.201700618.

Samanta, A., Zhao, A., Shimizu, G. K. H., Sarkar, P. and Gupta, R. (2011) Post-combustion CO_2 capture using solid sorbents: a review, *Industrial & Engineering Chemistry Research*, 51 (4), pp. 1438–1463.

Schott, J. A., Wu, Z., Dai, S., Li, M., Huang, K. and Schott, J. A. (2017) Effect of metal oxides modification on CO_2 adsorption performance over mesoporous carbon, *Microporous and Mesoporous Materials*, 249, pp. 34–41. DOI:10.1016/j.micromeso.2017.04.033.

Schlienger, S., Alauzun, J., Michaux, F., Vidal, L., Parmentier, J., Gervais, C., Babonneau, F., Bernard, S., Miele, P. and Parra, J.B., 2012. Micro-, mesoporous boron nitride-based materials templated from zeolites. *Chemistry of Materials*, *24*(1), pp.88-96.

Sevilla, M. and Fuertes, A. B. (2011a) Sustainable porous carbons with a superior performance for CO_2 capture, *Energy & Environmental Science*, 4 (5), pp. 1765–1771.

Sevilla, M. and Fuertes, A. B. (2011b) Sustainable porous carbons with a superior performance for CO_2 capture, *Energy and Environmental Science*, 4 (5), pp. 1765–1771. DOI:10.1039/c0ee00784f.

Sezginel, K. B., Keskin, S. and Uzun, A. (2016) Tuning the gas separation performance of CuBTC by ionic liquid incorporation, *Langmuir*, 32 (4), pp. 1139–1147.

Shtansky, D. V, Firestein, K. L. and Golberg, D. V (2018) Fabrication and application of BN nanoparticles, nanosheets and their nanohybrids, *Nanoscale*, 10 (37), pp. 17477–17493.

Silva, L. A., Guerini, S. C. and Lemos, V. (2006) Electronic and structural properties of oxygen-doped BN nanotubes, *IEEE Transactions on Nanotechnology*, 5 (5), pp. 517–522.

Singh, G., Kim, I. Y., Lakhi, K. S., Joseph, S., Srivastava, P., Naidu, R. and Vinu, A. (2017a) Heteroatom functionalized activated porous biocarbons and their excellent performance for CO_2 capture at high pressure, *Journal of Materials Chemistry A*, 5 (40), pp. 21196–21204. DOI:10.1039/c7ta07186h.

Singh, G., Kim, I. Y., Lakhi, K. S., Joseph, S., Srivastava, P., Naidu, R. and Vinu, A. (2017b) Heteroatom functionalized activated porous biocarbons and their excellent performance for CO_2 capture at high pressure, *Journal of Materials Chemistry A*, 5 (40), pp. 21196–21204. DOI:10.1039/c7ta07186h.

Singh, J. and Dhar, D. W. (2019) Overview of carbon capture technology: microalgal biorefinery concept and state-of-the-art, *Frontiers in Marine Science*, 6, pp. 29.

Singh, R. S. (2015) Influence of oxygen impurity on electronic properties of carbon and boron nitride nanotubes: A comparative study, *AIP Advances*, 5 (11), pp. 117150.

Song, Q., Fang, Y., Liu, Z., Li, L., Wang, Y., Liang, J., *et al.* (2017) The performance of porous hexagonal BN in high adsorption capacity towards antibiotics pollutants from aqueous solution, *Chemical Engineering Journal*, 325, pp. 71–79.

Song, Q., Liang, J., Fang, Y., Cao, C., Liu, Z., Li, L., Huang, Y., Lin, J. and Tang, C. (2019) Selective adsorption behavior/mechanism of antibiotic contaminants on novel boron nitride bundles, *Journal of Hazardous Materials*, 364 (May 2018), pp. 654–662. DOI:10.1016/j.jhazmat.2018.10.054.

Song, Q., Liang, J., Fang, Y., Guo, Z., Du, Z., Zhang, L., *et al.* (2020) Nickel (II) modified porous boron nitride: An effective adsorbent for tetracycline removal from aqueous solution, *Chemical Engineering Journal*, 394 (Ii), pp. 124985. DOI:10.1016/j.cej.2020.124985.

Su, F., Lu, C., Cnen, W., Bai, H. and Hwang, J. F. (2009) Capture of CO2 from flue gas via multiwalled carbon nanotubes, *Science of The Total Environment*, 407 (8), pp. 3017–3023. DOI:https://doi.org/10.1016/j.scitotenv.2009.01.007.

Sun, Q., Li, Z., Searles, D. J., Chen, Y., Lu, G. and Du, A. (2013) Charge-controlled switchable CO_2 capture on boron nitride nanomaterials, *Journal of the American Chemical Society*, 135 (22), pp. 8246–8253.

Tan, X., Tahini, H. A. and Smith, S. C. (2016) Hexagonal boron nitride and graphene in-plane heterostructures: An experimentally feasible approach to charge-induced switchable CO_2 capture, *Chemical Physics*, 478, pp. 139–144. DOI:10.1016/j.chemphys.2016.04.001.

Tang, C., Bando, Y., Huang, Y., Yue, S., Gu, C., Xu, F. and Golberg, D. (2005) Fluorination and electrical conductivity of BN nanotubes, *Journal of the American Chemical Society*, 127 (18), pp. 6552–6553.

Thangaraj, V., Bussiere, J., Janot, J. M., Bechelany, M., Jaber, M., Subramanian, S., Miele, P. and Balme, S. (2016) Fluorescence Quenching of Sulforhodamine Dye over Graphene Oxide and Boron Nitride Nanosheets, *European Journal of Inorganic Chemistry*. DOI:10.1002/ejic.201501153.

The Global CCS Institute (2019) *New wave of CCS activity: Ten large-scale projects announced*. Available from: https://www.globalccsinstitute.com/news-media/latest-news/new-wave-of-ccs-ambition-ten-large-scale-projects-announced/ [Accessed 7 October 2020].

Thommes, M., Kaneko, K., Neimark, A. V, Olivier, J. P., Rodriguez-Reinoso, F., Rouquerol, J. and Sing, K. S. W. (2015) Physisorption of gases, with special reference to the evaluation of surface area and pore size distribution (IUPAC Technical Report), *Pure and Applied Chemistry*, 87 (9–10), pp. 1051–1069.

To, J. W. F., He, J., Mei, J., Haghpanah, R., Chen, Z., Kurosawa, T., *et al.* (2016)

Hierarchical N-doped carbon as CO_2 adsorbent with high CO_2 selectivity from rationally designed polypyrrole precursor, *Journal of the American Chemical Society*, 138 (3), pp. 1001–1009.

Tokarev, A., Kjeang, E., Cannon, M. and Bessarabov, D. (2016) Theoretical limit of reversible hydrogen storage capacity for pristine and oxygen-doped boron nitride, *International Journal of Hydrogen Energy*, 41 (38), pp. 16984–16991. DOI:10.1016/j.ijhydene.2016.07.010.

Tonda, S., Kumar, S., Kandula, S. and Shanker, V. (2014) Fe-doped and -mediated graphitic carbon nitride nanosheets for enhanced photocatalytic performance under natural sunlight, *Journal of Materials Chemistry A*. DOI:10.1039/c3ta15358d.

Transforming Industry through CCUS (2019), *Transforming Industry through CCUS*. Available from: https://www.iea.org/reports/transforming-industry-through-ccus [Accessed 7 October 2020].

Tu, D., Liao, H., Deng, Q., Liu, X., Shang, R. and Zhang, X. (2018) Renewable biomass derived porous BCN nanosheets and their adsorption and photocatalytic activities for the decontamination of organic pollutants, *RSC Advances*, 8 (39), pp. 21905–21914.

United Nations Climate Change (2016) The Paris Agreement. Available from: https://unfccc.int/process-and-meetings/the-paris-agreement/the-paris-agreement [Accessed 16 December 2019].

United States Environmental Protection Agency [no date] No Title. Available from: https://www.epa.gov/ghgemissions/global-greenhouse-gas-emissions-data [Accessed 7 October 2020].

Vernon-Parry, K. D. (2000) Microscopy : An introduction, *III-Vs Review*, 13 (4), pp. 40–44.

Vinu, A., Terrones, M., Golberg, D., Hishita, S., Ariga, K. and Mori, T. (2005) Synthesis of mesoporous BN and BCN exhibiting large surface areas via templating methods, *Chemistry of Materials*, 17 (24), pp. 5887–5890.

Wang, C., Chen, Z., Yao, X., Chao, Y., Xun, S., Xiong, J., Fan, L., Zhu, W. and Li, H. (2018a) Decavanadates anchored into micropores of graphene-like boron nitride:

Efficient heterogeneous catalysts for aerobic oxidative desulfurization, *Fuel*, 230 (May), pp. 104–112. DOI:10.1016/j.fuel.2018.04.153.

Wang, D., Xue, Y., Wang, C., Ji, J., Zhou, Z. and Tang, C. (2019a) Improved capture of carbon dioxide and methane via adding micropores within porous boron nitride fibers, *Journal of Materials Science*, 54 (14), pp. 10168–10178.

Wang, J., Hao, J., Liu, D., Qin, S., Chen, C., Yang, C., *et al.* (2017) Flower stamen-like porous boron carbon nitride nanoscrolls for water cleaning, *Nanoscale*, 9 (28), pp. 9787–9791. DOI:10.1039/c7nr03084c.

Wang, M., Bai, Y., Zhang, B., Zhong, B., Yu, Y., Zhang, J., Huang, X. and Wen, G. (2019b) Large scale fabrication of porous boron nitride microrods with tunable pore size for superior copper (II) ion adsorption, *Ceramics International*, 45 (6), pp. 6684–6692. DOI:10.1016/j.ceramint.2018.12.157.

Wang, Y., Low, Z.-X., Kim, S., Zhang, H., Chen, X., Hou, J., *et al.* (2018b) Functionalized Boron Nitride Nanosheets: A Thermally Rearranged Polymer Nanocomposite Membrane for Hydrogen Separation, *Angewandte Chemie - International Edition*, 57 (49), pp. 16056–16061. DOI:10.1002/anie.201809126.

Wang, Y., Meng, J., Tian, Y., Chen, Y., Wang, G., Yin, Z., *et al.* (2020) Deep Ultraviolet Photodetectors Based on Carbon-Doped Two-Dimensional Hexagonal Boron Nitride, *ACS Applied Materials & Interfaces*, 12 (24), pp. 27361–27367. DOI:10.1021/acsami.0c05850.

Webley, P. A. and Danaci, D. (2020) Chapter 5: CO_2 Capture by adsorption processes, RSC Energy and Environment Series. Vol. 2020-Janua. DOI:10.1039/9781788012744-00106.

Wei, H., Deng, S., Hu, B., Chen, Z., Wang, B., Huang, J. and Yu, G. (2012) Granular Bamboo-Derived Activated Carbon for High CO_2 Adsorption: The Dominant Role of Narrow Micropores, *ChemSusChem*, 5 (12), pp. 2354–2360.

Wei, Y., Wu, P., Luo, J., Dai, L., Li, H., Zhang, M., *et al.* (2020) Synthesis of hierarchical porous BCN using ternary deep eutectic solvent as precursor and template for aerobic oxidative desulfurization, *Microporous and Mesoporous Materials*, 293, pp. 109788. DOI:https://doi.org/10.1016/j.micromeso.2019.109788.

Weng, Q., Wang, X., Bando, Y. and Golberg, D. (2014) One-Step Template-Free Synthesis of Highly Porous Boron Nitride Microsponges for Hydrogen Storage, *Advanced Energy Materials*, 4 (7), pp.1301525.

Weng, Q., Wang, X., Wang, X., Bando, Y. and Golberg, D. (2016) Functionalized hexagonal boron nitride nanomaterials: emerging properties and applications, *Chemical Society Reviews*, 45 (14), pp. 3989–4012.

Weng, Q., Wang, X., Zhi, C., Bando, Y. and Golberg, D. (2013) Boron nitride porous microbelts for hydrogen storage, *ACS Nano*, 7 (2), pp. 1558–1565.

Williams, D. B. and Carter, C. B. (1996) The transmission electron microscope, in: *Transmission electron microscopy*. Springer, pp. 3–17.

Wu, J. and Zhang, W. (2009) Tuning the magnetic and transport properties of boron-nitride nanotubes via oxygen-doping, *Solid State Communications*, 149 (11–12), pp. 486–490.

Wu, L., Xue, M., Qiu, S.-L., Chaplais, G., Simon-Masseron, A. and Patarin, J. (2012) Amino-modified MIL-68 (In) with enhanced hydrogen and carbon dioxide sorption enthalpy, *Microporous and Mesoporous Materials*, 157, pp. 75–81.

Wu, P., Wu, Y., Chen, L., He, J., Hua, M., Zhu, F., *et al.* (2020) Boosting aerobic oxidative desulfurization performance in fuel oil via strong metal-edge interactions between Pt and h-BN, *Chemical Engineering Journal*, 380 (June 2019), pp. 122526. DOI:10.1016/j.cej.2019.122526.

Wu, P., Zhu, W., Chao, Y., Zhang, J., Zhang, P., Zhu, H., *et al.* (2016a) A template-free solvent-mediated synthesis of high surface area boron nitride nanosheets for aerobic oxidative desulfurization, *Chem. Commun.*, 52 (1), pp. 144–147. DOI:10.1039/C5CC07830J.

Wu, P., Zhu, W., Chao, Y., Zhang, J., Zhang, P., Zhu, H., *et al.* (2016b) A template-free solvent-mediated synthesis of high surface area boron nitride nanosheets for aerobic oxidative desulfurization, *Chem. Commun.*, 52 (1), pp. 144–147. DOI:10.1039/C5CC07830J.

Wu, P., Zhu, W., Dai, B., Chao, Y., Li, C., Li, H., Zhang, M., Jiang, W. and Li, H. (2016c) Copper nanoparticles advance electron mobility of graphene-like boron nitride for

enhanced aerobic oxidative desulfurization, *Chemical Engineering Journal*, 301, pp. 123–131. DOI:10.1016/j.cej.2016.04.103.

Xiao, F., Chen, Z., Casillas, G., Richardson, C., Li, H. and Huang, Z. (2016) Controllable synthesis of few-layered and hierarchically porous boron nitride nanosheets, *Chemical Communications*, 52 (20), pp. 3911–3914.

Xiao, F., Naficy, S., Casillas, G., Khan, M. H., Katkus, T., Jiang, L., Liu, H., Li, H. and Huang, Z. (2015) Edge-hydroxylated boron nitride nanosheets as an effective additive to improve the thermal response of hydrogels, *Advanced Materials*, 27 (44), pp. 7196–7203.

Xie, S.-Y., Wang, W., Fernando, K. A. S., Wang, X., Lin, Y. and Sun, Y.-P. (2005) Solubilization of boron nitride nanotubes, *Chemical Communications*, (29), pp. 3670–3672.

Xie, Y., Kocaefe, D., Chen, C. and Kocaefe, Y. (2016) Review of research on template methods in preparation of nanomaterials, *Journal of Nanomaterials*, 2016, pp. 11.

Xiong, J., Di, J., Zhu, W. and Li, H. (2020a) Hexagonal boron nitride adsorbent: Synthesis, performance tailoring and applications, *Journal of Energy Chemistry*, 40, pp. 99–111. DOI:10.1016/j.jechem.2019.03.002.

Xiong, J., Li, H., Yang, L., Luo, J., Chao, Y., Pang, J. and Zhu, W. (2017) Metal-free boron nitride adsorbent for ultra-deep desulfurization, *AIChE Journal*, 63 (8), pp. 3463–3469.

Xiong, J., Luo, J., Di, J., Li, X., Chao, Y., Zhang, M., Zhu, W. and Li, H. (2020b) Macroscopic 3D boron nitride monolith for efficient adsorptive desulfurization, *Fuel*, 261 (October 2019), pp. 116448. DOI:10.1016/j.fuel.2019.116448.

Xiong, J., Luo, J., Yang, L., Pang, J., Zhu, W. and Li, H. (2018) Boron defect engineering in boron nitride nanosheets with improved adsorptive desulfurization performance, *Journal of Industrial and Engineering Chemistry*, 64, pp. 383–389. DOI:10.1016/j.jiec.2018.04.001.

Xiong, J., Yang, L., Chao, Y., Pang, J., Zhang, M., Zhu, W. and Li, H. (2016) Boron Nitride Mesoporous Nanowires with Doped Oxygen Atoms for the Remarkable Adsorption Desulfurization Performance from Fuels, *ACS Sustainable Chemistry and*

Engineering 4(8), pp.4457–4464. DOI:10.1021/acssuschemeng.6b01156.

Xiong, J., Zhu, W., Li, H., Yang, L., Chao, Y., Wu, P., *et al.* (2015) Carbon-doped porous boron nitride: Metal-free adsorbents for sulfur removal from fuels, *Journal of Materials Chemistry A*, 3 (24), pp. 12738–12747. DOI:10.1039/c5ta01346a.

Yang, C., Liu, D., Chen, Y., Chen, C., Wang, J., Fan, Y., Huang, S. and Lei, W. (2019) Three-Dimensional Functionalized Boron Nitride Nanosheets/ZnO Superstructures for CO_2 Capture, *ACS Applied Materials and Interfaces*, 11 (10), pp. 10276–10282. DOI:10.1021/acsami.8b20775.

Yang, H., Xu, Z., Fan, M., Gupta, R., Slimane, R. B., Bland, A. E. and Wright, I. (2008) Progress in carbon dioxide separation and capture: A review, *Journal of Environmental Sciences*, 20 (1), pp. 14–27.

Yang, S., Zhan, L., Xu, X., Wang, Y., Ling, L. and Feng, X. (2013) Graphene-Based Porous Silica Sheets Impregnated with Polyethyleneimine for Superior CO_2 Capture, *Advanced Materials*, 25 (15), pp. 2130–2134.

Yazaydın, A. O., Snurr, R. Q., Park, T.-H., Koh, K., Liu, J., LeVan, M. D., *et al.* (2009) Screening of metal− organic frameworks for carbon dioxide capture from flue gas using a combined experimental and modeling approach, *Journal of the American Chemical Society*, 131 (51), pp. 18198–18199.

Yin, J., Yang, Z., Bi, L., Ren, S., Yan, G., Wang, Y. and Huang, X. (2020) Electronic and magnetic properties of Fe-doped narrow zigzag boron nitride nanoribbons, *Materials Today Communications*, 22 (August 2019), pp. 100753. DOI:10.1016/j.mtcomm.2019.100753.

Yin, L.-W., Bando, Y., Golberg, D., Gloter, A., Li, M.-S., Yuan, X. and Sekiguchi, T. (2005) Porous BCN nanotubular fibers: growth and spatially resolved cathodoluminescence, *Journal of the American Chemical Society*, 127 (47), pp. 16354–16355.

Yin, Y. and Chen, Y. (2011) Synthesis and growth mechanism of BCN nanowires, *Materials Letters*, 65 (15), pp. 2476–2478. DOI:https://doi.org/10.1016/j.matlet.2011.05.026.

Yoo, G. Y., Lee, W. R., Jo, H., Park, J., Song, J. H., Lim, K. S., *et al.* (2016) Adsorption

of Carbon Dioxide on Unsaturated Metal Sites in M2(dobpdc) Frameworks with Exceptional Structural Stability and Relation between Lewis Acidity and Adsorption Enthalpy, *Chemistry - A European Journal*, 22 (22), pp. 7444–7451. DOI:10.1002/chem.201600189.

Younas, M., Sohail, M., Kong, L. L., Bashir, M. J. K. and Sethupathi, S. (2016) Feasibility of CO_2 adsorption by solid adsorbents: a review on low-temperature systems, *International Journal of Environmental Science and Technology*, 13 (7), pp. 1839–1860.

Zahedi, E., Babaie, M. and Bahmanpour, H. (2016) Adsorption properties of boroxol ring doped zigzag boron nitride nanotube toward NO molecule using DFT, *International Journal of Modern Physics B*, 30 (17), pp. 1650101. DOI:10.1142/S0217979216501010.

Zhang, H., Yu, J., Chen, Y. and Fitz Gerald, J. (2006) Conical boron nitride nanorods synthesized via the ball-milling and annealing method, *Journal of the American Ceramic Society*, 89 (2), pp. 675–679.

Zhang, J. (2013) Design and synthesis of metal organic frameworks for co2 separation and catalysis. Rutgers University.

Zhang, J., An, L., Zhang, B., Zhang, J., Yu, Y. and Wang, C.-M. (2019a) Interlayer friction properties of oxygen-doped hexagonal boron nitride bilayers, *EPL*, 127 (1). DOI:10.1209/0295-5075/127/16003.

Zhang, J., Liu, D., Han, Q., Jiang, L., Shao, H., Tang, B., Lei, W., Lin, T. and Wang, C. H. (2019b) Mechanically stretchable piezoelectric polyvinylidene fluoride (PVDF)/Boron nitride nanosheets (BNNSs) polymer nanocomposites, *Composites Part B: Engineering*, 175. DOI:10.1016/j.compositesb.2019.107157.

Zhang, N., Liu, H., Kan, H., Wang, X., Long, H. and Zhou, Y. (2014) The preparation of high-adsorption, spherical, hexagonal boron nitride by template method, *Journal of Alloys and Compounds*, 613, pp. 74–79. DOI:10.1016/j.jallcom.2014.05.161.

Zhang, N., Zhang, T., Kan, H., Wang, X., Long, H. and Cui, X. (2015a) The effect of the boron source composition ratio on the adsorption performance of hexagonal boron nitride without a template, *Materials Chemistry and Physics*, 163, pp. 331–336.

Zhang, T., Zhang, J., Wen, G., Zhong, B., Xia, L., Huang, X., Zhao, H., Wang, H. and Qin, L. (2018) Ultra-light h-BCN architectures derived from new organic monomer with tunable electromagnetic wave absorption, *Carbon*, 136, pp. 345–358. DOI:10.1016/j.carbon.2018.05.001.

Zhang, X., Li, W. and Lu, A. (2015b) Designed porous carbon materials for efficient CO2 adsorption and separation, *New Carbon Materials*, 30 (6), pp. 481–501.

Zhao, Y., Liu, Z., Cao, C., Wang, C., Fang, Y., Huang, Y., *et al.* (2017) Self-sacrificed template synthesis of ribbon-like hexagonal boron nitride nano-architectures and their improvement on mechanical and thermal properties of PHA polymer /639/301/357/551 /639/301/357/1018 /128 /145 article, *Scientific Reports*, 7 (1), pp. 1–6. DOI:10.1038/s41598-017-08524-7.

Zheng, W. (2020) Ultrasonic-assisted Compatibility Industrial Nanomaterials Manufacturing and Microstructure Analysis, *Acta Microscopica*, 29 (2).

Zhi, C., Bando, Y., Tang, C., Honda, S., Sato, K., Kuwahara, H. and Golberg, D. (2005) Covalent functionalization: towards soluble multiwalled boron nitride nanotubes, *Angewandte Chemie International Edition*, 44 (48), pp. 7932–7935.

Zhi, C. Y., Bando, Y., Terao, T., Tang, C. C., Kuwahara, H. and Golberg, D. (2009) Chemically activated boron nitride nanotubes, *Chemistry–An Asian Journal*, 4 (10), pp. 1536–1540.

Zhou, M., Chen, Z., Yang, P., Wang, S., Huang, C. and Wang, X. (2020) Hydrogen reduction treatment of boron carbon nitrides for photocatalytic selective oxidation of alcohols, *Applied Catalysis B: Environmental*, 276, pp. 118916. DOI:https://doi.org/10.1016/j.apcatb.2020.118916.

Zhou, X., Chu, W., Zhou, Y., Sun, W. and Xue, Y. (2018) DFT simulation on H 2 adsorption over Ni-decorated defective h-BN nanosheets, *Applied Surface Science*, 439 (May), pp. 246–253. DOI:10.1016/j.apsusc.2017.12.238.

Zhu, H.-L., Han, Q.-X., Wu, J., Meng, X.-L. and Cui, H.-Z. (2016) Large scale synthesis of nanoporous BN flake with high surface areas, *Journal of Crystal Growth*, 434, pp. 19–24.

Zukal, A., Kubů, M. and Pastva, J. (2017) Two-dimensional zeolites: Adsorption of

carbon dioxide on pristine materials and on materials modified by magnesium oxide, *Journal of CO_2 Utilization*, 21 (July), pp. 9–16. DOI:10.1016/j.jcou.2017.06.013.